DETERMINATION OF THE LEAK SIZE CRITICAL TO PACKAGE STERILITY MAINTENANCE

by

Scott W. Keller

Dissertation submitted to the Faculty of Virginia Polytechnic Institute and State University in partial fulfillment of the requirements for the degree

of

Doctor of Philosophy

in

Food Science and Technology

Dr. Joseph E. Marcy, Chair
Dr. Cameron R. Hackney
Dr. Barbara Blakistone
Dr. George H. Lacy
Dr. W. Hans Carter, Jr.

Key words: imposed pressure, imposed vacuum, microbial ingress, package sterility, threshold leak size, critical leak size, package defect, sterility maintenance**,** surface tension

August 1998

Blacksburg, Virginia

DETERMINATION OF THE LEAK SIZE CRITICAL TO PACKAGE STERILITY MAINTENANCE

Scott W. Keller

ABSTRACT

This study was divided into four sections: the literature review; the mechanism by which a package defect becomes a leak; and the imposed pressures generated within a package during distribution; comparison of the threshold leak size to the critical leak size and their effect on loss of package sterility; and the relationships between microorganism characterisitics and the threshold leak size, and their effect on the critical leak size.

Section II. The mechanism by which a package defect converts to a leaker in an effort to develop a relationship between the threshold leak size and loss of package sterility was studied. The threshold leak size is the hole size at which the onset of leakage occurs. The threshold pressure is that which is required to initiate a leak. Leak initiation was studied in terms of the interaction between three components: liquid attributes of liquid food products, defect size, and pressures required to initiate liquid flow.

Liquid surface tension, viscosity, and density were obtained for sixteen liquids. The imposed pressures (P_o) required to initiate flow through microtubes of IDs 0, 2, 5, 7, 10, 20 or 50 μm, were measured using 63 test cells filled with safranin red dye, tryptic soy broth, and distilled water with surface tensions of 18.69 mN/m, 44.09 mN/m, and 64.67

mN/m, respectively. Significant differences were found between observed threshold pressures for safranin red dye, tryptic soy broth, and distilled water ($p < 0.05$). Liquids with small surface tensions such as safranin red dye required significantly lower threshold imposed pressures than liquids with large surface tensions such as distilled water ($p < 0.05$). An equation was developed to quantify the relationship between liquid surface tension, threshold imposed pressure, and defect size. Observed threshold pressures were not significantly different ($p > 0.05$) than those predicted by the equation.

Imposed pressures and vacuums generated within packages during random vibration and sweep resonance tests were measured for brick-style aseptic packages (250 ml), metal cans size 76.2-mm x 114.3-mm (425 ml), quart gable top packages (946 ml), one-half gallon gable top packages (1.89 L) and one-gallon milk jugs (4.25 L). Significant differences were found between packages for observed generated pressures during vibration testing ($p < 0.05$). An equation to calculate the threshold like size based on liquid surface tension and imposed pressure was established.

Section III. The onset of liquid flow through a defect as a result of imposed positive pressures or vacuum were linked to the sterility loss of a package. Five-hundred sixty-three test cells, each with microtubes of 0, 2, 5, 7, 10, 20 or 50 μm, manufactured to simulate packages with defects, were biochallenged via an aerosol concentration of 10^6 cells/cm^3 of *Pseudomonas fragi* Lacy-1052, under conditions of imposed positive pressure or vacuum of 20.7, 13.8, 6.9, 0, -6.9, -13.8, -20.7 kPa, respectively and temperatures of 4°, 25° and 37°C. A statistically significant relationship between loss of

sterility due to microbial ingress in test cells and the initiation of liquid flow were found ($p < 0.05$). Microbial ingress was not found in test cells with microtube IDs of 2 μm. Leak sizes critical to the sterility maintenance were found to be different based on the liquid surface tension, and imposed package pressures. The threshold leak size where the onset of liquid flow was initiated, and the critical leak size at which loss of sterility occured were not significantly different ($p > 0.05$).

Section IV. The effects of microorganism size and motility, and the imposed pressure required to initiate liquid flow, on the leak size critical to the sterility of a package were measured. *Pseudomonas fragi* Lacy-1052, *Bacillus atrophaeus* ATCC 49337, and *Enterobacter aerogenes* ATCC 29007 were employed to indicate loss of package sterility. One hundred twenty-six microtubes with interior diameters (I.D.s) of 5, 10, and 20 μm and 7 mm in length were used as the manufactured defects. Forty-two solid microtubes were used as a control. An equation was used to calculate imposed pressures sufficient to initiate the flow of tryptic soy broth through all defects. No significant differences were found for loss of sterility as a result of microbial ingress into test cells with microtube ID sizes of 5, 10, and 20 μm between the test organisms ($p > 0.05$). Interactions between the initiation of liquid flow as a result of imposed pressures, and the sterility loss of test cells were significant ($p < 0.05$).

Key words: imposed pressure, imposed vacuum, microbial ingress, package sterility, threshold leak size, critical leak size, package defect, sterility maintenance**,** surface tension

Dedicated to Madison

“There is nothing more difficult to take in hand, more perilous to conduct or more uncertain in its success, than to take the lead in the introduction of a new order of things, because the innovator has for enemies all those who have done well under the old conditions, and lukewarm defenders in those who may do well under the new.”

N. Machiavelli: II Principle, 1513

ACKNOWLEDGMENTS

I wish to express my sincere appreciation to my Committee members, Dr. Cameron Hackney, Dr. Barbara Blakistone, and Dr. Hans Carter for making time in their busy lives for their professional advices and guidance. I would like to express my sincere gratitude to Dr. Joseph Marcy, Dr. George Lacy and Verlyn Stromberg for their patient but rigorous coaching. I would like to thank Dr. Richy Davis of V.P.I. & S.U., Dr. Wes Hoffman and Dr. Peter Pollock of the Carbon research Division of the Phillips Laboratory, Department of Defense, for their considerable efforts. I would like to thank Harriett Williams and John Chandler for their technical support, assistance on my project**.** Dr. Corey Berends for contributing his thoughtful insights, wonderfully engaging brainstorming chats, and great friendship, deserves many thanks. To my good friends Dr. Bruce Zoecklein and Jimmy Bragg for their moral support, fly-fishing instruction and general misguidence,...thanks, it was so much fun! I would like to thank the Center for Aseptic Packaging and Processing Studies (CAPPS), and the National Science foundation for full financial support for this project and sponsored visits for presentations in Copenhagen, Denmark and Hsinchu-City, Taiwan.

TABLE OF CONTENTS

LIST OF TABLES, FIGURES AND APPENDICES

SECTION II

SECTION III

SECTION IV

INTRODUCTION

Sterility maintenance assurance continues to be a prominent concern for producers of aseptically packaged products. Such producers have aggressively embraced new technologies and materials to manufacture flexible and semi-rigid packaging. Aseptic technology and material's usage have created dilemmas over methods by which aseptic package integrity should be evaluated.

One hundred percent on-line inspection and evaluation of packaged products remains a top priority for producers of aseptically packaged products. More than seventy manufacturers produce on-line package inspection systems, nine of which specialize in leak/seal testing (Noone, 1996a). Thirty-nine major producers offer eight closure types in an effort to reduce loss of seal integrity (Noone, 1996b). Commercially available closure styles range from flip top to twist open/close, with twelve features from child resistant to push-on/twist-off (Noone, 1996b). Although many technologies have been developed to maintain package sterility, a key problem remains unresolved; the leak size at which container sterility is jeopardized, or, the critical leak size.

Presently, disturbing disparities exist between leak sizes which are readily detectable using current on-line technology, and the speculated value for the critical leak size. It has been suggested that package inspection systems are available which can provide sufficient safety assurance at detection levels of 10 μm for pinholes and 50 μm for channel leaks (Yam, 1995). However, the critical leak size is believed to be $\leq$ 10 μm

for channel leaks (Blakistone et al., 1996).

Microleaks, which cause loss of sterility for both aseptically packaged food and medical devices, pose significant risk due to difficulties associated with detection. Sterility maintenance of an aseptically packaged product must be based on an understanding of conditions which place package sterility in jeopardy. Such was the intent of this study.

OBJECTIVES

The objective of this study was to determine the microleak defect size(s) critical to sterility maintenance of aseptic packages. The desired results of this study are a quantification of factors affecting sterility loss of aseptic packages, and the creation of a model to predict the likelihood of sterility loss. Such a model could be used to generate guidelines to produce package sterility assurance levels similar to process sterility levels used for low-acid foods.

1. **Role of Defect Size** To understand the role of defect sizes in the process of microbial ingress under ambient conditions.

2. **Role of Temperature, Imposed Pressure or Vacuum** To independently measure the influence of temperature, imposed pressure and imposed vacuum on

the threshold defect size and determine their relationship to the sterility maintenance of an aseptic package.

3. **Package Vibration** To measure, under ambient conditions, the influence of vibration (distribution simulation) on the threshold defect size.

4. **Develop Mathematical Model** To mathematically characterize the mechanism(s) responsible for loss of package sterility. To develop a mathematical model that will predict the ability of a package to maintain sterility.

SECTION I: LITERATURE REVIEW

LOSS OF PACKAGE STERILITY

The goal of shelf stable food manufacturers is to produce commercially sterile products that will maintain their sterility until they reach the consumer (Placencia et al., 1986). Aseptic packaging was developed to achieve this goal.

Manufacturers of packaging technology have responded well to the changing demands of consumers. This is reflected in product sales. In 1995, sales of products in controlled/modified atmosphere/vacuum packaging surpassed totals for canned or frozen foods (Brody, 1996). The same year, 10 billion aseptic packages were distributed to retailers and institutions (Brody, 1996). To increase our understanding of possible mechanisms responsible for the loss of sterility in aseptic packages, we will review problems associated with other packages with longer histories.

Cans

Heat processed food products in cans have been available in Europe and the United States for more than a century (Anema and Schram, 1980). The incidence of sterility loss of canned foods is well documented, but poorly understood.

Contamination of canned products may occur when microorganisms pass through a seam in the container. Such contamination is called "leaker spoilage" (Michels and

Schram, 1979). Michels and Schram (1979) reported three types of post process contamination due to leaker spoilage: "1) spoilage with acid and gas formation; 2) spoilage with acid formation, but with no gas formation (flat sour spoilage); 3) bacterial growth with neither acid or gas formation."

Many researchers consider leakers to be the primary source of post process contamination and loss of product sterility (Anema and Schram, 1980; Davidson and Pflug, 1981; Placencia et al., 1988; Anderson, 1989; Kamei et al., 1991). Post process leakage has been linked to microbial spoilage of commercially canned foods more than any other single factor (Gilchrist et al., 1985). An estimated 90% of can spoilage in the United States is due to post process contamination (Segner, 1979). Between 1921 and 1979, 154 incidents of food poisoning were associated with post process contamination due to leakage (Stersky et al., 1980).

Put and Warner (1972) listed three main factors that influence spoilage of canned products as a result of post process handling: 1) the condition of the can double seams, 2) bacterially contaminated cooling water, and 3) abuse from can filling and handling equipment. Contaminated cooling water used in production facilities may eventually make contact with the package contents through pinholes or channel leakers. Bacteria may be conveyed along with the cooling water, to an environment conducive to survival and growth (Put and Warner 1972). Pflug et al. (1981) confirmed these findings by studying swollen cans of low-acid foods at the retail level.

Whether leakage occurs during cooling operations or on wet runways, water

appears to be a common carrier of bacteria that contributes to post process spoilage (Rey et al., 1982). Wet and dirty, rough post cooling handling and impact with conveyor belt surfaces, increases the incidence of post process contamination of containers as well (Bashford, 1947; Put and Warner, 1972). Post process contamination of flexible retort pouches may occur in much the same way as that of cans (Michels and Schram, 1979).

Although the incidence of sterility loss in cans is well documented, the cause of occurrence is often circumstantial. Pflug et al. (1981) collected 1,104 swollen cans from retail food markets over a 17-month period. He concluded that 314 (28.4%) of the swollen cans resulted from major container defects. The remaining 790 cans demonstrated swelling as a result of; "a) typical leaker spoilage, 86%, b) typical under processing spoilage, 7%, c) thermophilic spoilage, 1%, and d) non microbial swells, 6%."

Pflug et al. (1981) found the incidence of spoilage to vary between 2.1 and 78.4 cans per 100,000 sold (0.0021 to 0.0784%). The incidence rate of can spoilage depended on the type of food packaged. The largest number of swelled cans were those that contained dog food (78.4 cans), various types of fish (65.4 cans) and stew (36.6 cans).

Flexible Pouches and Semi-rigid packages

Flexible and semi-rigid packages are the result of advances in packaging materials and a competitive technology market. These containers were developed as an

alternative technology to cans, and are generally constructed of layers of various polymers, paperboard and/or metals. Each layer is situated, with respect to the other, to provide various strength and barrier properties.

The first large scale commercial use of flexible packages was in Italy, in 1965 (Michels and Schram, 1979). Since then, flexible packages have been used to package a wide variety of products, especially in the food and medical device manufacturing industries. Packaging experts estimate that 50 to 70% of all recalls of medical devices are due to packaging defects, 40% of which can be attributed to improper packaging (Bryant, 1988).

Lampi (1980) suggested that leakers in flexible pouches could occur as a result of wrinkles in the seal area due to food material entrapped within the seal or via holes in the packaging material. Nichols (1989) reported that seal contamination, poor control of sealing parameters, mechanical alignment problems, and changes in packaging materials contribute to seal failure (i.e., leakers) in flexible and semi-rigid packages. McEldowney and Fletcher (1990a) suggested that leakers may occur via temporary holes in the material of flexible and semi-rigid packages. Careful manual handling of dry sterilized flexible and semi-rigid packages is an acceptable practice, and can keep pinholes to acceptably low levels (Michels and Schram, 1979; Anema and Schram, 1980).

Materials used to construct flexible and semi-rigid packages often fail to adequately protect the food product under normal storage and distribution conditions due to physical, mechanical and structural deficiencies of the package. Flexible and semi-

rigid packages are susceptible to various imposed defects, such as burst defects and seal creep, due to abuses via shock and vibration during product storage and distribution. Package construction may vary depending on the type of machinery used to form, fill and seal the aseptic package.

Flexible Pouches and Semi-rigid Package Construction

The construction of flexible pouches and semi-rigid packages differ considerably from that of metal cans. Metal alloys are used for the construction of cans while plastics, paperboard, aluminum foil or composites of these materials are used for the construction of flexible and semi-rigid packages. Heat sealability and peelability represent keen areas of concern for the mechanical construction of these packages (Arndt, 1992).

Sterility maintenance of flexible and semi-rigid packages depend on parameters such as sealing temperature, sealing pressure and dwell time, all of which must operate in the confines of a specific range (material dependent) to ensure adequate sealing. Such parameters are commonly changed to accommodate the type and combination of packaging materials. For example, sometimes a shorter dwell time may be used with a higher sealing temperature (Arndt, 1992).

Seal Integrity of Flexible Pouches and Semi-rigid Packages

Seal integrity of flexible and semi-rigid packages greatly influences shelf-life and, inevitably, consumer confidence in the product. Nichols (1989) reported that seal

contamination, poor control of sealing parameters, mechanical alignment problems, and changes in packaging materials contribute to seal failure in flexible and semi-rigid packages. Anema and Schram (1980) concluded that flexible and semi-rigid packages can maintain sterility and reach consumers in excellent condition if careful control is maintained during sealing of the package.

Barrier, Migration, and Material Structural Properties of Flexible and Semi-rigid Packages

Barrier and migration properties of the material(s) used in the construction of semi-rigid and flexible containers must also be considered. Migration occurs when gases permeate and pass through the packaging material. Gas migration often results in a reduction of shelf-life and quality of the product (Placencia et al., 1988). Materials which allow migration may also create opportunities for gas leakage or permeation through seams via channel leakers or through the body wall of the containers via pin hole leaks. Permeation may also occur through the bound polymer layers in laminated barrier plastic sources (Reich, 1985).

An issue not well documented concerns the biobarrier properties of polymer packaging materials. Materials used in the construction of flexible and semi-rigid packages may fail to adequately protect food products under normal storage and distribution conditions due to physical, mechanical and structural deficiencies of the package along with inadequacies of the material to act as a biobarrier. Without

standardized methodologies for the testing of packaging materials for biobarrier properties, current packaging materials used for flexible and semirigid packages may be misused (Placencia et al., 1986). Packages constructed of materials untested for biobarrier efficiacy may have a higher propensity for loss of sterility (Placencia et al., 1986).

DEFECT AND LEAK DETECTION

One hundred percent on-line, nondestructive inspection of packaged products for the detection of defects remains an elusive goal for manufacturers. Equipment capable of detecting package micro-defects was developed before the threshold defect (pin hole or channel leaker) size critical to sterility maintenance and integrity of a package were established.

Gnanasekharan and Floros (1994) cited three major obstacles to be resolved prior to the development of a reliable, 100% on-line inspection system. They are; the size of leaks that occur in real life, the minimum leak size for microbial contamination to occur, and the minimum leak size that can be rapidly and reliably detected.

Flexible and semi-rigid packages often undergo temporary shapes caused by forces within the environment, such as abuses incurred during storage and distribution. Due to characteristics inherent in flexible and semi-rigid packages, more opportunities

for complex disfigurement or breach of seal integrity exist than with cans (Kamei et al., 1991).

Gnanasekharan and Floros (1994) argue that small leaks in packages under vacuum, such as cans, may permit ingress of microorganisms due to the presence of pressure differentials. Similar size holes in aseptic or other packaging whose interior pressure is closer to that of ambient atmospheric conditions may not permit microbial ingress. Therefore, the threshold defect size critical to sterility maintenance of cans may not be the same threshold as that for flexible and semi-rigid packages. Most defect/leak detection tests in use today, including biotesting, were developed for the evaluation of cans. Such tests fail to consider the environment which flexible or semi-rigid packages may need to tolerate, or the influence of events, such as temporary deformation of a package, on the sterility maintenance of the package.

In an effort to measure the ability of flexible or semi-rigid packages to maintain sterility, several methods of defect detection have been developed (Gilchrist et al., 1989). The methods of defect detection can be classified into two categories; gross examination, and fine examination.

Defect Detection

Gross examination focuses on abnormalities detectable by sight or touch such as, mechanical defects, perforations, delamination, swelling, flex cracks, and malformations, which can provide insight as to the cause of the defect. Defects are measured and noted

as containers are inspected (Arndt, 1992). If evidence of microbial intrusion is present, further investigation is required.

Fine examination employs microscopy, SLAM (scanning laser acoustic microscopy), SAM (scanning acoustic microscopy), ultrasound, etc., and can be used in combination with direct visual inspection. Fine examination can be helpful when difficulties exist in detecting problem areas within seals of the containers (Arndt, 1992).

Leak Detection

Current leak detection testing methods involve some variations of tests which use either a chemical or a gas as a leak indicator. These leak testing techniques measure the escape or entry of liquids or gases (pressurized or evacuated) from systems designed to contain them. The escape of gases or liquids are a result of pressure differentials formed between the interior and the exterior of the package (Anderson, 1989; Axelson and Calvin, 1991). Leaks of sufficient size to allow passage of the test chemical or gas, may be identified and sometimes located. Equations used to model the dynamics of gas, liquid or mass transfer through leaks are based on tube diameters $\geq$ 1000 μm, not 10, 20 or 50 μm pin holes such as those found in food packages (Alves and Boucher, 1963; Fuchs, 1964).

The following techniques are accepted methods for leaker detection, identification and characterization within flexible and semi-rigid containers.

Air Leak Testing

The objective of the air leak test is to identify leakers by observing a measurable pressure loss within the container. Two methods of air leak testing are the dry method and the wet method.

The dry method requires injection of air into the container until a standard pressure is reached. The standard pressure used for testing should be less than the burst pressure for the package. The process is monitored for a period of 60 seconds using a pressure gauge (Arndt, 1992).

The wet method uses the same approach as the dry method except that the container is completely submerged. Leaks are detected visually as a result of the presence of bubble streams rather than by pressure changes identified by a pressure gauge (Anderson, 1989; Placencia and Peeler, 1990; Arndt, 1992).

Burst Testing

Burst resistance, or burst pressure, is defined as the internal container pressure required to cause failure of the container seal (Matty et al., 1991). Burst testing is used to determine the ability of a sealed container to withstand various internal pressure and is considered a general indicator of abuse resistance (Arndt, 1992). Measurements for burst resistance are reported in $kPa/cm^2/sec$. Restrained and unrestrained burst tests are used to identify a separation between packages with strong seals and those with weak seals by determining the pressure at which seal failure occurs (Arndt, 1992).

Restrained, or static burst testing, allows a steady increase of internal pressure (usually 6 kPa/cm^2/sec) to a pressure slightly less than that required to cause seal failure, and is held for 30 seconds (Anderson, 1989). Unrestrained, or dynamic burst testing, involves a steady increase of internal pressure (usually 6 kPa/cm^2/sec) until seal failure occurs.

Two factors influence parameters for burst resistance: package pressurization rate and restraint height (Matty et al., 1991). The pressurization rate is defined as the rate at which the internal pressure of the package under use or abuse (test) is increased. The restrained height is defined as the distance above the container flange when the package lid is allowed to flex freely via expansion or contraction (Matty et al., 1991).

Chemical Etching

Chemical etching allows visual examination of the package area(s) suspected of leakage. Etching is a process by which the laminated seal area is separated into the original constituent components. This etching process removes overlying layers from multi-laminated materials to reveal the seal of the package (Arndt, 1992). This process allows package with known defects in the seal (found using the etching technique) to be compared to the exterior of packages suspect of defects before etching.

To facilitate etching, materials are soaked in tetrahydrofuran (THF) to remove the outer polyester layer by softening adhesives and/or inks (Arndt, 1992). The package sample is then soaked in 6 N HCL to remove any traces of aluminum foil, if applicable.

The materials are then rinsed. Ink pattern and dispersion are then observed and checked for leaks and channels within the fused area. The samples may then be placed on an overhead projector so that a visual inspection maybe rendered (Arndt, 1992).

Compression Test

The compression test offers three techniques to determine the effects of weight/exterior pressure on the seal integrity of the container: static method, dynamic method, and squeeze test.

Using the static method, a sealed sample container is placed on a flat surface while a flat weight is placed on top. The weight is allowed to remain on top of the container for a predetermined period of time or until deformation resulting in seal breach occurs (Arndt, 1992).

The dynamic method consist of a sealed sample container placed on a flat surface while a continuously increasing force is exerted on the top of the container at a constant rate. The maximum force the container will resist without traces of leakage due to loss of seal integrity is observed (Arndt, 1992).

The squeeze test consists of applying a manual kneading action that forces the contents of the container to come into contact with the interior seal surface area of the package. During the test, the observer checks the package for leaks and delamination around the seal areas and on the exterior walls of the package (Arndt, 1992).

Positive results occur when holes are found somewhere on the package, such as in the seal or in the seam. Holes result when measurable movement of the top plate of the package is observed (Arndt, 1992).

Negative results occur when no loss of seal integrity is identified by measurable movement of the top plate of the package. False positive results occur in packages that are underfilled or that simulates failure without loss of seal integrity (Arndt, 1992).

Distribution Test

A distribution, or abuse, test can simulate various stresses such as vibration, compression and impact at levels similar to those expected during normal distribution. All sample packages should be incubated at 37°C under ASTM laboratory conditions of 23 ± 2°C and 50 ± 5% relative humidity for a period of two weeks. After testing, all packages are examined for defects or damage as a result of treatment. Packages that are not affected by the treatment should be incubated for an additional 14 days at 37°C and then visually inspected for indications of defects or damage (Arndt, 1992).

Electester

The electester is capable of detecting changes in the viscosity of liquids within a package as a result of microbial fermentation. Shock waves are used to determine viscosity variations within the package. Packages containing microbial activity due to post process or other contamination will result in the creation of a more viscous fluid that

adsorbs more shock waves when compared to non contaminated packages (Anderson, 1989; Arndt, 1992). The sample packages to be tested are incubated at 37°C for 4 days. The packages are rotated 90° and returned to their original position very quickly to create a shock wave for viscosity measurement. The wave formed by the motion is then observed on an oscilloscope and wave lengths are compared to non contaminated containers. Positive results occur when the wave formed by the motion dampens more quickly or slowly than normal. Negative results occur when the wave falls within normal limits, indicating that no microbial contamination is present.

Electroconductivity

This test is identifies defects by using electric current. Flexible packages constructed of plastic are generally poor conductors of electricity, therefore any breach in the surface of the plastic package acts as an effective conduit to the current (Axelson and Calvin 1991; Arndt, 1992). A conductivity meter or probe is placed on the outside of the package, while another probe is placed inside of the package. The package is then submersed in 1% NaCl in water (a brine solution).

Positive results occur when a current flow is completed, indicating a breach in the seal. Negative results occur when a current flow does not exist, indicating an intact seal.

Helium Leak Test

The helium leakage technique is used primarily to study the influence of can

structural defects on barrier properties (Put and Warner, 1972; Gilchrist et al., 1985; Gilchrist et al., 1989). Test container preparations consist of evacuation by a 2-stage rotary vacuum pump. When the pressure falls to $< 10^{-1}$ torr, helium is sprayed around the outside of the package. If any quantity of helium penetrates the seams of the package, it is detected by a mass spectrometer according to the amount found (Put and Warner, 1972).

Cautions must be observed when using the helium leak test to detect defects in flexible packages (Arndt, 1992). Sealed pouches are generally placed on their side in a helium pressurization tank. Use of flexible pouches requires careful maintenance of the helium pressurization tank at approximately 207 kPa/cm^2. Pressures greater than 345 kPa/cm^2 generally result in false positives for leakage, whereas less than 207 kPa/cm^2 (between 69 and 138 kPa/cm^2) may reduce the sensitivity of the test. Problems have been noted during flexible package tests when pressure was carefully maintained at 207 kPa/cm^2. For example, greater than 69 kPa/cm^2 may cause laminated material to distend or stretch near the seal, resulting in temporary closure of channel leakers, especially those with less than a 20 µm diameter (Gilchrist et al., 1985; Gilchrist et al., 1989).

Manganese Ion Test

The manganese ion test, performed simultaneously with a bio-test, is able to detect small traces of Mn^{+2} passing through the compromised areas in, on, or near the package seams (Put and Warner, 1972; Anderson, 1989). Processed packages are

mechanically abused and allowed to cool in a 7% solution of $MnSO_4$ containing 10^7 cells/mL (the bacteria used should be insensitive to Mn). After the packages have cooled, the contents of each package are filtered through a membrane, and the number of bacteria which enter the package can be enumerated. The filtrate may be used to calorimetrically estimate the amount of $MnSO_4$ which entered each package.

Bubble-forming Test

A bubble-forming solution can be added the surface area of the package. Care must be taken so that no bubbles are created by the process itself. A sensitivity of 10^{-5} atm cm^3/s can be achieved with this method (Anderson, 1989). The bubble-forming test is easy and inexpensive to use. A disadvantage is that the size of the leak is difficult to determine using this method.

Bubble Test

A bubble test is one of the most commonly used methods for identifying leaks in a package. The package is immersed in a liquid. A positive test results if any bubbles originate from the package surface, which indicates the presence of a leak. Use of this method allows detection of holes down to 0.005" in size. To increase the sensitivity of this test, a pressure differential between the package environment and its interior can be created by creating a partial vacuum in a chamber with the package inside, or by heating the package to create an internal pressure (Anderson, 1989).

BIOTESTING

Biotesting is a destructive test method that uses microorganisms for leak detection, with characteristics such as motility or non-motility, rather than a chemical or a gas. The objective of a biotest is to verify the post process contamination potential of a food container via microbial ingress (Folinazzo et al., 1968). Most food product manufacturers would prefer the availability of a physical test rather than a microbiological or biotest. Biotests are employed to develop and compare physical test results with microbial test results to assess the limits of new evaluation methods (Bryant, 1988).

Immersion Biotest

The precedence for immersion biotesting has its roots in practical observation. Anema and Schram (1980) found when quick drying of the containers was applied, after cooling, package sterility could be maintained under hygienic conditions, as demonstrated via immersion biotesting.

Immersion biotesting consists of submerging the test package into a solution comprised of a high concentration of microorganisms referred to as test or indicator organisms. Immersion biotesting has been used extensively for integrity testing of can double seams and has become the standard test method. Immersion biotesting of cans has set the precedence for integrity testing of semi-rigid and flexible packages as well.

Biotesting allows the manufacturer to evaluate the package's ability to maintain sterility under severe conditions. Microorganisms, in concentrations ranging between 10^6 and 10^9 colony forming units (CFU/mL), are used as leak indicators. Leakage is determined by growth of the test microorganism within the test container.

Cans used for biotesting are pre-screened by immersion in water. Cans that leak 0.01 mL of air at 25°C and 0 kPa in 15 seconds are considered good candidates for a biotest experiment (Put et al., 1980).

Arndt (1992) described a method of immersion biotesting which consisted of a temperature controlled water bath and agitation in a solution. The solution contained either *Enterobacter aerogenes* for foods with a pH > 5.0, or *Lactobacillus cellobiosis* for foods with a pH ≤ 5.0, both of a 10^7 CFU/mL concentration. Filled cans were sterilized and cooled in sterile water. Put et al.(1980) filled the test cans with 1/3 citrate broth which contained (by percentages): sodium citrate, 0.25; $Na(NH_4)HPO_3$, 0.1; NaCl, 0.5; and placed them in distilled water at a pH 6.8. Part of the cooling water surrounding the seam was removed by vaporization via a vacuum system and replaced by water or citrate broth inoculated with various concentrations of test organisms (Put et al., 1980). The exterior seam of the container remained in contact with the infected medium at a constant temperature for a predetermined period before being washed with tap water. A portion of the containers remained wet, while the rest were allowed to dry. After a predetermined time, all containers were allowed to stand at a constant temperature, for various times. Leaks generally became evident during this incubation period (organism

dependent) as indicated by container swell (as a result of microbial production of gas within the container), and broth turbidity. Test organism(s) selected should have caused fermentation of the food product if the container was penetrated, but should not be pathogenic.

Each container, according to its schedule for standing time period was then removed from the area so that its contents could be membrane filtered to provide a count (CFU/mL) of infiltrating bacteria (Put et al., 1980). Common modifications to this bio-test include the addition of 0.1% glucose to the citrate broth and variations of standing time.

Gilchrist et al. (1989) used immersion biotests in conjunction with helium gas and fluorescence dye leak tests to determine the seal integrity of flexible retort packages. The pouches were constructed of a trilaminate of polyethylene, aluminum, and polypropylene. Pouch dimensions were 6.5" x 8.5" and 12" x 14" with a total laminate thickness of 0.005 inch. Holes were made in the pouches using one of two methods: 1) using a laser to melt through the material to produce holes in the range of 17 μm to 81 μm, or 2) by forcing a stainless-steel wire through the material, producing holes in the range of 22 μm to 175 μm. The pouches were commercially sterilized for 20 minutes at 121°C in a still retort. Sterile pouches were placed in tryptic soy broth (TSB) containing a concentration of 10^8 *E. coli*/ml for two hours, and agitated every 15 minutes. Pouches were removed from the TSB and incubated at 37°C for 20-24 hours. Gilchrist et al. (1989) found that bacteria was able to pass thorough holes down to 20 μm. Premeasured

holes revealed that the hole size had decreased from 20 μm to 5 μm due to handling of the pouch.

Most flexible and semi-rigid containers used to aseptically package food or medical devices are not immersed in concentrated bacterial suspensions during storage and distribution (Gnanasekharan and Floros, 1994; Reich, 1985). Therefore, immersion biotest methods employed to evaluate can seam integrity, when applied to flexible and semi-rigid packages, may not be practical indicators of the package's ability to maintain sterility. Immersion biotesting of flexible and/or semi-rigid aseptic packages for sterility maintenance force an evaluation of the package under conditions that the packages were not intended to tolerate during normal storage and distribution..

Bioaerosols

Package sterility evaluation methods that employ bioaerosols simulate conditions similar to those which the package will be expected to tolerate during storage and distribution. Bioaerosols found in nature vary greatly in concentration. Reich (1985) reported the average airborne microbial level in hospitals to be 125 cfu/m^3. Lenhart et al. (1982) found the airborne concentration at the entrance of a poultry shackling line to be 6.5 x 10^5 CFU/m^3, of which 1% to 3% were Gram-negative and contributed approximately 918.4 ng/m^3 of airborne endotoxins. Factors such as species variability, air temperature, humidity, irradiation, or trace materials in the air influenced microbiological viability, and lifespan (Reist, 1993).

The literature has produced much justification for the creation of new methods and standards for aseptic package evaluation. Immersion biotesting, a method traditionally used for the evaluation of canned products, is currently the transient technology used to evaluate aseptic package integrity. The foundations of the immersion biotest method consist of exposure of aseptic packages to a condition they will not be expected to tolerate during storage and distribution. Therefore, the food packaging industry must establish an integrity test to replace biochallenge via traditional immersion testing for the evaluation of aseptic packages. Reich (1985), Placenia et al. (1986), Chen et al. (1991), Blakistone et al. (1996) and Keller et al. (1996) have laid the foundation for such a test method.

Reich (1985) used an airflow-nebulizer approach for controlled microbial exposure to the package. The purpose of the investigation was to determine the effectiveness of an intact package as a microbial barrier under conditions of microbiological challenge, representative of that which the package will be expected to tolerate during distribution (Reich, 1985).

Holes were made in Tyvek^{TM} lidding material of thirty-five packages with a Tesla coil to simulate defects. All materials were examined with the aid of a scanning electron microscope (SEM) to verify hole size uniformity. Hole sizes consistently yielded diameters of 40 ± 5 μm (Reich, 1985). Each of the packages was subjected to a microbial challenge concentration of 4 x 10^4 *B. subtilis* ATCC 9372 spores per cubic meter, a microbial challenge far in excess of what might be found during actual product

use conditions (Reich, 1985).

The microbial distribution demonstrated a homogeneous dispersion of challenge organisms throughout the chamber. After 72 hours of ambient incubation, pacakges within the chamber demonstrated indicator organism growth (Reich, 1985). This indicated that the complete system represented a consistent and valid microbial challenge method to the barrier properties of the product.

Using a similar method to that of Reich (1985), Placenia et al. (1986) found the microbial challenge via exposure-chamber method to be a reliable test of the barrier properties of a packaging product. Using this method, a single, 1 µm-diameter pore could be detected 55.6% of the time when a bacterial exposure of 10^3 CFU/mL was employed (Placenia et al., 1986). Results demonstrated detectability increases as the bacterial concentrations or pore diameter increased (Placenia et al., 1986).

Chen et al. (1991) developed a spray cabinet technique, and added a new dimension to the research of Reich (1985) and Placenia et al. (1986). In addition to microbial challenge, Chen et al. (1991) observed the effects of shock and vibration on the sterility of a package.

The objective of Chen's et al. (1991) research was to determine the microbial integrity of paper board laminate packages. The method assessed the effect of a simulated distribution test on package integrity. *Lactobacillus cellobiosus* ATCC 11739 at a 2.5 x 10^6 cells/mL concentration was used for immersion and aerosol tests. Two hundred juice packages were used in the study; 40 containers were tested as blank

controls, 120 packages were sprayed and/or immersion tested and 40 packages were biotested via inoculated spray (20 for a 60 minute exposure, and 20 for a 15 minute exposure).

Three pinhole diameter sizes were used, 5, 10, and 15 μm, and capped over an unspecified number of 30 mL glass vials. Test vials were sprayed with or immersed in *Lactobacilli* 2.5 x 10^6 CFU/ml for 15, 30, 60, and 90 minutes and incubated for 48 hours at 35-37°C. Microorganism growth within the containers was determined by carbon dioxide production in the headspace of the package. Ten and 15 μm size holes were detected after 90 minutes of immersion testing. 10-μm pinholes were detected after 15 minutes of spraying. Chen et al. (1991) concluded that the spray cabinet technique detected pinholes of 5-15 μm more easily than the immersion method. The difference between the spray cabinet technique and immersion method was significant ($P < 0.05$) for the 10 μm orifices (Chen et al., 1991).

Chen et al. (1991) employed abuse testing to physically test package integrity under simulated distribution conditions. A sequential test, consisting of a hydraulic shock test (flat drop), static compression, resonant vibration, hydraulic shock (end drop) and random vibration, was developed. Eighteen packages (15% of total test packages) showed obvious leakage after exposure to the abuse tests (Chen et al., 1991).

Blakistone et al. (1996) examined the critical defect dimension threshold using 10 and 20 μm internal diameter (ID) nickel microtubes that were 5 and 10 mm in length. The microtubes were sealed into plastic pouches and integrity tested by immersion into

Pseudomonas fragi at concentrations of 10^2 and 10^6 CFU/mL. Forty-four percent (44%) of the pouches tested positive for microbial ingress, indicating that the threshold defect value must be below 10 μm. Microbial concentration was found to be significant (P< .05) at 10^6 CFU/ml. The interaction of concentration, and time was also significant at 10^2 CFU/ml after 30 min exposure and 10^6 CFU/ml after 15 min. Channel length was not statistically significant. The difference of contamination rates between immersion and aerosol biotesting demonstrates the importance of test methods for package evaluation that simulate the actual conditions the package will be expected to tolerate during storage and distribution (Blakistone et al., 1996).

Keller et al. (1996) employed a bioaerosol method to determined the effect of test organism motility, concentration, aerosol exposure time, hole diameter and length on the sterility of flexible retortable pouches. Microtubes with 10 and 20 µm hole diameters of 5 and 10 mm lengths were used to simulate defects in 128 flexible pouches. An aerosol with a 2.68 µm mean particle size comprised of 10^2 or 10^6 CFU/ml source concentrations of motile or nonmotile *Pseudomonas fragi* TM 849 was introduced into a 119,911 cm^3 chamber for exposures of 15 or 30 minutes. Six pouches showed test organism growth after a 72-hour incubation period. Microbial ingress was significant (P < .05) for motile test organisms with source concentrations of 10^6 CFU/ml (Keller et al., 1996).

AEROSOL THEORY

The atmosphere in contact with the outside surface of a package may contain a variety of air borne contaminants, including toxin producing bacteria (Kamei et al., 1991). Such contaminants may be suspended and transported great distances within an aerosol (Bovallius et al., 1978). Once in contact with the package, characteristics of the bacteria such as motility, ability to multiply and multiplication rates are thought to increase the likelihood of ingress and contribute to post process contamination of a sterile package (Put and Warner, 1972; Dimmick et al., 1979). Therefore, aerosols are presented in this study in light of their abilities to pose as a transport mechanism for an airborne bacteria.

Definition of an Aerosol

Williams and Loyalka (1991) defined aerosols as a suspension of particles in a gas. Aerosols are typically characterized by large residence times, small sizes and large numbers. This results in large surface areas for interactions with the host medium, substantial effects on the transmission of light (i.e., scattering and absorption), and size ranges from 0.001 μm to 50 μm (Williams and Loyalka, 1991).

Heterodispersed, Polydispersed, and Monodispersed Aerosols

Aerosols are typically classified as heterodispersed, polydispersed, or monodispersed (Raabe, 1976). Heterodspersed aerosols consist of particles that vary widely in size as well as physical and chemical characteristics. Polydispersed implies

homogeneity of physical and chemical characteristics with widely different particle sizes and aerodynamic properties (Raabe, 1976). Monodispersed aerosols are homogeneous in the basic chemical and physical characteristics, including composition, physical density, and relative uniformity of particle size, and aerodynamic properties (Raabe, 1976).

Aerosol theory may be considered in terms of statistical mechanics, kinetic theory, continuous medium, fluid dynamics, and aerodynamics. The statistical mechanics perspective describes an aerosol as a large collection of molecular spheres in random motion around each other, but that may be in ordered motion overall (Reist, 1993). The kinetic theory highlights the non equilibrium gaseous portion of the aerosol. The continuous medium perspective compares aerosols to an interlocking syrup such as molasses or water. The fluid dynamics perspective consists of a study of the microscopic gas medium properties. The aerodynamics perspective identifies a gas in which the particles are suspended. The suspended particles are considered, from a molecular point of view, as a continuous medium (Reist, 1993).

Microorganisms suspended within an aerosol are called bioaerosols and illustrate the need for an eclectic perspective of aerosol theory. The primary mechanisms essential for the generation of bioaerosols are thought to occur naturally; fine comminution of infected solid materials, such as rain beating on rotting vegetation, and atomization of liquid suspensions, such as a cough or sneeze (Darlow, 1969). Both comminution and atomization produce aerosols with liquid, gas and solid phases.

Considerations for Aerosol Selection

Considerations important for determining the appropriate aerosol to use, as well as to describe the operation of the nebulizer are the output rate and concentration of usable aerosol, the volumetric rate of air, the evaporation losses of liquid which are independent of the viable aerosol, the droplet size distribution, the volume of liquid required for proper operation, and the maximum unattended operating time (Raabe, 1976). The nebulizer selected for this study was based on four additional criteria: the ability of the aerosol generator to consistently produce a particle size capable of transporting the test organism, absence of microbial injury to test organisms as a result of aerosol production, regulated flow rate, and production of relative humidity with low condensation.

Several assumptions must be accepted when using an aerosol. Such assumptions are that leak paths are short and changes in the gas take place instantaneously (Romarao and Tien, 1988; Simpson et al., 1989; Williams and Loyalka, 1991). The ratio of the chamber cross-sectional area to the orifice area is postulated to be very large. Despite the continuous change with time of flow rate, the acceleration of the fluid and the forces causing it are negligible (Williams and Loyalka, 1991). Coagulation and deposition may occur due to Brownian and gravitational motion of aerosol particles (Simpson et al., 1989). The size and shape of an aerosol particle determines the residence time of the aerosol, along with heat and mass transfers to the particles (Williams and Loyalka, 1991).

Aerosol Generators

There are three primary types of aerosol generators; compressed air nebulizers, ultrasonic nebulizers, and dust blowers (Raabe, 1976). Compression nebulizers generate droplets by shattering a liquid stream in fast moving air. Examples of compressed air generators are: DeVilbiss No. 40, Dautrebande D-30, Lauterbach nebulizer, collision nebulizer, Laskin nebulizer, Wright nebulizer, Lovelace nebulizer, Retec X-70/N nebulizer, Babington nebulizer, and the hydrosphere nebulizer. Ultrasonic nebulizers employ vibrations to initiate formation of droplets (Raabe, 1976). Dust blowers use air flow at low pressures to create airborne particles.

The bioaerosol used in this study was generated using a Wright compressed air nebulizer. The Wright nebulizer is characterized by a collection surface near the disintegration point of the nebulizer jet. This placement of the collection surface allows a higher concentration of useable aerosol within a certain size range than other nebulizers (Raabe, 1976). The outlet of the liquid feed tube is placed near the point of minimum static pressure of the air jet emitted from a small orifice (0.074 cm ID) so that liquid is drawn into the jet flow. The jet flow is directed into a small compartment, sprayed through a larger hole (0.16 cm ID) and impinged upon an open-sided flat collector over a short distance (0.116 cm). Only smaller droplets are able to make the turns, while the larger droplets collect on the baffle (Raabe, 1976). Large droplets deposited on the baffle are then forced to the edge by the airstream where they are extensively aerosolized. This causes the output of small droplets to be greatly enhanced (Raabe,

1976). The average particle diameter size produced by the Wright compressed air nebulizer is $\leq$ 10 μm.

The characteristics of the ultimate aerosol produced by the generator used depends not only upon the generation method, but on the physical and chemical nature of the source material (Raabe, 1976). Temperature and humidity conditions as well as treatment received also strongly influence the aerosol produced (Raabe, 1976).

Aerosol Particle Size

Great discrepancies exist within the literature in terms of which optimal aerosol particle size is required to effectively transfer a viable microorganism to create a bioaerosol. Reich (1985) used a nebulizer that produced particles ranging from 0.3 mm to 2.0 mm. Placenia et al. (1986) used a particle size range was between 0.3 μm and 10 μm. Chen et al. (1991) used 4 L per minute of sterile broth infected with *Lactobacilli*; the aerosol particle size was not specified.

Particle size distribution of atmospheric non-bioaerosols covers five orders of magnitude, from a radius of 0.001 μm to 100 μm and can be difficult to measure (Jaenicke, 1976). The particle size of naturally occurring bioaerosols averages $\leq$ 3.5 μm although aerosol sizes are known to change with environmental conditions (Bovallius et al., 1978; Adams et al., 1985). Dimmick et al.(1979) reported that as bioaerosol droplet/particle size was increased from 4 μm to 6 μm in diameter, bacterial cell division

occurred. A mean particle size of $\leq$ 3.5 μm reduces the possibility of cell division during aerosol residence and settling periods and permits greater control over test organism concentrations (Dimmick et al., 1979). Bausum et al. (1982) found aerosols with high concentrations of bacteria to have aerodynamic particle sizes ranging from 4.1 μm to 5.9 μm. The total percentage of particles found, ranging from μm and 5 μm in size, was between 39 % to 62%. The higher average particle size and lower bacterial counts found by Bausum et al. (1982) may be attributed to a relative humidity range of 5% to 32%, with an average of 18%, as opposed to the range of 32% to 70%, with an average of 55%, found in the earlier phase of their research. Aerosol strength was positively correlated with relative humidity (Bausum et al., 1982).

In this study, bioaerosol particle sizes with an average aerodynamic mean size of 2.68 μm were used. Aerosol particles of this size (i.e., fine particle sizes $\leq$ 3.5 μm) are relatively stable suspensions in a gaseous medium of liquid particles (Raabe, 1976). Fine particles have settling speeds that are influenced more by density and geometric diameter than by gravity (Raabe, 1976).

Aerosol Particle Behavior

Particles within an aerosol may coagulate. Coagulation describes the process of adhesion or fusion of two particles as a result of contact by touch or collision. Such contact occurs due to relative velocity differentials between the aerosol particles. Relative velocity results from: gravitational settling, turbulence, acoustic forces,

temperature changes, density gradients, light, and Brownian motion (Williams and Loyalka, 1991). Brownian motion is the irregular movement of small particles suspended in a fluid, due to the random impact of molecules on their surface, as a result of temperature fluxuations. Resting particles may be resuspended due to surface heating, depressurization of a containment area, or lift forces exerted by gas flows.

Simpson et al. (1989) showed that particles moved within a container from high temperature zones to low temperature zones, an effect called thermophoresis. Thermophoresis can be defined as the steady state under the influence of a temperature gradient where aerosol particles move with constant velocity towards lower temperatures. Hydrosols, which are particles suspended in a liquid, were found to act identical to aerosols (Simpson et al., 1989).

Mean Free Pathway

Fluid dynamics employs molecular theory to predict kinetic behavior of particles within a fluid medium. Models have been developed that consider energy balances and states of bulk fluid masses a macroscopic level. These models are constructed of statistical mechanics justified and correlated to experimental data usually consisting of observed properties of gases.

Aerosols are often composites of liquids, gases, and solids, of which the primary component exerts the greatest influence on the behavior characteristics of the particle. Because aerosol particles are continually undergoing molecular bombardment, their

pathways are curves rather than straight lines. A fundamental theory that models the physical and kinetic properties as well as the interaction of a particle during movement is brought to light in a discussion of the mean free pathway.

The mean free pathway is defined as the average distance a molecule will travel in a gas before it collides with another molecule (Campbell, 1973; Reist, 1984). This distance is related to molecular spacing but recognizes that all molecules are in a constant state of motion, thus more widely separated than if they were firmly bound to each other (Spurney, 1972; Reist, 1984).

The number of molecules struck per centimeter can be expressed as

$$\pi = \sigma^2 n \quad (1)$$

where σ is the molecular diameter (d_A), or the collision cross section

$$\sigma = \pi d^2 \quad (2)$$

where d is the diameter of the collision area. The collision frequency can be defined as

$$z = \sigma N C_{av} \quad (3)$$

where N is the number of molecules per unit volume, C_{av} is the distance a molecule travels per a unit time, and z is the number of collisions experienced (Campbell, 1973). Therefore, the mean free pathway can be calculated as follows,

$$MFP = \frac{1}{\sqrt{2\, n \pi \sigma^2}} \quad (4)$$

or

$$\lambda = \frac{C_{av}}{z} = \frac{1}{\sigma N} \quad (5)$$

where λ is the mean free pathway. It is important to note here that the above equations have not incorporated considerations for particle behavior in viscous materials at solid interfaces.

Bioaerosols

Bioaerosols are somewhat different from non-bioaerosols in that the number of *living* particles per unit volume are more prone to non-uniform coagulation (Reist, 1993). The mean free path of the molecules is replaced by the apparent free path of the aerosol particulate. The apparent free path is the average distance over which the particulate loses all correlation with the initial direction of its motion (Fuchs, 1972; Teltsch et al., 1980). The mean particulate size increases and had an increase in flow rate as well (Fuchs, 1972).

Colliods versus Aerosols

The literature depicts significant disparities between immersion and aerosol biotest results. Much of the disparity rests in the fundamental differences between the

mechanism of microorganism transport within each test method. For the purpose of this comparison, the definition of a colloid is restricted to a particle in a liquid, and an aerosol is a particle in a gas.

Some general differences between a colloid and an aerosol are the influence of viscosity on particle transport, buoyancy effects, refractive index and optical detection, ion concentration, biological activity, and evaporation and condensation.

Influence of Viscosity on Particle Transport

High viscosity liquid mediums reduce the transport potential for colloid particles compared to particles of the same size in aerosols. Expressions such as "slip" and mean free pathway (MFP), used to describe and quantify particle motions within aerosols, increase the disparity between transport potentials (Hunter, 1985; Cooper, 1989). The degree of difference between the transport potential for each method is determined somewhat by the characteristics of the particle. Common particle categories consist of rigid spherical particles and anisotropic particles. Rigid spherical particles translate and rotate independently, in a magnitude equivalent to imposed force (Russel et al., 1989). The rotational and translational motions of anisotropic particles are coupled (Russel et al., 1989). Principally, this relationship and disparity between transport potentials for rigid spherical and anisotropic particles have been characterized in terms of particle velocity for pair interactions between torque-free spheres

$$U = \sum_{j=1}^{2} \omega_{ij} \cdot F_j \qquad (6)$$

where *i* represent particles 1 and 2, ω_{ij} is the mobility tensors separation dependent response of the *i*th and *j*th spheres and U is the resultant velocity.

Buoyancy-induced Flows and Transports

Effects resulting from buoyancy-induced flow and transport reduce the migration velocity of colloidal particles within a liquid compared to that of an aerosol (Cooper, 1989). Much of the buoyancy effect can be attributed to the particle size distribution within the liquid suspension and the changing body force relationship between the local density and gravity. The net effect of this body or buoyancy force can be expressed as

$$B = g(\rho - \rho_r) \qquad (7)$$

where B is the buoyancy force, g is the local body force due to gravity, ρ is the density and ρ_r is the reference density (Gebhart et al., 1988). Changes in particle size may result in solution density changes.

Due to the potentially significant influence of particle size on the properties of the solution or test fluid, it is important to use particle-sizing techniques to determine an "equivalent" sphere size for the calculation of settling rates or vertical velocities. Turbulence generated within the system near the wall region may significantly influence buoyancy related effects for a liquid and an aerosol due to particle stream wise flow movement and vertical velocity changes. The stream wise component, or direction of flow, for particles within a liquid tends to be less than the local mean velocity, while the

vertical component tends to be tends to be greater (Streeter, 1961; Niño and Garcia, 1996). Most of these effects are realized during entrainment (Streeter, 1961). Detailed methodologies for particle size analysis and effects resulting from buoyancy-induced flows and transport can be found in Gebhart et al. (1988).

Refractive Index of Aerosols

Aerosol particles are often distributed with respect to both size and chemical composition (Friedlander, 1970). Such distribution produces a substantial effect on the transmission of light in terms of scattering and absorption (Kerner et al., 1972; Williams and Loyalka, 1991). High refractive indexes, such as those produced by large particle sizes in a liquid, result in reduced contrast between the colloidal particle and its medium when compared to an aerosol particle (Cooper, 1989).

Knowledge of particle size and distribution facilitates the reproducibility of aerosols for package integrity testing via bioaerosols. Particle sizes, as well as other important characteristics that effect particle transport such as the coagulation rate, can be determined for polydispersed and monodispersed aerosols by using the diffusion method of particle size determination in combination with refractive index measurements (Fuchs, 1972).

Ion Concentration

Liquids generally contain higher concentrations of ions than aerosols do. As a

result, electrical double-layers can form around charged particles in liquids, lending behaviors difficult to model, particularly for particle to particle and surface interactions (Cooper, 1989).

Biological Activity

Biological activity within an aerosol is typically measured using filtration methods. The filtration process is inherently an unsteady-state process. Filtration is the capture of particles on a filter (Cooper, 1989). The accumulation of deposited particles on the filter continuously changes the structure of the filter media (Romarao and Tien, 1988). The presence of particles on a filter not only affects the collection efficiency of the filter, but also contributes to a pressure drop across the filter. Pressure drops or gradients develop due to increased drag resistance of the liquid or air flow (Ramarao and Tien, 1988). Pressure gradients may reduce the efficiency of the filter and permit passage of microorganisms as well as create problems for liquid systems such as inaccurate biological counts, and loss of sterility of downstream systems (Cooper,1989).

Evaporation and Condensation

Evaporation and condensation can change the nature of, and even destroy an aerosol and the suspended particles. Condensation results from the aggregation of particles suspended in aerosolled liquid. As the aerosol particle size increases, the settling velocity increases. Similar processes that may occur within a fluid are solvation

and precipitation (Cooper, 1989).

THRESHOLD LEAK SIZE

Definition of a Leak

Guazzo (1994) defined leakage as the sum of convection and diffusion forces. The driving force that contributes to a flow rate as the result of convection across the leak is the pressure differential (Board, 1980, Guazzo, 1994). Anderson (1989) defined leaks as actual through-wall discontinuity or passage through which a fluid flows or permeates.

Anderson (1989) identified four types of flow through a leak based on the volume of capillary flow, molecular flow ($\leq 10^{-6}$ atm cm^3/s), transitional flow (10^{-4} to 10^{-6} atm cm^3/s), laminar flow (10^{-2} to 10^{-6} atm cm^3/s), and turbulent flow ($\geq 10^{-2}$ atm cm^3/s).

Two types of capillary effects are thought to occur within the defined flow ranges outlined above; capillary effects of the first kind, and capillary effects of the second kind (Fuchs, 1972). Capillary effects of the first kind consist of increased vapor pressure over a convex surface. Capillary effects of the second kind include the dependence of the pressure inside the droplet on its size and density (Fuchs, 1972). The capillary effects of the second kind are the effects of interest in this study.

Placencia and Peeler (1990) found that some manufacturers consider pore/leaker size itself to be an indicator of a packaging material's integrity. Therefore, it is

important to determine the relationship between hole/leaker size and biotest results.

Leak Studies

Packaging researchers consider leakers to be the primary source of post process contamination (Anema and Schram, 1980; Rey et al., 1982; Placencia et al., 1988; Kamei et al., 1991). Packages with vacuums, or that maintain constant pressure differences between their interior and exterior, such as cans after retorting, may be at greater risks for post-process contamination by leakers than those at atmospheric pressures (Put et al., 1980; McEldowney and Fletcher, 1990a). The risks for such packages result from the slow equilbration of pressure differentials during cooling that provide opportunity for microbial ingress if a leaker is present (Arndt, 1992).

Relationships between vacuums in cans with defects and loss of sterility as a result of microbial ingress into the package are widely documented (Put and Warner, 1972; Put et al., 1980). However, McEldowney and Fletcher (1990a) found that bacterial ingress into a package was not proportional to vacuum forces, suggesting that packages with large vacuums may be at no greater risk than those with low internal vacuums. McEldowney and Fletcher (1990b) found several other factors such as vacuum, viscosity of the contents, leakage pathway size and shape, bacterial morphology, concentration and population composition to be key influences for can spoilage. Likewise, Put and Warner (1972) reported that leakage was largely a function of an inverse relationship between bacterial cell size and the package content's viscosity, and was proportional to leakage

channel size in the presence of a viscous medium. Put et al. (1980) attributed permanent leaks in cans to: a) improper can construction, b) poor quality compounds, and c) improper seam tightness or side seam soldering.

The diameter, profile, shape and length of the leak pathway may have a measurable effect on capillary action within the passage way of the double seam of metal cans. Gnanasekharan and Floros (1994) suggested that factors such as length to diameter ratio of the leak, the internal geometry of the leak (straight/tortuous or smooth/rough) and the pressure differential across the leak interface, must be considered. Jarrosson (1992) and Keller et al. (1996) found no significant relationship between leaker length and diameter, although leak diameter itself was significant. Reichs (1985) suggested that the probability of detecting a microhole (i.e., leaker), via microbial ingress, increased as pore or hole diameter increased.

Howard and Duberstein (1980) found that under specific conditions certain types of water borne bacteria penetrated 0.2 μm membrane filters and therefore speculated that the minimum hole size critical to sterility maintenance and integrity of the package (i.e., the threshold leak size) is between 0.2 μm and 0.4 μm. This range was selected based on the size of membrane filters used routinely for aseptic packaging applications with little significant microbial contamination. Lampi (1980) showed that bacterial penetration via holes of less than 10 μm was unlikely. Lake et al. (1985), during an extensive four-year study, found that leaks must be considerably larger than 1 μm for bacterial penetration to occur. Gilchrist et al. (1985) showed that bacterial contamination of cans from cooling

water requires pinholes larger than 5 μm. McEldowney and Fletcher (1990a,b) found that holes of 1 μm permitted microbial entry under certain conditions. Chen et al. (1991) reported that 5 μm pin holes allowed microbial aerosol penetration. Jarrosson (1992) found that a 20 μm diameter hole with a 5 mm channel length permitted microbiological contamination in Meal Ready to Eat (MRE) pouches. Much of the discrepancy over the threshold leak size in the aforementioned studies rest in the inability to manufacture and maintain the integrity of the leak size during retorting and/or experimentation. This is especially true for small hole diameters, those with 10-20 μm internal diameters (Gnanasekharan and Floros, 1994; Jarrosson, 1992).

Reich (1985) suggests that any microbial challenge test used should not be too severe, with respect to the level of CFU/ml exposure, but rigorous enough to yield results with a comfortable safety factor. He suggests that bioaerosol biotesting be used in place of immersion biotesting.

Immersion biotests typically use concentrations as high as 10^9 CFUs/ml. Reich (1985) suggested that bioaerosol concentrations of $> 10^4$ cells/cm^2 are far in excess of what might realistically be found in product-use conditions. Further, Reich (1985) suggested that use of bioaerosols for biotesting may create an environment that more closely imitates that of storage and distribution conditions. Therefore, integrity testing using bioaerosols may yield information that more accurately characterizes the ability of a package to maintain sterility.

A disadvantage of biotesting is that test results are not immediate. Biotesting

requires days rather than seconds or minutes to receive the results. Immersion biotesting using contaminated cooling water in a still vertical retort found leakers down to 20 μm, while helium tests have identified leakers down to 3 μm (Gilchrist et al., 1989). An effort has been made by some scientists, however, to establish correlations between biotest methods and the more rapid chemical/physical test methods (Placencia and Peeler, 1990).

Microorganisms as Leak Indicators

Microorganisms have been used by many researchers for leak/integrity testing via immersion and bioaerosol biochallenge. Put et al. (1980) used a suspension of *Clostridium intermedius* to biotest glass jars. Effects of organism attributes, such as motility versus non motility, on post process contamination of the jars were not considered in that experiment. Reich (1985) used a bacterial spore suspension of *Bacillus subtilis* ATCC 9372 for his biotesting experiment. A bacterial spore suspension of *Bacillus subtilis* var. *niger* was again used by Placencia et al. (1986). Davidson and Pflug (1981) recovered mesophilic, aerobic, nonsporeforming microorganisms and mixed cultures containing aerobic and anaerobic sporeformers from spoiled canned foods retrieved at the retail level.

McEldowney and Fletcher, (1990b) reported that, in general, *Pseudomonas sp.*, did not initiate leakage at a rate faster than nonmotile strains. They also found that high cell concentrations of 5.4×10^{10} cells/ml show less leak initiation than cells of all other

concentrations (McEldowney and Fletcher, 1990b). Put et al. (1980) suggest that under static conditions, the frequency of reinfection was enhanced primarily by concentration and secondarily as a result of the motility of the infiltrating bacteria. Guazzo (1994) advised that size, motility, and viability within the test environment of the microorganism are all important selection criteria for test microorganisms.

Motile Microorganisms

Motile organisms display a variety of shapes via expansion and contraction, as well as modes of locomotion, thereby allowing the organism to enter areas not accessible to nonmotile organisms (Lee et al., 1993). Such characteristics may not be exhibited by nonmotile organisms.

Organism motility may be explained in part by chemotaxis. Chemotaxis may be described as the ability of cells to detect concentration gradients of certain chemicals in their environment and to bias their movement based on that gradient (Lauffenburger and Calcagno, 1983). Positive chemotaxis occurs when organism movement is biased toward a high concentration of attractants, where as negative chemotaxis occurs when the movement of the organism is biased toward a lower concentration of repellents (Lauffenburger and Calcagno, 1983).

The role of chemotaxis, or motility in general, in microbial populations is not well understood (Lauffenburger and Calcagno, 1983). A comprehensive theory to

predict the effects of competition between two bacterial populations with differing growth, as to the kinetic and motility properties, determination of a population supremacy over a competing population, or potential for co-existence is not available (Lauffenburger and Calcagno, 1983). Three possible non-trivial steady-state configurations or possibilities that may be exhibited by competing microorganisms are: when species one survives and species two dies out, when species two survives and species one dies out, and when species one and two coexist (Lauffenburger and Calcagno, 1983).

FLUID FLOW THEORY

Many theories concerning the flow of liquids through a capillary/defect are present in the literature. Various equations incorporate the specific dimensions of the flow pathway, usually in terms of capillary length and internal diameter (ID). Conditions such as temperature, pressure, and fluid properties (i.e., viscosity and density) have received much consideration and have been incorporated in various models.

Fluid flow theory, or fluid mechanics, is the study of the effects of fluids in motion or at rest on boundaries of solid surfaces and/or other fluids (White, 1986a). Fluid mechanics can be described using either eulerian and lagrangian methods. Eulerian methods define the fluid flow field by determination of the pressure field $p(x, y, z, t)$ of the flow pattern (White, 1986a).

The lagrangian method describes the movement of a particle through a fluid during flow, and the motion of isolated fluid droplets (White, 1986a). Largrangian descriptions of fluids permit considerations such as the velocity field functions (pressure, density, and temperature), displacement vectors, acceleration vectors, local angular velocity vectors (internal energy, enthalpy, entropy, specific heat), convective acceleration, transport properties (i.e., coefficient of viscosity, thermal conductivity), and volume fluxuation through a surface (White, 1986a).

Definition of a Fluid

Fluids may be defined as materials that present no resistance to shear deformation (Campbell, 1973). Shear deformation may occur, however, during continuous relative motion between layers of the fluid material or at the fluid solid interface. Such stress-strain rate relationships, or viscosity, can be used as a measure of the fluidity of the material. A low absolute viscosity is characteristic of extreme fluidity, whereas high absolute viscosities indicate the absence of fluidity.

In general terms, fluids can be divided into two categories, newtonian and nonnewtonian. The general behaviors are named after Sir Isaac Newton, who first documented the resistance law in 1687 (White, 1986a). Newtonian fluids exhibit linear, primary thermodynamic characteristics with respect to viscosity. The properties of the fluid vary with temperature and pressure (White, 1986a).

Nonnewtonian fluids do not exhibit linear relationships with respect to

temperature and pressure. Distinct categories under the heading of nonnewtonian fluids include dilatant (shear-thickening), plastic (strong thinning effect), rheopectic (gradually increasing shear stress), and thixotropic (gradually decreasing shear stress) fluids. Plastic fluids may have a pseudoplastic quality, or shear-thinning, where the fluid exhibits decreasing resistance with increasing stress (White, 1986a).

Fluid Viscosity

Viscosity is considered a secondary thermodynamic variable in that thermodynamics are generally used to characterize the effects of heat on a static system. Fluids are generally in variable motion and exhibit constantly changing properties. Examples of primary thermodynamic variables are quantities such as pressure, temperature and density.

Viscosity is used to characterize the behavior of a specific fluid-mechanical property. It is the measure of the resistance of fluids to deformation, change or steady flow (White, 1986a; ASTM D-445, 1996; ASTM D-446, 1996). Such resistance is generally reported in dyne-seconds per cm^2. A kinematic viscosity is the ratio of viscosity to density and is reported in stokes, a c.g.s. unit of kinematic viscosity. Poise is a c.g.s. unit of absolute viscosity. The name "Poise" was adopted from the name of J. L. Poiseuille, whom established the pressure-drop law in 1840. Poiseuille's equation that characterizes fluid flow through a vertical tube is as follows

$$v = \frac{\pi p r^4}{8 l \eta} \quad (8)$$

where l is the length of the tube, r is the tube radius, p is the difference in pressure at the tube ends, η is the coefficient of viscosity and v is the volume of fluid (Weast and Astle, 1980).

Poiseuille's equation can be modified to consider laminar flow through a tube in a horizontal position as follows

$$\Delta p = \frac{8 \mu L Q}{\pi R^4} \quad (9)$$

where L is the entrance length, and Q is the flow volume (White, 1986b).

Methods for Measuring Viscosity

There are several methods available by which the viscosity of a fluid can be quantified. The following methods and equations focus on viscosity with respect to flow efflux times and volumes observed and measured using glass Cannon-Fenske and Cannon-Ubbelohde semi-micro capillary kinematic viscometers.

Glass capillary viscomters must be calibrated prior to use. The purpose of calibration is to provide a baseline under experimental conditions such as temperature and relative atmospheric pressure for a standard fluid such as water. Calibrations can be calculated using the following methods

$$C_1 = \frac{(t_2 \times C_2)}{t_1} \quad \textbf{(10)}$$

where C_1 is the calibration constant of the viscometer being calibrated and is dependent on the gravitational acceleration at the place of calibration, t_1 is the flow time to the nearest 0.1 s, C_2 is the constant of the calibrated viscometer, and t_2 is the flow time to the nearest 0.1 s in the calibrated viscometer (ASTM D-445, 1996; ASTM D-446, 1996). A correction can be applied were the acceleration of gravity exceeds 0.1%,

$$C_2 = (g_1 / g_2) \times C_1 \quad \textbf{(11)}$$

where g_1 and g_2 are the acceleration of gravity (ASTM D-446, 1996).

Kinematic viscosity can be calculated as a function of the viscometer dimensions

$$v = (10^6 \pi g D^4 H t / 128 V L) - E / t^2 \quad \textbf{(12)}$$

where v is the kinematic viscosity in mm^2/s, g is the acceleration due to gravity in m/s^2, D is the diameter of the capillary, L is the length of the capillary, H is the average distance between the upper and lower reference lines, V is the volume (m^3) of liquids that pass through the capillary per a given flow time t, and E is the kinetic energy correction factor (ASTM D-446, 1996). To negate the effect of the kinetic energy factor, E/t^2, a viscometer of sufficient capillary diameter and length should be selected so that the flow time is greater than 200 s (ASTM D-445, 1996; ASTM D-446, 1996). An arbitrary maximum flow time of 1000 s is recommended, although longer times can be used.

Surface Tension

Surface tension refers to the work done to stretch the surface of a fluid (Woodruff, 1973). The calculated value for viscosity can be corrected for the effects of fluid surface tension and density. The corrected value can be expressed as follows

$$C_2 = C_1[(1 + (2/gh)\cdot(1/r_u - 1/r_l)\cdot(\gamma_1/\rho_1 - \gamma_2/\rho_2)] \quad \textbf{(13)}$$

where g is the acceleration of gravity, h is the driving head, r_u is the average radius of the upper meniscus, r_l is the average radius of the lower meniscus, γ is the surface tension (N/m), and ρ is the density (kg/m^3) (ASTM D-446, 1996).

Two fluids, either liquid or gas, in contact with each other that are not allowed to expand, will form an interface between themselves. Such interfaces comprise several layers of molecules of various packing densities. More closely packed molecules found deep within the liquid repel each other, whereas loosely packed molecules at the surface attract each other (Caskey and Barlage, 1971; Somasundaran et al., 1974. White, 1986a). These complex interfacial regions between the fluids are described in fluid mechanics as surface tension.

Nine methods are commonly employed to measure the surface tension of fluids in air, vacuum or immersed in a liquid: capillary height, drop weight, Wilhelmy plate, the Du Noüy ring, Sessile and Pendent drop, maximum pull on a rod, maximum bubble pressure, spinning drop, and vibrating jet (Harkins and Brown, 1919; Washburn, 1921; Bartell and Whitney, 1932; Bartell and Walton, 1934; Harkins and Anderson, 1937;

Addison, 1943; Burick, 1950; Defay and Hommelen, 1958; Ross and Haak, 1958; Defay and Hommelen, 1959; Lucassen-Reynders, 1963; Butler and Bloom, 1966; Princen et al., 1967; Paddy, 1972; Paddy et al., 1975; Rotenburg et al., 1983; Lunkenheimer et al., 1984; Mysels, 1986; Oss, 1994). All these methods of measuring surface and interfacial tensions were founded upon the equation introduced by Laplace:

$$\Delta P = \sigma(1/R_1 + 1/R_2) \quad \textbf{(14)}$$

where the Laplace pressure difference, Δp equals the product of the surface tension σ with consideration of the fractional effects generated by the radii of curvature R_1 and R_2 (Harkins and Brown, 1919; Paddy, 1969; Oss, 1994). The method used in this study was the Du Noüy ring method.

The Du Noüy Ring Method

Precise surface tension measurements can be made with the platinum Du Noüy ring. This method takes advantage of the fact that the adhesion of a liquid to the platinum ring is greater than the cohesive forces of the liquid to itself. The platinum ring is balanced on the torsion arm of a surface tension meter. The is immersed 0.3 cm below the fluid surface. The force required to break the ring free of the fluid surface, or the force required to overcome the cohesion of the liquid (2σ) is the apparent surface tension. The surface tension can be calculated by

$$\sigma = \frac{mg}{4\pi r} F \qquad (15)$$

where *mg* is the force applied from the torsion arm to the ring of radius r. The relationship may also be written as

$$S = P \times F \qquad (16)$$

where S and P are the absolute and apparent values respectively, for surface tension. The correction factor F can be defined by

$$(F - a)^2 = \frac{4b}{(\pi R)^2} \times \frac{P}{(D - d)} + K \qquad (17)$$

where R is the radius of the platinum ring, r is the radius of the wire of the ring, D is the density of the lower phase, d is the density of the upper phase (for two phase systems), K = 0.04534 - 1.679 r/R, C is the circumference of the ring, a = 0.725, and b = 0.0009075. The correction factor accounts for the weight of the fluid that remains on the ring after detachment (Harkins and Brown, 1919).

REFERENCES

Adams, A. J., D. E. Wennerstrom and M. K. Mazumder. 1985. Use of bacteria as model nonspherical aerosol particles. J. Aerosol Sci. 16(3):193-200.

Addison, C. C. 1943. The properties of freshly formed surfaces: Part I. The application of the vibrating-jet technique to surface tension measurements of mobile liquids. J. Chem. Soc. 535-541.

Anderson, G.L. 1989. Leak testing. p. 50-57. *In* 9th ed. Nondestructive Evaluation and Quality Control: Metals Handbook. AOAC, Arlington, VA.

Anema, P. J. and B. L. Schram. 1980. Prevention of post process contamination of semi-rigid and flexible containers. J. Food. Prot. 43(6):461-464.

Alves, G. E. and D. F. Boucher. 1963. Fluid and particle mechanics. p. 9-10. *In* R. H. Perry, C. H. Chilton and S. D. Kirpatrick (ed). Chemical Engineering Handbook. McGraw Hill, New York.

Arndt, G.W. 1992. Examination of flexible and semirigid containers for integrity. p.322-368. *In* 7th ed. Bacteriological Analytical Manual. AOAC, Arlington, VA.

ASTM D-445. 1996. Standard test method for kinematic viscometers of transparent and opaque liquids (the calculation of dynamic viscosity). p. 169-176. *In* Am. Soc. For Testing and Materials. Philadelphia, PA.

ASTM D-446. 1996. Standard specifications and operating instructions for glass capillary kinematic viscometers. p. 177-199. *In* Am. Soc. For Testing and Materials. Philadelphia, PA.

Axelson, L. and S. Calvin. 1991. Aseptic integrity and microhole determination of packages by gas leakage detection. Packaging Technol. and Sci. 4:9-20.

Bartell, F. E. and C. E. Whitney. 1932. Adhesion tension. J. Phys. Chem. 36:3115-3126.

Bartell, F. E. and C. W. Walton, Jr. 1934. Alteration of the surface properties of stibnite as revealed by adhesion tension studies. J. Phys. Chem. 38:503-511.

Bashford, T. E. 1947. Infected cooling water and its effect on spoilage in canned foods.

J. Appl. Bacteriol. 10:46-49.

Bausum, H. T., S. A. Schaub, K. F. Kenyon and M. J. Small. 1982. Comparison of coliphage and bacterial aerosols at a wastewater spray irrigation site. Appl. Environ. Microbiol. 43:28-38.

Blakistone, B. A., S. W. Keller, J. E. Marcy, G. H. Lacy, C. R. Hackney and W. H. Carter, Jr. 1996. Contamination of flexible pouches challenged by immersion biotesting. J. Food Prot. 59(7):764-767.

Board, R. G. 1980. The avian eggshell; a resistance network. J. Appl. Bacteriol. 48:303-313.

Bovallius, A., B. Bucht, R. Roffey and P. Anas. 1978. Long-range air transmission of bacteria. Appl. Environ. Microbiol. 35(6):1231-1232.

Brody, A. L. 1996. Integrating aseptic and modified atmosphere packaging to fulfill a vision of tomorrow. Food. Technol. 28(4):56-66.

Bryant, M. 1988. Packaging failures: Quality in design doesn't end with the finished product. Med. Dev. & Diag. Ind. 10(8):30-33.

Burick, E. J. 1950. The rate of surface tension lowering and its role in foaming. J. Colloid Sci. 5:421-436.

Butler, J. N. and B. H. Bloom. 1966. A curve-fitting method for calculating interfacial tension from the shape of a sessile drop. Surf. Sci. 4:1-17.

Campbell, R.G. 1973. Introduction. p. 1-44. *In* Foundations of Fluid Flow Theory. Addison-Wesley Publishing Company, Reading, MA.

Caskey, J. A. and Barlage, W. B. 1971. An improved technique for determining dynamic surface tension of water and surfactant solutions. J. Colloid Interface Sci. 35: 46-52.

Chen, C., B. Harte, C. Lai, J. Pestka and D. Henyon. 1991. Assessment of package integrity using a spray cabinet technique. J. Food. Prot. 54(8):643-647.

Cooper, D. W. 1989. Monitoring containment particles in gases and liquids: A review. p. 1-33 *In* K.L. Mittal (ed). Particles in Gases and Liquids 1: Detection,

Characterization and Control. Plenum Press, New York.

Darlow, H. M. 1969. Safety in the microbiological laboratory. p. 220-245. *In* Norris, J.R. and D. W. Ribbons (ed). Methods in Microbiology. Vol. 1. Academic Press, New York.

Davidson, P. M. and I. J. Pflug. 1981. Leakage potential of swelled cans of low-acid foods collected from supermarkets. J. Food. Prot. 44(9):692-695.

Defay, R. and J. R. Hommelen. 1958. Measurements of dynamic surface tensions of aqueous solutions by the oscillating jet method. J. Colloid Sci. 13:553-564.

Defay, R. and J. R. Hommelen. 1959. Measurement of dynamic surface tensions of aqueous solutions by the falling meniscus method. J. Colloid Sci. 14:401-410.

Dimmick, R. L., H. Wolochow and M. A. Chatigny. 1979. Evidence for more than one division of bacteria within airborne particles. Appl. Environ. Microbiol. 38(4): 642-643.

Folinazzo, J. F., J. J. Kiloran and D. T. Maunder. 1968. Bio-test method for determining integrity of flexible packages of shelf-stable foods. Food. Technol. 22:615-618.

Friedlander, S. K. 1970. The characterization of aerosols distributed with respect to size and chemical composition. J. Aerosol Sci. 1:295-307.

Fuchs, N. A. 1964. Classification of aerosols: size and shape of aerosol particles. Chapter 4. *In* The Mechanics of Aerosols. Macmillan Co., London.

Fuchs, N. A. 1972. Some new methods and devices for aerosol studies. p.200-211. *In* T.T. Mercerm P.E. Morrow and W. Stöber (ed.). Assessment of Airborne Particles, Fundamentals, Applications, and Implications to inhalation Toxicity. Charles C. Thomas Publisher, Springfield, IL.

Gebhart, B., J. Yogesh, M. Roop and B. Sammakia. 1988. General Formulation of Buoyancy-Induced Flows. Chapter 2. *In* Buoyancy-Induced Flows and Transport. Hemisphere Publishing Corp., New York.

Gilchrist, J. E., B. S. Dhierdra, D. C. Radle and R. W. Dickerson. 1989. Leak detection in flexible retort pouches. J. Food. Prot. 52(6):412-415.

Gilchrist, J. E., U. S. Rhea, R. W. Dickerson and J. E. Campbell. 1985. Helium leak

test for micron-sized holes in canned foods. J. Food Prot. 48(10):856-860.

Gnanasekharan, V. and J. D. Floros. 1994. Package integrity evaluation: Criteria for selecting a method. Part I. Pack. Technol. and Eng. 3(6):67-72.

Guazzo, D. M. 1994. Package Integrity Testing. p. 247-276. *In* 2nd ed, M. J. Akers (ed). Parenternal Quality Control. Mercel Dekker, New York.

Harkins, W. D. and T. F. I. Anderson. 1937. A simple accurate film balance of the vertical type for biological and chemical work, and a theoretical and experimental comparison with the horizontal type II. Tight packing of a monolayer by ions. J. Am. Chem. Soc. 59:2189-2197.

Harkins, W. D. and F. E. Brown. 1919. The determination of surface tension (free surface energy), and the weight of falling drops: The surface tension of water and benzene by the capillary-height method. J. Am. Chem. Soc. 41:499-524.

Howard, G. and R. Duberstein. 1980. A case of penetration of 0.2 μm rated membrane filters by bacteria. J. Parental Drug Assoc. 34(2): 95-102.

Hunter, R. J. 1985. Rheological and sedimentation behavior of strongly interacting colloidal systems. p. 184-202. *In* H. F. Eicke (ed). Modern Trends of Colloid Science in Chemistry and Biology. Birkhäuser Verlag, Boston.

Jaenicke, R. 1976. Methods for Determination of Aerosol Properties. p. 469-475. *In* Fine Particles, Aerosol Generation, Measurement, Sampling, and Analysis. Academic Press, Inc. New York.

Jarrosson, B. P. 1992. Closure Integrity of Heat Sealed Aseptic Packaging Using Scanning Acoustic Microscopy. Virginia Polytechnic Institute and State University, Department of Food Science and Technology, M.S. Thesis.

Kamei, T., J. Sato, A. Natsume and K. Noda. 1991. Microbiological quality of aseptic packaging and the effect of pinholes on sterility of aseptic products. Pack. Technol. and Sci. 4:185-193.

Keller, S. W., J. E. Marcy, B. A. Blakistone, G. H. Lacy, C. R. Hackney and W. H. Carter, Jr. 1996. Bioaerosol exposure method for package integrity testing. J. Food. Prot. 59(7): 768-771.

Kerner, M., E. Matijevíc, G. Nicolaon and D. D. Cooke. 1972. Preparation of liquid aerosols and their particle size analysis by light scattering. p.153-168. *In* T. T.

Mercerm, P. E. Morrow and W. Stöber (ed). Assessment of Airborne Particles, Fundamentals, Applications, and Implications to Inhalation Toxicity. Charles C. Thomas Publisher, Springfield, IL.

Lake, D. E., R. R. Graves, R. S. Lesniewski and J. E. Anderson. 1985. Post-processing spoilage of low-acid canned foods by mesophilic anaerobic sporeformers. J. Food Prot. 48(3):221-226.

Lampi, R. A. 1980. Retort pouch: The development of a basic packaging concept in today's high technology era. J. Food Process Eng. 4:1-18.

Lauffenburger, D. and P. B. Calcagno. 1983. Competition between two microbial populations in a nonmixed environment: Effect of cell random motility. Biotechnol. Bioeng. 25:2103-2125.

Lee, J., I. Akira, J. Theroit and K. Jacobson. 1993. Principles of locomotion for simple-shaped cells. Nature. 362:167-171.

Lenhart, S. W., S. A. Olenchock and E. C. Cole. 1982. Viable sampling for airborne bacteria in a poultry processing plant. J. Toxicol. Environ. Health. 10:613-619.

Lucassen-Reynders, E. H. 1963. Contact angle and adsorption on solids. J. Phys. Chem. 67:969-972.

Lunkenheimer, K., C. Hartenstein, R. Miller and K. D. Wantke. 1984. Investigations of the methods of the radically oscillating bubble. Colloids and Surfaces. 8:271-288.

Matty, J. T., J. A. Stevenson and S. A. Stanton. 1991. Packaging for the 90's: Convenience versus shelf stability or seal peelability versus seal durability. Food Pack. Technol. 4(4): 74-90.

McEldowney, S. and M. Fletcher. 1990a. A model system for the study of food container leakage. J. Appl. Bacteriol. 69:206-210.

McEldowney, S. and M. Fletcher. 1990b. The effect of physical and microbiological factors on food container leakage. J. Appl. Bacteriol. 69:190-205.

Michels, M. J. M. and B. L. Schram. 1979. Effect of handling procedures on the post process contamination of retort packages. J. Appl. Bacteriol. 47:105-111.

Mysels, K. J. 1986. Improvements in the maximum bubble-pressure method of measuring surface tension. Langmuir J. 2:428-432.

Nichols, P. 1989. Container integrity of heat sterilized food. PIRA packaging Division, Slough, England.

Niño, Y. and M. H. Garcia. 1996. Experiments on particle-turbulence interactions in the near-wall region of an open channel flow: Implications for sediment transport. J. Fluid Mech. 326:285-319.

Noone, W. J. 1996a. Packaging inspection systems making their presence felt. Pack. Technol. and Eng. 5(4):27-35.

Noone, W. J. 1996b. Closures: Opportunities knock. Pack. Technol. and Eng. 5(7):21-27.

Oss, C. J. 1994. Contact angle and surface and interfacial tension determination. p. 89-127. *In* Interfacial Forces in Aqueous Media. Marcel Dekker, Inc., New York.

Paddy, J. F. 1969. Surface tension: Part 1. Theory of surface tension, Part 2. The measurement of surface tension. Surf. Colloid Sci. 1:39-251.

Paddy, J.F. 1972. Tables of profiles of axisymmetric menisci. J. Electroanal. Chem. Interfacial Electrochem. 37:313-316.

Paddy, J. F., A. R. Pitt and R. M. Pashley. 1975. Menisci at a free liquid surface tension from the maximum pull on a rod. J. Chem. Soc. 1(71):1919-1931.

Pflug, I. J., P. M. Davidson and R. G. Holcomd. 1981. Incidence of canned food spoilage at the retail level. J. Food Prot. 44(9):682-685.

Placencia, A. M., G. S. Oxborrow and J. T. Peeler. 1986. Package integrity methodology for testing the biobarrier of porous packaging. Part II: FDA exposure-chamber method. Med. Dev. and Diag. Ind. 8(4) 46-53.

Placencia, A. M., M. L. Arin, J. T. Peeler and G. S. Oborrow. 1988. Physical tests are not enough. Med. Dev. and Diag. Ind. 10(9): 72, 74-78.

Placencia, A. M. and J. T. Peeler. 1990. Relationship of bubble point to microbial penetration in medical packaging. TAPPI J. 73:255-257.

Princen, H. M., I. Y. Z. Zia and S. G. Mason. 1967. Measurement of interfacial tension

from the shape of a rotating drop. J. Colloid Interface Sci. 23-99-107.

Put, H. M. C. and W. R. Warner. 1972. The Mechanism of microbiological leaker spoilage of canned foods: a review. J. Appl. Bacteriol. 35:7-27.

Put, H. M. C., H. T. Witvoet and W. R. Warner. 1980. Mechanism of microbiological leaker spoilage of canned foods: Biophysical aspects. J. Food. Prot. 43(6): 488-497.

Raabe, O. G. 1976. The Generation of Aerosols of Fine Particles. p.57-68. *In* Fine Particles, Aerosol Generation, Measurement, Sampling, and Analysis. Academic Press, Inc., New York.

Reich, R. R. 1985. A method for evaluating the microbial barrier properties of intact packages. Med. Diag. Ind. 7(3):80, 82, 86-88.

Reist, P. C. 1984. Introduction to Aerosol Science. Macmillian Publishing Co., London.

Reist. P. C. 1993. Aerosol Science and Technology. 2nd ed. McGraw-Hill, Inc., New York.

Rey, C. R., G. A. Halaby, E. V. Lovgren and T. A. Wright. 1982. Evaluation of a membrane filter test kit for monitoring bacterial counts in cannery cooling waters. J. Food Prot. 45:1087-1090.

Romarao, B. V. and C. Tien. 1988. Calculations of drag forces acting on particle dendrites. Aerosol Sci. and Technol. 8:81-95.

Ross, S. and R. M. Haak. 1958. Inhibition of foaming. IX. Changes in the rate of attaining surface tension equilibrium in solutions of surface-active agents on addition of foam inhibitors and foam stabilizers. J. Phys. Chem. 62:1260-1264.

Rotenburg, Y., L. Boruvka and A. W. Newmann. 1983. Determination of surface tension and contact angle from shapes of axisymmetric fluid interfaces. J. Colloid Interface Sci. 93:169-183.

Russel, W. B., D. A. Saville and W. R. Schowalter. 1989. Particle capture. p. 366-393. *In* Colloidal Dispersions. Cambridge University Press, Cambridge.

Segner, W. P. 1979. Mesophilic aerobic sporeforming bacteria in the spoilage of low-

acid canned foods. Food Technol. 33(1):55-59.

Simpson, D. R., M. M. R. Williams and S. Simons. 1989. Modeling of aerosols in coupled chambers. Nuc. Sci. and Eng. 101:259-268.

Somasundaran, P., M. Danitz and K. J. Mysels. 1974. A new apparatus for measurements of dynamic interfacial properties. J. Colloid Interface Sci. 48:410-416.

Spurney, K. R. 1972. Aerosol filtration by means of analytical pore filters. p. 67-68. *In* T. T. Mercerm P. E. Morrow and W. Stöber (ed). Assessment of Airborne Particles, Fundamentals, Applications, and Implications to inhalation Toxicity. Charles C. Thomas Publisher, Springfield, IL.

Stersky, A., E. Todd and H. Pivnick. 1980. Food poisoning associated with post process leakage (PPL) in canned foods. J. Food Prot. 43(6):465-476.

Streeter, V. L. 1961. Turbulence. p. 1-10. *In* 1st ed. Handbook of Fluid Dynamics. McGraw-Hill Book Company, Inc., New York.

Teltsch, B., H. I. Shuval and J. Tadmor. 1980. Die-away kinetics of aerosolized bacteria from sprinkler application of wastewater. Appl. Environ. Microbiol. 39:1191-1197.

Washburn, E. W. 1921. The dynamics of capillary flow. Phys. Rev. 2(7):273-283.

Weast, R. C. and M. J. Astle. 1980. p. F-130. *In* 60th ed. Chemical Rubber Company Handbook of Chemistry and Physics. CRC Press, Boca Raton, FL.

White, F. M. 1986a. Viscous flow in dusts. p. 1-43. *In* 2nd ed. Fluid Mechanics. McGraw-Hill, Inc., New York.

White, F. M. 1986b. Viscous flow in dusts. p. 305-306. *In* 2nd ed. Fluid Mechanics. McGraw-Hill, Inc., New York.

Williams, M. M. R. and S. K. Loyalka. 1991. Aerosol Theory and Practice. Pergamon Press, Oxford, UK.

Woodruff, D. P. 1973. Interfacial free energy and the γ-plot. p. 1-11. *In* The Solid-Liquid Interface. Cambridge University Press, New York, N.Y.

Yam, K. 1995. On-line, non-destruction system inspects integrity of pouches. Pack. Technol. and Eng. 4(5):46-49.

SECTION II: APPLICATION OF FLUID MODELING TO DETERMINE THE THRESHOLD LEAK SIZE FOR LIQUID FOODS

(Paper formatted for submission to the Journal of Food Protection)

ABSTRACT

This study examined the mechanism by which a package defect converts to a leaker in an effort to develop a relationship between the threshold leak size and loss of package sterility. The threshold leak size is the hole size at which the onset of leakage occurs. The threshold pressure is that which is required to initiate a leak. Leak initiation was studied in terms of the interaction between three components: liquid attributes of liquid food products, defect size, and pressures required to initiate liquid flow.

Liquid surface tension, viscosity, and density were obtained for sixteen liquids. The imposed pressures (P_o) required to initiate flow through microtubes of IDs 0, 2, 5, 7, 10, 20 or 50 μm, were measured using 63 test cells filled with safranin red dye, tryptic soy broth, and distilled water with surface tensions, of 18.69 mN/m, 44.09 mN/m, and 64.67 mN/m, respectively. Significant differences were found between observed threshold pressures for safranin red dye, tryptic soy broth, and distilled water ($p < 0.05$). Liquids with small surface tensions, such as safranin red dye, required significantly lower threshold imposed pressures than liquids with large surface tensions, such as distilled water ($p < 0.05$). An equation was developed to quantify the relationship between liquid surface

tension, threshold imposed pressure, and defect size. Observed threshold pressures were not significantly different ($p > 0.05$) than those predicted by the equation.

Imposed pressures and vacuums generated within packages during random vibration and sweep resonance tests were measured for aseptic packages brick-style (250 ml), metal cans size 76.2-mm x 114.3-mm (425 ml), quart gable top packages (946 ml), one-half gallon gable top packages (1.89 L) and one-gallon milk jugs (4.25 L). Significant differences were found between packages for observed generated pressures during vibration testing ($p < 0.05$). An equation to calculate the threshold size based on liquid surface tension and imposed pressure was established.

Key Words: threshold leak size, threshold pressure, surface tension, distribution, random vibration test, sweep resonance test

INTRODUCTION

Aseptic packaging technology is employed to provide shelf stable food products for consumer use. This technology relies on the maintenance of a hermetic seal to assure package sterility. Sterility of aseptic packages may be lost during storage and distribution due to the presence of defects in the seal area or package body as a result of abusive handling (*14*). Defects in the seal area may be created during the sealing process as well.

Examinations of packages where post process contamination occurred showed that liquid food product within the defect linked the package contents to the exterior surface of the package and resulted in loss of package sterility (*2, 12, 15, 20, 26, 33, 34, 36*). Microorganisms traversed the liquid filled defect, entered the package and contaminated its contents *(16, 22, 23, 27, 31, 32*). Such package examinations focused more on the physical attributes of invading microorganisms found within the packages rather than conditions that lead to microbial ingress through the leaker (*1, 9, 24*).

Packages are expected to tolerate numerous conditions during storage and distribution while protecting their contents from influences that may jeopardize sterility. Forces exerted on the package, or that result from movement of the contents within the package, may inflict damage without affecting sterility (*35*). The magnitudes of such forces incurred by or generated within a food package during distribution, and their significance to the sterility maintenance of the package is not known (*28, 32, 35*). The magnitudes of forces sufficient to cause loss of package sterility by converting a defect to

a leaker appear to comprise the bulk of the concern.

Since defects become leakers as a result of filling with liquids, an understanding of the dynamics of liquid movement is important. For the purposes of this study, we will focus on the flow of liquid from the package interior, through a defect, to the gaseous exterior of the package or liquid to air contact.

Much of leak theory is based the Hagen-Poiseuille model for the volumetric rate of liquid flow (*2*).

$$Q = \frac{\pi \rho R^4}{8 \eta L} (p_1 - p_2) \qquad (1)$$

Hagen-Poiseuille's law relates the effect of viscosity η, capillary radius of R, capillary length L, and total pressure differential of $(p_1 - p_2)$ to the volumetric rate of flow Q, of liquids and gases *(2, 10, 11, 37*). However, the Hagen-Poiseuille equation fails to consider resistance offered by liquids prior to the initiation of liquid flow. To initiate liquid flow, the pressure imposed on the liquid must be of a sufficient magnitude to exceed the resistance to movement offered by the liquid surface tension. The liquid surface tension is the specific surface free energy of the liquid gas interface (*37*).

Variations of Hagen-Poiseuille's equation have been used to describe the flow of gases and liquids for the purpose of leak detection (*2, 18, 19, 20*). Values produced by these equations have been correlated to leak detection devices capable of determining pressure changes via package lid or side panel deflection (*18*). Using the Hagen-Poiseuille

equation, relationships between volumetric flow rates through leakers and contamination of packages as a result of microbial ingress have been estimated (*18, 19, 20, 30*). Still, such equations have failed to produce a critical leak size, or the hole size at which the onset of microbial ingress into a package occurs.

The association of leakers and the loss of package sterility is well documented (*28, 29, 30,* 34). However, the process by which a defect becomes a leaker, and the relationship between a defect and the loss of package sterility is poorly understood. In an effort to understand the relationship between the defect size found within a package and the loss of package sterility, this study measured the pressures necessary to convert defects into leaks, or the threshold pressure. The threshold pressure is the amount of force required to initiate liquid flow through a defect of a given interior diameter (ID). The defect size at which the onset set of liquid flow results is called the threshold defect size

The goals of this study were to measure the effect of defect size and liquid surface tension on the pressure required to initiate liquid flow, determine the internal pressure packages will generate during simulated distribution, and to produce an equation for the calculation of the threshold defect size.

MATERIALS

Microtubes

Nickel microtubes were supplied by the Phillips Laboratory, Fundamental Technology Division, Carbon Research Laboratory, Edwards Air Force Base, CA through a Cooperative Research and Development Agreement (*21*). Sixty-three microtubes with IDs of 0, 2, 5, 7, 10, 20 and 50 μm and 7 mm in length, were used as the manufactured defects. Solid microtubes (no holes) were used as controls.

Test cells

Glass test cells were developed to facilitate measurements of the imposed pressure required to initiate liquid flow through a microtube. The glass test cell dimensions are 8 cm [H] x 5 cm [D]. Each test cell consists of a 45 mm [H] x 15 mm [D] glass vial (3 ml capacity) encased in a 85-ml glass water jacket (Fig. 1). The vial and the jacket have one entry and one exit port each. The vial has a glass lug for a septa closure.

Viscometry

Cannon-Fenske two-bulb viscometers, sizes 50 and 100, and a Cannon-Ubbelohde size 100, three bulb, semi-micro viscometer (Cannon Instrument Company, State College, PA) were employed to measure the efflux times of eighteen liquids. Two-bulb

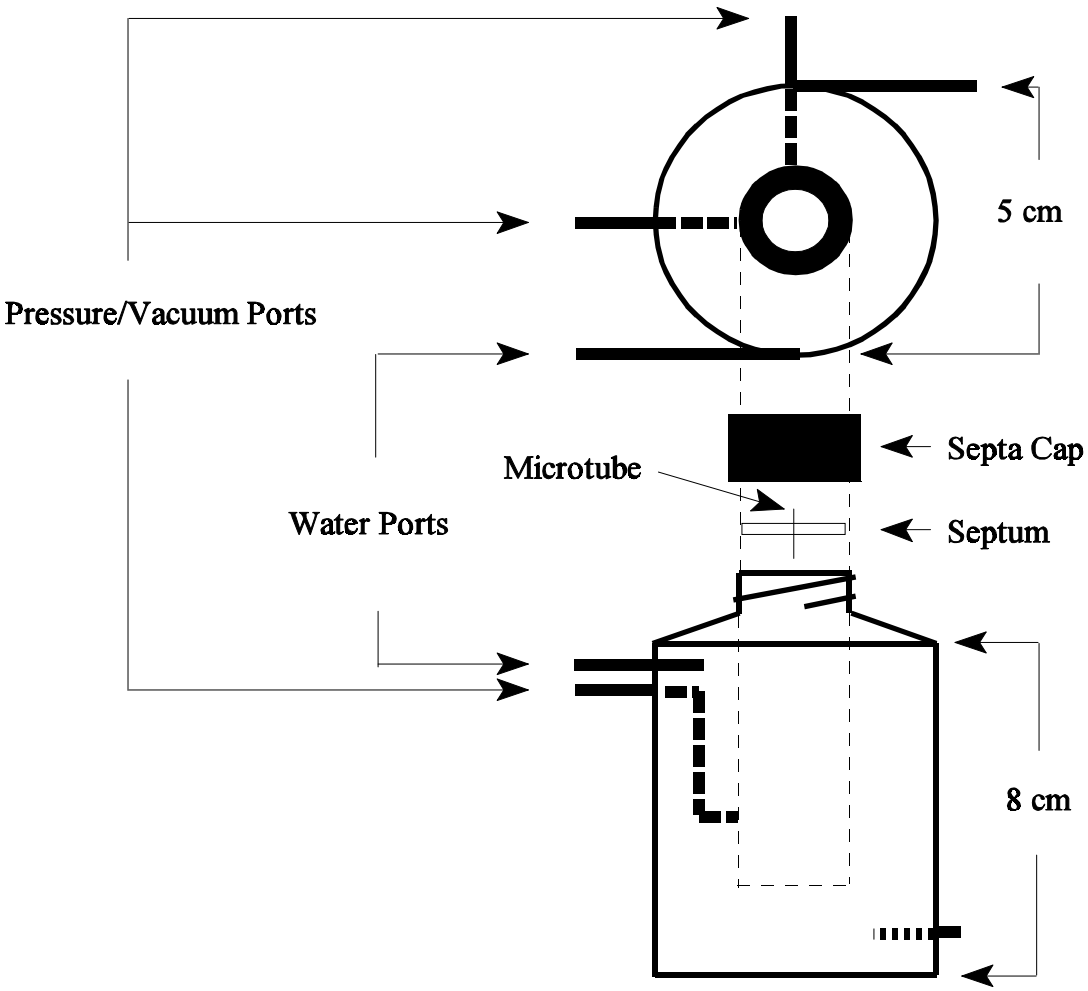

FIGURE 1. *Test cell showing pressure/vacuum ports, water ports, dimensions, septa cap, septum, and microtube position.*

viscometers were used for Newtonian sample liquids and a three-bulb viscometer was used for liquid samples that exhibited shear-thinning. A water bath regulator was employed to maintain a temperature of 25 ± 0.1 °C.

Density Measurements

Density measurements (g/cm^3) were collected for eighteen liquids using a DA-300 density/specific gravity meter (Mettler/Toledo Instruments, Toledo, OH) at 25°C. Filtered liquid samples (2 ml) were injected into the internal measuring cell of the density/specific gravity meter. A measuring time of ≤ 600 s was used.

Imposed pressure

An in-line pressure gauge (model HHP701-2, Omega Engineering, Inc., Stamford, CT) with a detection range of 138 kPa of vacuum or positive pressure, and a resolution and accuracy of 0.05% and ± 0.15% FS, respectively, was employed to measure the pressure imposed on sample liquids inside the test cells.

Packages for simulated distribution testing

Four of each of the following package types were used for vibration testing; metal cans size 76.2 mm x 114.3 mm (425 ml), brick style aseptic packages (250 ml), one-quart paper board, gable top milk packages (946 ml), one-half gallon paper board, gable top milk packages (1.89 L) and one-gallon plastic milk jugs (4.25 L). The top of each

package was fitted with 33 mm x 23 mm two-way stopcock low pressure chromatography fixtures (Bio-Rad Laboratories, Hercules, CA). Packages were filled with water to their respective capacities to produce head space values typical for the package type. The atmosphere inside all packages was equilibrated to 0.00 kPa. One of each package type was used as a control.

Package holding device

A package holding device constructed of Lexan® with a 30.5 cm (L) x 18.0 cm (W) foundation platform and an 18-cm x 18 cm adjustable fitting panel was used for simulated distribution testing. Countersinks were manufactured into the foundation platform and the adjustable fitting panel to minimize package contact as well as to ensure desired package placement during simulated distribution vibration test. Five, 45 cm (L) x 0.95 cm outside diameter threaded rods were used to connect and adjust the fitting panel to the foundation platform. Access holes in the fitting panel allowed easy placement of the packages and prevented tube crimping.

Vibration table

A vertical electro hydraulic vibration tester (VEVT), with an accelerometer mounted on the underside of the table, directly below the package holding device, was used for simulated distribution vibration testing. Control spectrum assurance level II prescribed by ASTM, was used for inducement of pressure within test packages (*6, 7, 8*).

METHODS

Surface tension measurements

Surface tensions of eighteen liquids were measured at 25°C employing the du Nöuy method using a platinum iridium ring with a circumference of 5.925 cm, an R/r ratio of 53.077, and a surface tensiomat (model 21, Fisher Scientific, Atlanta, GA) (*1*). Sample liquids were filtered via 0.3 μm sized filters (No. 4210, Gelman Sciences, Ann arbor, MI), prior to surface tension measurements.

Viscosity measurements

Viscosity measurements were performed as prescribed by ASTM guidelines (*4*). Ten ml of each of the sample fluids was filtered via 0.3 μm sized filters, prior to insertion into the viscometers. Liquid temperatures were allowed to equilibrate to the 25°C water bath. Viscometer sizes were selected so that liquid flow times were greater than 200 s. Values for efflux times (s) were converted to absolute viscosities with distilled water as the standard. Care was taken to maintain clean viscometers for reproducible results. Maintenance for viscometers were carried out as specified in ASTM (*5*).

Preparation of test cells

A 27-gauge syringe needle was used to puncture and penetrate the center of a silicone septum. Microtubes were inserted into the needle under a light microscope. The

syringe needle was removed from the septum, leaving the microtube in place. The internal diameter of each microtube was measured using a light microscope (model BH-2, Olympus, Lake Success, NY) equipped with video callipers (Fig. 2). Septums containing measured microtubes were positioned on top of the test cell finish. Glass lugs of the test cell were wrapped with Teflon™ tape, overlapping the top outside circular edge of the septum. Septa caps were placed over the septums and tightened. Silicone sealer (Dow Corning, Dayton, OH) was used to seal the septa surface around the microtube and the septum-septa cap contact area. Seal areas were tested for integrity using the dye test, air pressure and vacuum test (*3*).

Equation for the initiation of liquid flow

The equation for the initiation of liquid flow quantifies the pressure required to initiate flow of a liquid with a given surface tension through microtubes with IDs of 2, 5, 7, 10, 20, or 50 μm. The relationship between the pressure required to initiate liquid flow, and liquid surface tension is developed by

$$P_0 - P_L + \rho gL = \Delta P \qquad (2)$$

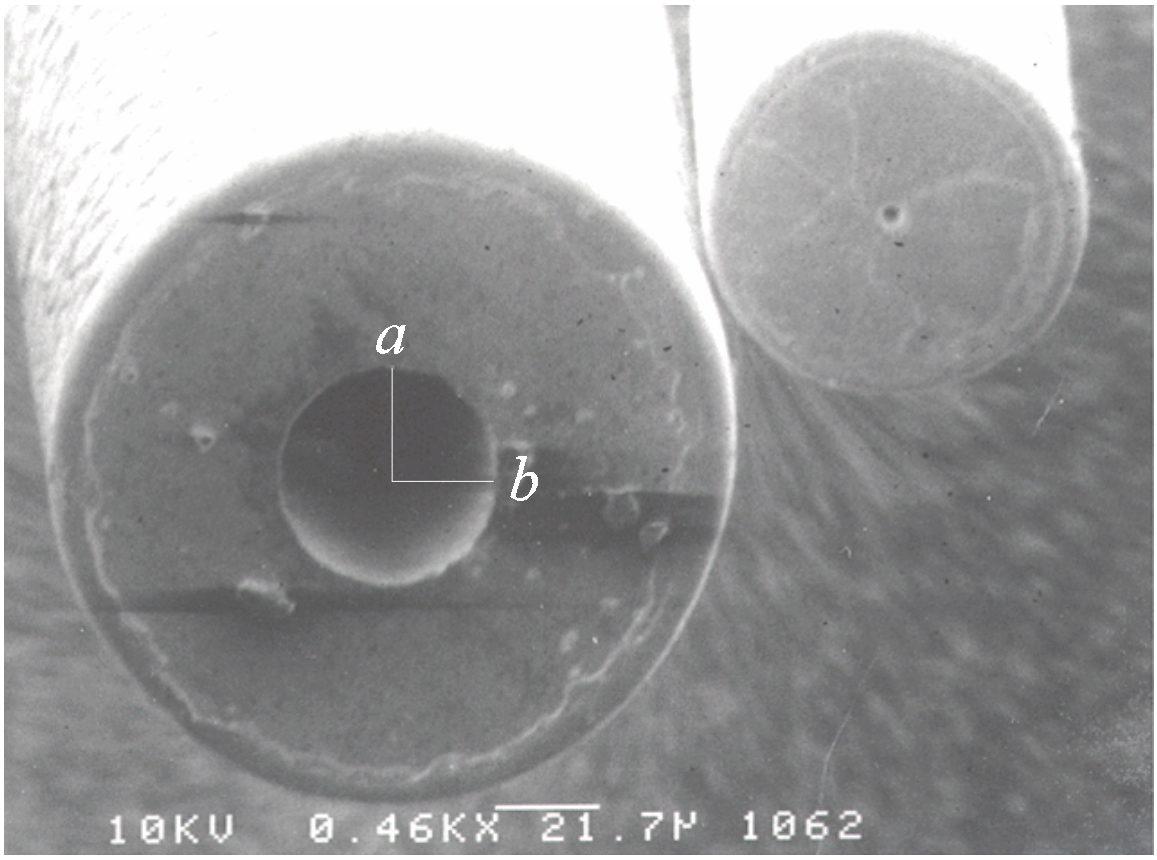

FIGURE 2. *End view of nickel microtubes with IDs of 50μm and 2μm, showing the radius a and b used to calculate the hydraulic diameter (D_H).*

where P_O is the imposed pressure, P_L is the internal pressure of the resultant droplet on the end of the microtube, ρ is the liquid density, g is the force of gravity, and L is the length of the microtube or fill height of the liquid (*10*). The term ρgL is called the liquid static head.

Since the value for P_L is difficult to obtain, the pressure was obtained by measuring the radius r of the droplet formed on the end of the microtube as a result of imposed pressure P_O. Pressure is linked to the surface tension by

$$\Delta P = 2\sigma / r \qquad (3)$$

where the pressure acting upon a liquid of a given surface tension σ, is a function of the tube diameter that will produce a liquid droplet of radius r (*38*). These relationships are the foundation for the equation for the initiation of liquid flow.

The product of the equation is the threshold pressure required to initiate liquid flow. Calculations for the threshold pressure required to initiate liquid flow are dependent on the imposed pressure P_O applied to create a droplet of radius r, on the end of a microtube of length L, for a liquid with a surface tension of σ, and a density of ρ, at an atmospheric pressure of P_{ATM} (*10, 38, 39*). The equation for the initiation of liquid flow is (*16, 38*):

$$P_0 > (P_{ATM} + 2\sigma / r - \rho gL) \qquad (4)$$

We will refer to Equation 4 as liquid flow model #1 (M1).

Imposed pressure measurements

Safranin red dye (3 ml) was filtered via 0.3 μm sized filters, and injected into each of seven test cells via a syringe. A fill height and liquid static head of approximately 4.35 cm and 2.58 mmHg, respectively, were achieved. Each of the seven test cells had one microtube of either 2, 5, 7, 10, 20, and 50 μm I.D.

Test cells were inverted, so that microtubes pointed downward. Each test cell was secured to an inverted light microscope (Olympus Model BH-2, Lake Success, NY) equipped with a video monitor. Test cells were adjusted to position the microtube perpendicular to the floor. The light microscope was adjusted so that the entire ID of each microtube was clearly visible. Positive pressures were imposed via an adjustable, electric pump (model ROA-P131-AA, Gast Co., Benton Harbor, MI) at an increase of 0.069 kPa per 10 s until a liquid droplet with a radius equal to the radius of the microtube appeared. The imposed pressures at which such liquid droplets were observed were designated the threshold imposed pressures. The droplet radius measurements were incorporated into M1 as the value for *r*. An in-line pressure gauge (model HHP701-2, Omega Engineering, Inc., Stamford, CT) was used to measure the imposed pressure.

Measurements for the droplet radius size *r*, resulting from the observed values for the threshold pressures were obtained for safranin red dye, tryptic soy broth, and distilled water. The observed threshold pressure values were compared to values produced by M1.

Random vibration, sweep and dwell resonance tests

The packaging holding device was secured to the VEVT (Lansmont Corp., East Lansing, MI) table top via a holding bracket bolted directly into the vibration table. Package and holding device areas of contact were minimized so as to reduce flex inhibition of the package body walls or side panels. The panels of the package holding device were secured to the package just tight enough so as to prevent movement. Adjustment nuts were torqued counter rotationally against each other to increase package holding device rigidity for continuous communication of table vibrations to the package. The foundation platform and the fitting panel were independently leveled.

Sweep and dwell resonance tests were performed using a controlled power spectral density (PSD) intensity, method B as specified in ASTM D999 (*6*). For sweep resonance tests, a continuous PSD frequency spectrum from 3.5 Hz to 150 Hz in increments of 0.01 Hz were used. Dwell resonance test were comprised of discrete sinusoidal PSD frequencies of 50 Hz and 150 Hz ± 3 Hz. All tests were conducted at an ambient laboratory temperature of 25°C.

Pressures generated within the packages during simulate distribution were measured via a general purpose 100 millivolt output pressure sensor (model PX302-015GV, Omega Engineering, Inc., Stamford, CT) with a detection range of 0 - 103.4 kPa positive pressure or vacuum. The pressure sensor was connected to a high speed load and strain gage meter (model DP-776, Omega Engineering, Inc., Stamford, CT) set at 500 samples per second. The strain gage meter was calibrated at 0.00, 34.6, 69.2 and 103.5

kPa. Imposed pressures generated from within the package were communicated to the sensor via a 3.2 mm (ID) x 6.4 mm (OD) x 10 cm (L) Tygon™ tubing attached to each package by a 33 mm (L) x 23 mm (W) 2-way stopcock (Bio-Rad Laboratories, Hercules, CA). Stopcocks on one of each package type were turned to the closed position and used as controls.

Replications

Procedures employed to measure surface tension, viscosity, and density values were replicated three times for each of the sixteen sample liquids. Safranin red dye, tryptic soy broth, and distilled water were selected to measure the imposed pressures required to initiate liquid flow because they represented the smallest, intermediate, and largest values for surface tension, respectively, of the liquids sampled. Procedures employed to measure pressures required to initiate liquid flow were replicated three times for each sample liquid per microtube ID size.

Vibration tests were replicated three times each for all package types. Sweep resonance tests were not replicated. Maximum and minimum values were observed for each test. For sweep resonance tests, the resonant frequency at which the maximum and minimum pressures were produced were observed.

Statistical analysis

A split plot statistical design was employed for measurements made using liquid samples in test cells. Microtube ID was the main plot, the surface tension and observed imposed pressures were the subplots. The ANOVA was employed for analysis of data (SAS Institute, Inc., Cary, NC). The same statistical design was employed to determine the significance between observed threshold pressures and predicted values produced by equations for initiation of liquid flow. Statistical significance was determined using tables (*25*)

A split plot design was also employed for pressure measurements made during random vibration tests. Liquid fill height was the main plot, liquid static head and pressure changes within a package were subplots. Statistical analysis were not performed on data from sweep resonance tests. Statistical significance was determined using tables (*25*).

RESULTS AND DISCUSSION

Controls

Test cell evaluation for integrity of seal areas using the dye, air pressure and vacuum tests confirmed that leakers were not present. Control packages prepared for random vibration and sweep resonance tests with stopcocks in closed position showed no changes in pressure during the tests.

Surface tension, viscosity, and density measurements

Liquid surface tensions of samples ranged from 18.69 ± 0.20 mN/m for safranin red dye, to 64.67 ± 0.25 mN/m for distilled water (Table 1). Viscosity values ranged from 8.97 ± 0.03 mm^2/s for distilled water to 69.66 ± 0.57 mm^2/s for evaporated milk. Values for density ranged from 0.80 g/cm^3 for safranin red dye to 1.05 g/cm^3 for 2% fat chocolate milk (Table 1).

Surface tension, threshold pressure, and mircotube ID size

Pressures imposed in test cells as a function of the liquid static head (ρhg) for a fill height of 4.35 cm, were 0.34 kPa, 0.43 kPa, and 0.42 kPa for safranin red dye, TSB, and distilled water, respectively. Differences in the densities of the liquid samples accounted for variations between liquid static head values.

The imposed pressures required to initiate liquid flow through microtubes with ID sizes of 2, 5, 7, 10, 20, and 50 μm were measured for safranin red dye, TSB, and distilled water. As expected, imposed pressure and liquid surface tension significantly effected the threshold leak size ($p \leq 0.05$). The pressure required to initiate flow of distilled water

TABLE 1. *Surface tension, viscosity and density values for fluids at 25 ℃.*

Fluid Measurements			
Product	Surface Tension (mN/m)	Viscosity (mm^2/s)	Density (g/cm^3)
Distilled Water	64.67 ± 0.25	8.97 ± 0.03	0.99 ± 0.00
Mott's Apple Juice	63.17 ± 0.70	12.08 ± 0.10	1.04 ± 0.00
Gatorade Orange Drink	60.89 ± 0.70	10.56 ± 0.13	1.02 ± 0.00
Hi-C Grape Drink	60.79 ± 0.30	12.35 ± 0.07	1.04 ± 0.00
Snapple Lemon Tea Drink	51.36 ± 0.20	11.16 ± 0.07	1.03 ± 0.00
Kroger's 0% Fat Skim Milk	46.07 ± 0.20	13.65 ± 0.05	1.02 ± 0.00
Ocean Spray Orange Juice	44.46 ± 0.70	15.35 ± 0.00	1.04 ± 0.00
Difco Tryptic Soy Broth	44.09 ± 1.00	9.51 ± 0.02	1.01 ± 0.00
Hawaiian Punch Fruit Punch	43.01 ± 0.00	12.39 ± 0.03	1.04 ± 0.01
Carnation Evaporated Milk	42.84 ± 1.00	69.66 ± 0.57	1.05 ± 0.01
Ocean Spray Grapefruit Juice	42.69 ± 0.05	13.08 ± 0.06	1.03 ± 0.01
Hawaiian Punch Fruit Juicy Red	41.57 ± 0.00	12.37 ± 0.03	1.04 ± 0.00
Hershey's 2% Fat Chocolate Milk	41.21 ± 0.45	13.33 ± 0.12	1.05 ± 0.00
Rhône-Poulenc Igepal CO 630 (surfactant)	28.81 ± 0.45	9.79 ± 0.03	0.99 ± 0.00
Parks 100% Mineral Spirits	22.63 ± 0.15	12.42 ± 0.00	0.79 ± 0.00
Safranin Red Dye	18.69 ± 0.20	26.01 ± 0.17	0.80 ± 0.00

The filtration process may remove components of some of these liquid products such as pulp from friut juice, and fat droplets from milk.

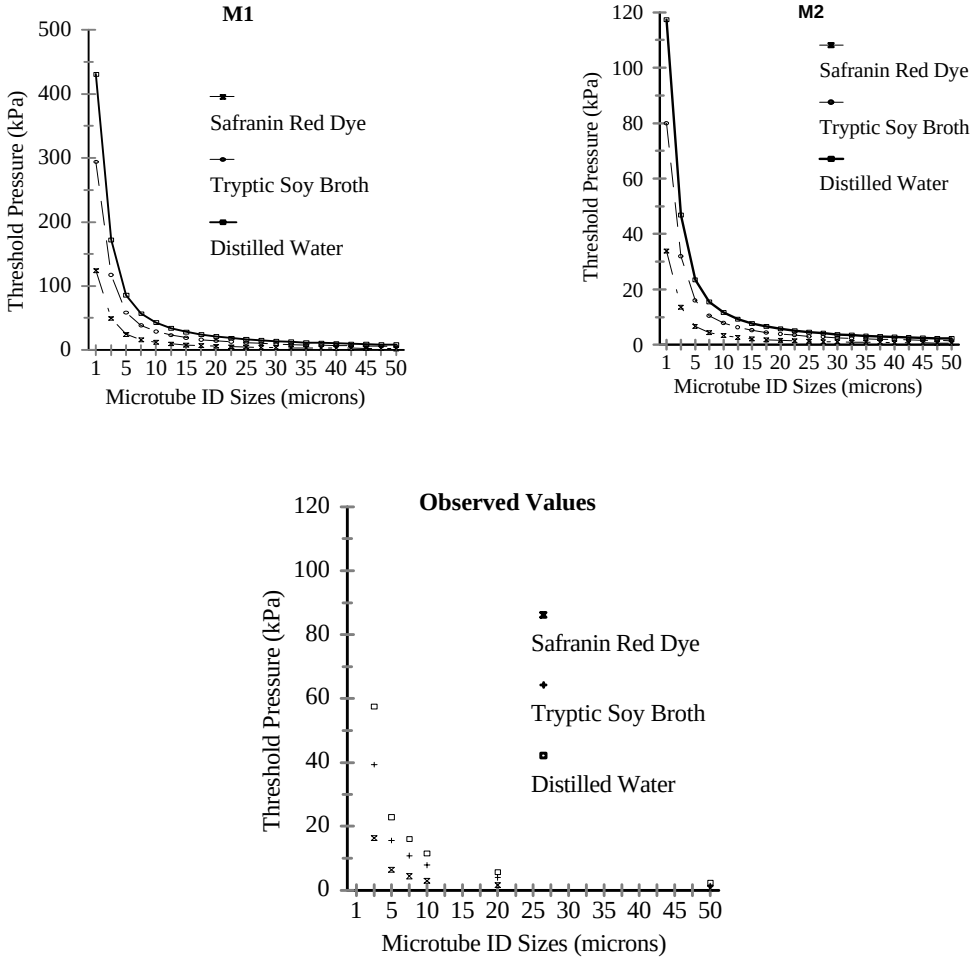

FIGURE 3. *Threshold pressures predicted by M1 (equation 4) and M2 (equation 6) compared to the observed values required to initiate flow of safranin red dye, tryptic soy broth, and distilled water with surface tensions of 18.69 mN/m, 44.09 mN/m and 64.67 mN/m, respectively.*

through a microtube with a 20-μm ID was 5.64 kPa whereas, a marginally larger imposed pressure of 6.33 kPa initiated flow of safranin red dye through a microtube with a 5-μm ID (Fig. 3). An increase in the liquid surface tension produced a decrease in the threshold pressure, per microtube ID size. The threshold pressure for safranin red dye for a microtube with a 2-μm ID was 16.34 kPa compared to 57.56 kPa for distilled water(Fig. 3). Differences between the threshold leak sizes and threshold pressures for these liquids are a result of differences in the magnitudes of their liquid surface tensions. Because the surface tension of sarfanin red dye (18.69 mN/m) is small relative to that of water, it offers less resistance to the initiation of liquid movement. As a result, safranin red dye requires less imposed pressure to initiate flow than liquids with large surface tensions such as distilled water (64.67 mN/m). Therefore, the threshold leak size is smaller for liquids with surface tensions similar to that of safranin red dye than those for liquids with much larger surface tensions such as distilled water, per imposed pressure. These findings differ from Amini and Morrow (*2*), McEldowney and Fletcher (*28*), and Floros and Gnanasekharan (*18*) in that leakers were attributed to pressure differentials between the inside and the outside of the package acting on the liquid viscosity of the product. The product of their research was a value for the leakage rate of a liquid or gas passing through a leaker. However, flow must be initiated prior to establishing a leakage rate. Liquid surface tension is an important component in the liquid flow imitation process. After liquid flow is initiated, equations that incorporate viscosity such as those proposed by Amini and Morrow (*2*) and Floros and Gnanasekharan (*18*) may be employed to determine leakage

rates.

Liquid flow model

Observed threshold pressures were significantly different ($p < 0.05$) than those calculated using M1. The observed threshold pressure for safranin red dye through a microtube with an ID of 2 μm was 16.34 kPa compared to the M1 predicted value of 48.05 kPa. Differences between observed threshold pressures and values derived employing M1 increased as values for liquid surface tensions increased, such as those for TSB and distilled water (Fig. 3).

Differences between the observed threshold pressures and M1 values are due, in part, to the method of leaker size determination employed by M1. Leaker dimensions for M1 were mathematically derived by relating the measured droplet radius produced by a liquid of a given surface tension to the imposed pressure required to produce the droplet. In an effort to reduce the difference between observed threshold pressures and pressures predicted by M1, the term $2\sigma/r$ was replaced by $4\sigma/D_H$ to permit calculation of the hydraulic diameter of each microtube (*13, 17*). By using the term D_H, the direct measurements of the leaker can be employed for the calculation of the threshold pressure.

The equation used to calculate values for the hydraulic diameter (D_H) employs measurements of the a and b radius for each microtube ID (Fig. 2). The hydraulic diameter value permits the calculation of diameters for tubes with circular or elliptical shapes. Hydraulic diameters (*13, 17*) for each microtube were calculated as follows

$$D_H = \frac{2ab}{\sqrt{\frac{a^2 + b^2}{2}}} \qquad (5)$$

A correction factor of 0.272 was incorporated into the equation as well. The correction factor is necessary due to the hydrophilic nature of the nickel microtubes. The resulting equation for the initiation of liquid flow #2 (M2) is (*16*),

$$P_O > P_{ATM} + [(4\sigma/D_H - \rho gL) \; x \; 0.272] \qquad (6)$$

Microtubes made of hydrophobic materials such as polypropylene may require a smaller correction factor. Microtubes made of these materials may require larger imposed pressures to initiate liquid flow than microtubes made of nickel, and therefore reduce the difference between observed values and those predicted by M1. Because of the hydrophilic nature of the microtubes used in this study, values for the threshold pressure and threshold leak size may be smaller than those resulting from usage of other materials. Therefore, observed values for the threshold pressures and threshold leak sizes are conservative.

Observed threshold pressures were not significantly different ($p > 0.05$) than those predicted by M2 (Fig. 3). For a microtube with a 5-μm ID, observed threshold pressures for safranin red, TSB, and distilled water were 6.34 kPa, 15.58 kPa, and 22.88 kPa, respectively, compared to 6.33 kPa, 15.43 kPa, and 23.62 kPa, respectively, predicted by

M2 (Fig. 3).

For ease of comparison of threshold values with results from prior research, observed threshold pressures for the safranin red dye, TSB, and distilled water were converted to leakage rates ($Pa \cdot m^3/s$) for each microtube ID size (Fig. 4). The Hagen-Poiseuille equation was employed to calculate volumetric flow rates using measurements of the threshold pressure and the resultant liquid droplet radius for safranin red dye, TSB, and distilled water (Equation 1). Volumetric flow rates were converted to leakage rates according to Guazzo (*20*).

Distilled water through a microtube with a 50-μm ID showed the largest leakage rate at 1.3×10^{-2} $Pa \cdot m^3/s$. Safranin red dye showed the smallest leakage rate at 4.2×10^{-6} $Pa \cdot m^3/s$ through a microtube with an ID of 2 μm. This is contrary to the findings of Put et al. (*34*) and Morton et al. (*30*) who reported that detectable liquid leakage occurred at rates > 10^{-5} $Pa \cdot m^3/s$. Morton et al. (*30*) found the detectable leakage limit using spiked water and nitrogen gas with a copper tracer element under an imposed pressure of 20.7 kPa through defects 330-μm wide by 290-μm deep, manufactured into the closure seal interface of parenteral vials. Using the same imposed pressure of 20.7 kPa as Morton et al. (*30*), calculations made using M2 to solve for leak size produced values for threshold leakers with significantly smaller ID sizes of 1.6-μm, 3.8-μm, and 5.6-μm for safranin red dye, TSB, and distilled water, respectively (Fig. 4). Therefore, the threshold leakage rate sought by Put et al. (*34*) and Morton et al. (*30*) is dependent on the surface tension of the liquid or gas used. Liquid or gas surface tensions were not examined in their study.

Now that the threshold pressures per microtube ID size and liquid surface tension have been established, it is important to determine the magnitude of pressure change that occurs within a package during distribution. It is equally important to determine the influence of liquid static head on such pressure changes. For this reason random vibration and sweep resonance tests were performed.

Random vibration tests

Significant differences ($p < 0.05$) were found between packages for observed generated pressures during vibration testing using the ANOVA and comparing to table values (*25*). Minimum and maximum pressures generated in one-gallon jugs were -0.71 and 1.86 kPa, respectively (Table 2). Aseptic packages produced the smallest vacuum at -0.25 kPa, and was attributed to flexing of the body wall panels. Metal cans developed the least amount of pressure during random vibration testing at 0.21 kPa. Low generated pressures observed for metal cans were attributed to package rigidity and absence of

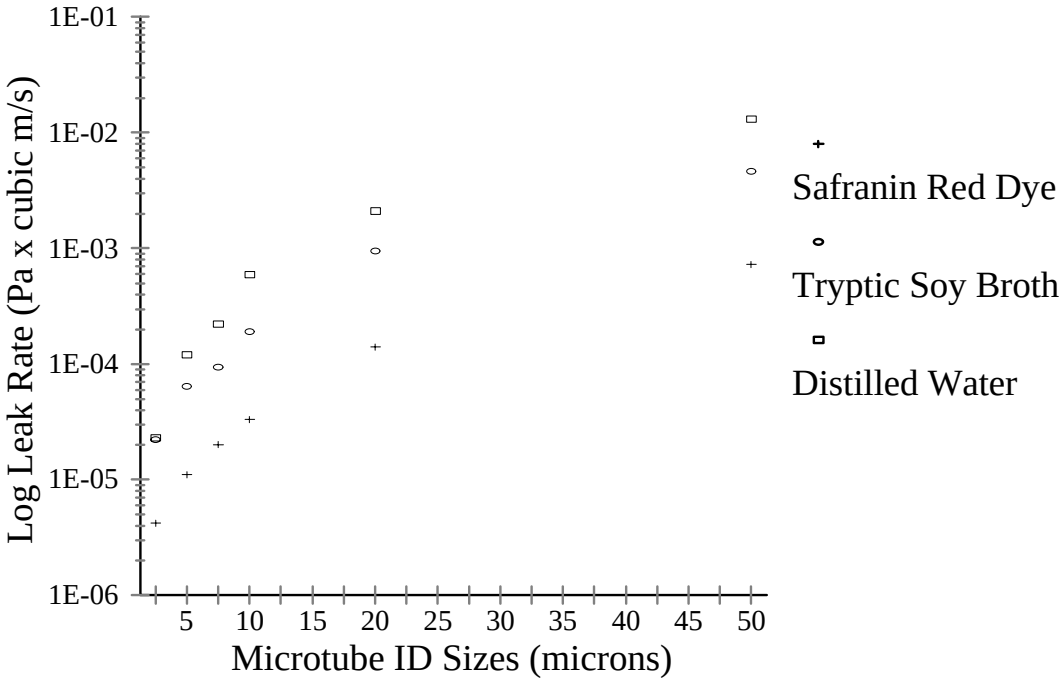

FIGURE 4. *Log leak rates through microtubes for safranin red dye, tryptic soy broth, and distilled water at 25 ℃.*

Table 2. *Imposed pressures generated inside water filled packages during random vibration testing at 25 ℃.*

		Observed Pressures (kPa)				
		Aseptic Package	Metal Can	Quart Carton	Half Gallon Carton	One Gallon Jug
Fill Volume		250 ml	425 ml	946 ml	1.89 L	4.25 L
Pressures[a]						
	Low	-0.25 ±0.03	-1.33 ±0.11	-1.79 ±0.39	-1.51 ±0.83	-0.71 ±0.19
	High	1.86 ±0.55	1.44 ±0.07	1.49 ±0.25	1.86 ±0.06	1.86 ±0.17
		Observed Pressures Corrected for Static Head (kPa)				
Static Head		0.98	0.96	1.87	1.87	2.17
Pressures[a]						
	Low	-1.23 ±0.03	-2.29 ±0.11	-3.66 ±0.39	-3.38 ±0.83	-2.88 ±0.19
	High	2.84 ±0.55	2.40 ±0.07	3.36 ±0.25	3.73 ±0.06	4.03 ±0.17

[a] Average of three samples

flexing of the package body during vibration test. Values were obtained by measuring pressure fluctuations within the head space of each package during their respective test. Pressure changes within the head space were intended to simulate those a defect in the seal of an aseptic package may encounter during distribution. Values for the observed pressure changes do not consider the effect of liquid static head. As a result, observed values for the minimum and maximum pressures generated during random vibration and sweep resonance testing are conservative.

The observed values for generated pressure can be corrected for static head by adding the static head pressure to the minimum and maximum observed pressures generated within the package (Table 2). Observed pressures were corrected for static head to simulate the maximum pressures a defect may encounter. The resultant corrected pressures are equivalent to those found at the lowest point of a package.

Employing the ANOVA, significant differences ($p < 0.05$) were found between values for the observed pressures generated within a package during vibration testing and observed pressures corrected for static head (*25*). Observed values for the minimum and maximum pressures generated within a quart carton, half-gallon carton, and a one gallon jug during random vibration testing were 1.49 kPa, 1.86 kPa, and 1.86 kPa, respectively, compared to values corrected for static head of 3.36 kPa, 3.73 kPa, and 4.03 kPa, respectively. Uncorrected values are of a sufficient pressure to initiate flow of liquids with small surface tensions, such as safranin red dye, through defects with ID sizes as small as 20-μm. However, the surface tension of safranin red dye is well below the surface tension

values of liquid food products measured in this study. The corrected pressures for the same packages are similar to the threshold pressure of 3.99 kPa required to initiate flow of TSB through a defect with an ID of 20-μm. Therefore, under the same conditions, flow will result for liquids with surface tensions equal to or less than that of TSB through defects with 20-μm IDs. Such liquid food products are fruit punch, evaporated milk, grapefruit juice, fruit drink and 2% fat chocolate milk, and require threshold pressures of 3.79 kPa, 3.77 kPa, 3.76 kPa, 3.65 kPa, and 3.62 kPa, respectively, to initiate flow through defects with 20-μm IDs (Table 2).

Sweep resonance tests

Maximum and minimum values of pressures for packages during sweep resonance testing are found in Table 3. Half-gallon cartons produced the largest value for imposed vacuum; 1.72 kPa at a resonance frequency of 25.1 Hz. One-gallon plastic milk jugs generated the largest value for imposed positive pressures; 2.21 kPa at a resonance frequency of 72.0 Hz.

During random vibration testing, general upward trend for imposed vacuum and positive pressure values were observed as the volumes and body panel sizes increased for packages. Such trends were not evident for packages during sweep resonance testing. The difference in the values are, in part, a result of the nature of the tests. A sweep

Table 3. *Maximum pressures generated inside water filled packages during sweep resonance testing at 25 °C.*

Package	Fill Volume	Vacuum (kPa)	Frequency (Hz)	Positive Pressure (kPa)	Frequency (Hz)
Aseptic package	250 ml	-1.31	15.00	1.65	45.40
Metal can	425 ml	-1.39	7.30	1.31	5.40
Quart carton	946 ml	-1.39	12.40	1.39	99.00
Half-gallon carton	1.89 L	-1.72	25.10	1.38	3.80
One-gallon jug	4.25 L	-1.03	56.00	2.21	72.00

resonance test consists of smooth transitions through vibration test frequencies. A random vibration test consists of abrupt changes of the test frequency causing immediate upward or downward directional changes of the test package. The abrupt changes cause liquids to compress and exert outward pressure on the body wall panels of the package. Packages with large surface areas like those on plastic jugs, permit the liquid to flex package panels to a greater degree than smaller packages. Liquid displacement and flexing of the package panels cause vacuums and impose positive pressures within the package.

Pressure and surface tensions have been identified as significant components in the onset of the initiation of liquid flow through a defect to establish a leaker. The conversion of defects to leakers is a significant process because leakers in packages result in post process contamination (*2,19,26*). Upon flow initiation, a fluid pathway through the defect that joins the sterile contents of the package to the surrounding environment is established. Hagen-Pouiseuille's equation has not been employed to characterize the interaction between the physical characteristics of liquid food products, and defect sizes found within packages to determine their contribution to the development of a leak. Characterization of a liquid product by its physical attributes such as surface tension has contributed to the quantification of forces required the onset of a leak.

Threshold leak size

In this study, we have quantified the role of surface tension and imposed pressure in converting a defect of a given ID size into a leak. Since no significant differences were

found between the observed threshold pressures and the threshold pressure values predicted by M2 for safranin red dye, tryptic soy broth, or distilled water, equation 6 can be rearranged to solve for the hydraulic diameter, or the threshold leak size as follows

$$D_H = 4\sigma\left(\frac{P_0}{0.272} + \rho gL\right)^{-1} \qquad (7)$$

Pressures generated within a package during random vibration testing can be substituted for the imposed pressure P_O. Surface tension and density values for liquid food products found in Table 1 can be substituted for σ and ρ, respectively. Values for the static head from Table 2 can be substituted for ρgL. The threshold defect size, per pressure and a static head for each liquid, were calculated for grapefruit juice, grape drink, and tea using these values (Fig. 5). An increase in pressure resulted in a decrease in the threshold leak size, as shown in Figure 5. A change of leaker location from the lowest point to the highest point in a package will change the threshold pressure and threshold leak size due to the difference of static head pressure. Therefore, as static head increases in a package, the amount of additional imposed pressure required to initiate liquid flow is reduced.

The difference between the values for the theshold pressure and the threshold leak size for liquids in packages with the same static head are due to the effects of liquid surface. The calculated theshold pressure and threshold leak size are shown for grapefruit juice, grape drink, and tea in Figure 5. Threshold pressure and threshold leak size differences for each liquid were due to dissimilarities between their liquid surface tensions.

The surface tension for grape drink was 60.79 mN/m compared those for tea and grapefruit juice at 51.36 mN/m and 42.69 mN/m, respectively (Table 1).

CONCLUSIONS

The magnitude of imposed pressures required to convert a defect to a leaker is dependent on the defect size and the surface tension of the liquid food product. To initiate a leak, the imposed pressure must over come the force of the liquid surface tension and initiate liquid flow through a microtube. As microtube ID size decreases, the threshold imposed pressure for a given liquid increases. As the surface tension decreases, the threshold pressure decreases for all microtube ID sizes.

The magnitude of imposed pressure required to initiate liquid flow is also dependent on the location of the defect due to differences in the static head pressures. Imposed pressures and vacuums generated within packages during random vibration testing are of sufficient magnitudes to initiate the flow of a liquid food products through microleaks with IDs of 20μm.

In the future, a relationship between the threshold leak size and the critical leak size may be established. The critical leak size is the defect size at which sterility of the package is lost. Such information would provide a foundation by which manufacturers could avoid inherently problematic conditions, as well as empirically evaluate and tailor leak detection equipment for their specific needs.

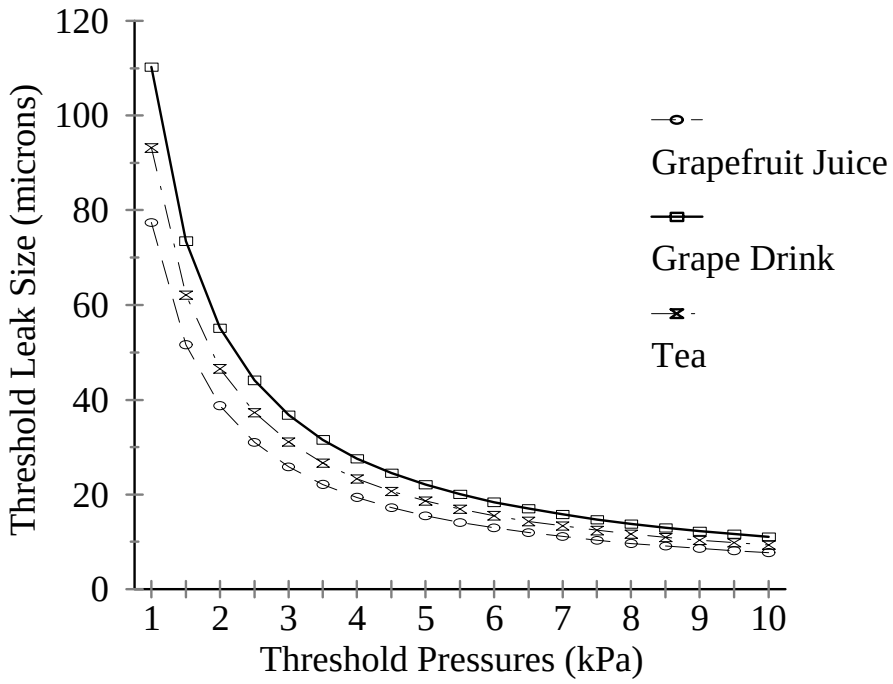

FIGURE 5. *Calculated threshold leak sizes per imposed pressure for grapefruit juice, tea, and grape drink with surface tensions of 42.69 mN/m, 51.36 mN/m, and 60.79 mN/m respectively. Calculations were based on a fill height of 10 cm.*

REFERENCES

1. Anonymous. 1996. Fisher Surface Tensiomat; Instruction. p. 10. Fisher Scientific, Atlanta, GA.

2. Amini, M. A. and D. R. Morrow. 1979. Leakage and permeation: Theory and practical applications. Package Dev. and Sys. May/June: 20-27.

3. Arndt, G.W. 1992. Examination of flexible and semirigid containers for integrity. Ch. 21A. *In* Bacteriological Analytical Manual, 7th ed. AOAC, Arlington, VA.

4. ASTM Committee D-445. 1996. *Standard Test Method for Kinematic Viscometers of Transparent and Opaque Liquids (the Calculation of Dynamic Viscosity)*, p. 169-176. Am. Soc. For Testing and Materials, Philadelphia, PA.

5. ASTM Committee D-446. 1996. *Standard Specifications and Operating Instructions for Glass Capillary Kinematic Viscometers*, p. 177-199. Am. Soc. For Testing and Materials, Philadelphia, PA.

6. ASTM. 1996. Standard Methods for Vibration Testing of Shipping Containers, D 999, p. 153-157. Am. Soc. For Testing and Materials, Philadelphia, PA.

7. ASTM. 1996. Standard Practice for Performance Testing of Shipping Containers and Systems, D 4169, p. 551-561. Am. Soc. For Testing and Materials, Philadelphia, PA.

8. ASTM. 1996. Standard Test Method for Random Vibration Testing of Shipping Containers, D 4728, p. 740-745. Am. Soc. For Testing and Materials, Philadelphia, PA.

9. Blakistone, B.A., S.W. Keller, J.E. Marcy, G.H. Lacy, C.R. Hackney, and W.H. Carter, Jr. 1996. Contamination of flexible pouches challenged by immersion biotesting. J. Food. Prot. 59 (7): 764-767.

10. Bird, R. B., W. E. Stewart, and E. N. Lightfoot. 1960[a]. Velocity distributions in laminar flow. Ch. 2, p. 46. *In* Transport Phenomena. John Wiley & Sons, Inc., New York.

11. Bird, R. B., W. E. Stewart, and E. N. Lightfoot. 1960[a]. Interphase transport in multicomponent systems. Ch. 21, p. 648. *In* Transport Phenomena. John Wiley & Sons, Inc., New York.

12. Butler, J.N. and Bloom, B.H. 1966. A curve-fitting method for calculating interfacial tension from the shape of a sessile drop, Surf. Sci. 4:1-17.

13. Beyer, W.H. (eds.). 1976. Standard mathematical table. 24th ed. Chemical Rubber Company. Cleveland, Ohio.

14. Chen, C., B. Harte, C. Lai, J. Pestka and D. Henyon. 1991. Assessment of package integrity using a spray cabinet technique. J. Food. Prot. 54(8):643-647.

15. Davidson, P. M. and I. J. Pflug. 1981. Leakage potential of swelled cans of low-acid foods collected from supermarkets. J. Food. Prot. 44(9):692-695.

16. Davis, R. 1998. Personal communication.

17. Denn, M. 1980. Pipe flow. Chapter 3. *In* Process Fluid Mechanics. Prentice-Hall, Inc., Englewood Cliffs, NJ.

18. Floros, J.D. and V. Gnanasekharan. 1995. Determination of critical leak size by analysis of gas and aerosol flow. Symposium Proceedings: "Advances in Aseptic Processing and Packaging Technologies," Copenhagen, Denmark. September 11-12.

19. Gilchrist, J. E., U. S. Rhea, R. W. Dickerson, and J. E. Campbell. 1985. Helium leak test for micron-sized holes in canned foods. J. Food Prot. 48(10):856-860.

20. Guazzo, D. M. 1994. Package Integrity Testing. *In* Parenternal Quality Control. M.J. Akers, (Ed.) , 2nd edition. p 247-276. Mercel Dekker, New York.

21. Hoffman, W. 1996. Cooperative research and development agreement. Phillips Laboratory, OLAC PL/RKFE, Edwards, CA.

22. Hurme, E.U., G. Wirtanen, L. Axelson-Larsson, N. A. M. Pachero, and R. Ahvenainen. 1997. Penetration of bacteria through microholes in semirigid and retort packages. J. Food. Prot. 60(5): 520-524.

23. Kamei, T., J. Sato, A. Natsume, and K. Noda. 1991. Microbiological quality of aseptic packaging and the effect of pinhole on sterility of aseptic products. Pack. Technol. and Sci. 4:185-193.

24. Keller, S. W., J. E. Marcy, B. A. Blakistone, G. H. Lacy, C. R. Hackney, and W. H. Carter, Jr. 1996. Bioaerosol exposure method for package integrity testing. J. Fd. Prot. 59(7): 768-771.

25. Koopman, L.H. 1987. Appendix Tables. p. 604. *In* Introduction to Contemporary Statistical Methods, 2nd ed. Duxbury Press, Boston.

26. McEldowney, S. and M. Fletcher. 1988. Bacterial desorption from food container and food processing surfaces. Mirob. Ecol. 15:229-237.

27. McEldowney, S. and M. Fletcher. 1990. A model system for the study of food container leakage. J. Appl. Bacteriol. 69:206-210.

28. McEldowney, S. and M. Fletcher. 1990. The effect of physical and microbiological factors on food container leakage. J. Appl. Bacteriol. 69:190-205.

29. Michels, M. J. M. and B. L. Schram. 1979. Effect of handling procedures on the post-process contamination of retort packages. J. Appl. Bacteriol. 47:105-111.

30. Morton, D. K., G. L. Nicholas, L. H. Troutman, and T. J. Ambrosio. 1989. Quantitative and mechanistic measurements of container/closure integrity. Bubble, liquid, and microbial leakage test. J. Parenteral Sci. and Technol. 43(3): 104-108.

31. Pflug, I. J., P. M. Davidson, and R. G. Holcomd. 1981. Incidence of canned food spoilage at the retail level. J. Food. Prot. 44(9),682-685.

32. Placencia, A. M., G. S. Oxborrow, and J. T. Peeler. 1986. Package integrity methodology for testing the biobarrier of porous packaging. Part II: FDA exposure-chamber method. Med. Dev. and Diag. Ind. 8(4) 46-53.

33. Put, H. M. C. and W. R. Warner. 1972. The Mechanism of microbiological leaker spoilage of canned foods: a review. J. Appl. Bacteriol. 35:7-27.

34. Put, H. M. C., H. T. Witvoet, and W. R. Warner. 1980. Mechanism of microbiological leaker spoilage of canned foods: Biophysical aspects. J. Food. Prot. 43(6):488-497.

35. Rey, C. R., G. A. Halaby, E. V. Lovgren and T. A. Wright. 1982. Evaluation of a membrane filter test kit for monitoring bacterial counts in cannery cooling waters. J. Food Prot. 45:1087-1090.

36. Stersky, A., E. Todd, and H. Pivnick. 1980. Food poisoning associated with post process leakage (PPL) in canned foods. J. Food Prot. 43(6):465-476.

37. Weast, R. C. and M. J. Astle. 1980. *Chemical Rubber Company Handbook of Chemistry and Physics*, 60th edition, p. F-130, CRC Press, Boca Raton, FL.

38. Whitaker, S. 1968. Introduction. In *Introduction to Fluid Mechanics*, Ch. 1, p. 22. Krieger Publishing Co, Malabar, FL.

39. White, F. M. 1986. Viscous flow in dusts. In *Fluid Mechanics*, 2nd edition. Ch. 1, p.1-43. McGraw-Hill, Inc., New York, NY.

APPENDIX A. MEASUREMENTS REQUIRED FOR THE EQUATION FOR THE INITIATION OF LIQUID FLOW

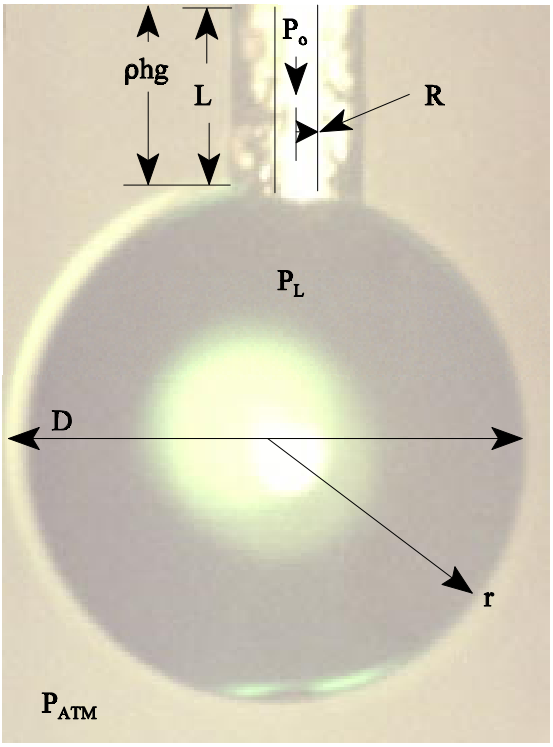

FIGURE 1. *Liquid droplet formation of diameter (D) and radius (r) on the end of a microtube with a 25μm radius (R) and 7 mm length (L) as a result of the combined forces of imposed pressure (P_o), liquid static head (ρhg), and atmospheric pressure (P_{ATM}).*

APPENDIX B. SURFACE TENSION MEASUREMENT METHOD

The following was established for the Fisher Surface Tensionmat, Model 21 for use with a 6-cm circumference platinum ring for the du Noüy method, to determine the apparent surface tension of model solutions.

A platinum-iridium ring of precisely known dimensions is suspended from a counter-balanced lever-arm. The arm is held horizontal by torsion applied to a taut stainless steel wire. Increasing the torsion of the wire will cause the arm and the ring to raise. The raised ring carries with it a film of the liquid in which it is immersed. The "apparent" surface tension can be found on the calibrated dial. Dial readings can be converted to "absolute" values by preparing a correction factor chart.

Materials

Clean glassware, fresh chromic-sulfuric acid cleaning mixture, distilled water.

Methods

Clean platinum ring and rinse in benzene, acetone, and distilled water. Air dry. Heat in the oxidizing portion of a Bunsen burner. Calibration consists of adjusting the torsion arm length so that the dial scale will read in dynes per centimeter. Secure the torsion arm. Cut a strip of paper to fit onto the ring. Release the torsion arm. Adjust the knob on the right

side of the case so that the index level of the arm is opposite the reference line of the mirror. Turn the knob beneath the main dial until the vernier reads zero. Secure the torsion arm. Place a standardized weight between 500 and 800 mg (e.g. 600 mg) on the paper platform. Release the torsion arm and adjust the knob on the right side of the case in a counterclockwise direction until the index level of the arm is opposite the reference line of the mirror. Record the dial reading to 0.10 division and secure the torsion arm. Calculate the apparent surface tension as follows:

$$S = (M \times g)/2L \qquad (1)$$

where, M is the weight placed on the paper platform in grams, g is the acceleration of gravity (cm/sec^2), L is the mean circumference of the ring (cm) and S is the apparent surface tension in dynes/cm.

Should the dial reading differ from the calculated value, the effective length of the torsion arm must be adjusted until these two values agree. This adjustment can be made by turning the knurled knob at the left end of the lever arm to move the hanger hook. Each unit of the scale should now represents a pull on the ring of 1 dyne/cm.

$$S = (0.500 \times 980)/(2 \times 6.02) = 40.7 \ dynes/cm \qquad (2)$$

A conversion factor may be multiplied by the scale reading to give a corrected surface tension in dynes per centimeter. After calibration, it is convenient to calculate the number of grams total pull on the ring that is represented by each scale division. This is done by

dividing the scale reading into the weight used for the calibration, (i.e., 0.500/40.7 =0.01229 g).

Measuring Surface Tension

Insert the clean platinum ring and check the plane of the ring. Set the dial and vernier at zero. Adjust the knob on the right side of the case until the index level of the arm is opposite the reference line of the mirror. Place the solution to be tested on the sample table. Raise the sample table until the ring is just submerged. About 1/8 inch immersion is considered sufficient. Release the torsion arm and adjust the knob on the right side of the case until the index level of the arm is opposite the reference line of the mirror. Be careful to keep the ring in the liquid during this manipulation. Turn the knob beneath the main dial until the vernier reads zero. Lower the sample table slowly until the ring is in the surface of the liquid, while at the same time adjusting the knob on the right side of the case to keep the index lined up with the reference mark on the mirror. These simultaneous adjustments must be carefully proportioned so that the ring system remains constantly in its zero position. Continue the two simultaneous adjustments until the distended film at the surface of the liquid breaks. The scale reading at the breaking point of the distended film is the apparent surface tension. As the breaking point is approached, the adjustments must be made more carefully and more slowly. Make at least two measurements. Record the temperature and the surface age at the time of the testing. Since the submerging of the ring may cause a significant disturbance of the surface, take the age as the elapsed time between

submersion and breakaway of the ring. In most cases, an accuracy of ± 5 s is reasonable.

Calculation and Report

The uncorrected surface tension must be multiplied by a correction factor, F, to give the corrected surface tension. F is a function of the contours of the liquid surface in the neighborhood of the ring at the instant of breakaway

$$F = f(R/r,\ R3/V) \tag{3}$$

where R is equivalent to $L/2\pi = 6.02\ cm/2\pi = 0.96$ cm, r is equal to 0.007 in or 0.018 cm, the ratio R/r is equal to 0.96/0.018 or $53.3 \approx 53$ and R^3 is 0.88. The following equation can be used as well

$$(F - a)^2 = \frac{4b}{(\pi R)^2} \times \frac{P}{(D - d)} + K \tag{4}$$

or

$$F = 0.7250 + \sqrt{\frac{0.0145 \times P}{C^2(D - d)} + 0.04534 - \frac{1.679 \times r}{R}} \tag{4a}$$

where F is the correction factor for surface tension, R is the radius of the ring, r is the radius of the wire of the ring, P is the apparent value or dial reading, D is the density of the lower phase, d is the density of the upper phase, K is equal to 0.04534 - 1.679 r/R,

C is the circumference of the ring, a is equal to 0.725 and b is 0.0009075.

The value of V can be calculated from the following equation:

$$V = M/(D - d) \qquad (5)$$

where M is the weight of liquid raised above the free surface of the liquid, D is the density of liquid, d is the density of air saturated with vapor of the liquid. To calculate M, multiply the tensiometer dial reading by the factor (0.01229 g).

APPENDIX C. EQUATION FOR THE INITATION OF LIQUID FLOW

The equations that follow consider the ambient, imposed, and droplet internal pressure and size of the resultant fluid droplet formed at the end of the microtube as a function of the internal diameter and length of the microtube.

$$P_0 - P_L = P_0 - [P_L - pgL] = P_0 - P_L + pgL \quad (1)$$

$$P_0 - P_L + pgL = \triangle P \quad (2)$$

Equations 2 and 3 establish ΔP from using different measurements. The relationship between the defect dimensions or hole size and the fluid surface tension is therefore established. ΔP can be defined as a function of the internal pressure within the droplet formed by a fluid of a known viscosity, imposed pressure and microtube length (equation 2), or in terms of surface tension and microtube radius (equation 3).

$$\triangle P = 2\sigma / r \quad (3)$$

Therefore, microbial ingress may be indirectly influenced by channel length in that the channel length is a value used to determine/calculate ΔP.

Next, the terms for fluid surface tension, fluid viscosity, atmospheric and imposed pressures are considered

$$P_O - P_L = P_O - [P_{ATM} + 2\sigma / r - pg] \quad (4)$$

$$P_O - [P_{ATM} + 2\sigma / r - pg] = P_O - P_{ATM} + 2\sigma / r + pgL - 2\sigma / r \quad (5)$$

The resultant equation permits the calculation of the internal droplet pressure as a function of surface tension and hole radius, rather than fluid density and hole length as shown in equations 1 and 2, internal droplet pressure:

$$P_L = P_{ATM} + 2\sigma / r \quad (6)$$

where P_O is the imposed pressure, P_L is the internal pressure in droplet, σ is the surface tension, r is the droplet radius, R is the tube radius, μ is the fluid viscosity, p is the fluid density, L is the capillary length, and g is the acceleration of gravity.

Since the internal pressure within the droplet can be calculated per a given hole size via measurement of the fluid droplet radius and fluid surface tension, an initiation for liquid flow equation can be established. The equation for liquid flow is:

$$P_0 - P_L > 0, \quad P_0 > P_{ATM} + [(2\sigma/r - pgL) \times 0.272] \qquad (7)$$

where 0.272 is a correction factor as explained in Section II.

Once flow is established, the flow rate of the fluid through the hole/defect can be determined. The flow rate is a key component for the calculation of the evaporation rate.

Values for the fluid flow rate and evaporation rate are important for the following reasons: 1) if the fluid flow rate is greater than the evaporation rate, the fluid in the hole/defect can provide a conduit or a pathway for ingress of microorganisms or chemicals into the package, 2) if the fluid flow rate is less than the evaporation rate, the fluid within the hole/defect will evaporate, leaving solids which may block or "plug" the hole.

The imposed pressure and the resultant droplet radius will be measured for model fluids of each surface tension, viscosity and density via pressure gauge and micro video calipers. These values will be used to calculate the criteria for flow, molar flow rate (equation 9) and evaporation rate (equation 12) for the model solution.

The criteria for flow will establish a small numerical range that will quantify the imposed force (i.e., pressure or vacuum) required to overcome the fluid characteristics so that flow is initiated. The flow value units are reported in psia or kPa. Capillary volumetric flow

$$Q = \frac{\pi (P_0 - P_L) R^4}{8 \mu L} \qquad (8)$$

Mass flow:

$$M = Q \times P_{water} \quad (9)$$

Molar Flow rate:

$$W_A = M / MW_{water} \quad (10)$$

The Molar Flow Rate (MFR) represents the fluid flow rate through a capillary. The evaporation rate quantifies the portion of fluid that phase shifts from liquid to gas form due to the surface area of a fluid at a given point and flow rate. The evaporation rate will be reported in units of g mole/cm^3.

$$W_A = k_{xm} \pi (2r)^2 [X_{Ao} - X_{A\infty} / 1 - X_{Ao}] \quad (11)$$

where k_{xm} is the mass transfer coefficient, X_{Ao} is the mole fraction of water in the capillary, and $X_{A\infty}$ is the mole fraction of water in air calculated from relative humidity measurements at 25°C.

$$X_{A\infty} = p_w / P_{ATM} = H_R p_w / 100\ p_{ATM} \quad (12)$$

where H_R is the (partial pressure of water/vapor pressure of water) x 100, p_w is the vapor pressures of water, and p_w is the partial pressure of water.

$$W_A = 4 \pi r^2 x k_{xm} [X_{Ao} - X_{A\infty} / 1 - X_{A\infty}] \quad (13)$$

considering the diffusion coefficient of water in air.

Because fluid surface tension decreases as temperature increases, the surface tension, viscosity and density for each model fluid will be measured at 4.4°C, ambient temperature (≈ 25°C) and 37°C. A model developed by Eötvös predicts a linear decrease in the surface tension per mole with increasing temperature. The model also predicts that the surface tension vanishes at the critical temperature (equation 14).

$$\sigma (M/p)^{2/3} = k(T_c - T) \qquad (14)$$

where M is the molecular weight of the liquid, p is the fluid density, T_c is the critical temperature of the liquid, T is the working temperature, σ is the surface tension, and where $k = (M/p)^{2/3}$.

APPENDIX D. DIAGRAM OF PACKAGE PREPARATION FOR VIBRATION TESTING, AND PACKAGE HOLDING DEVICE

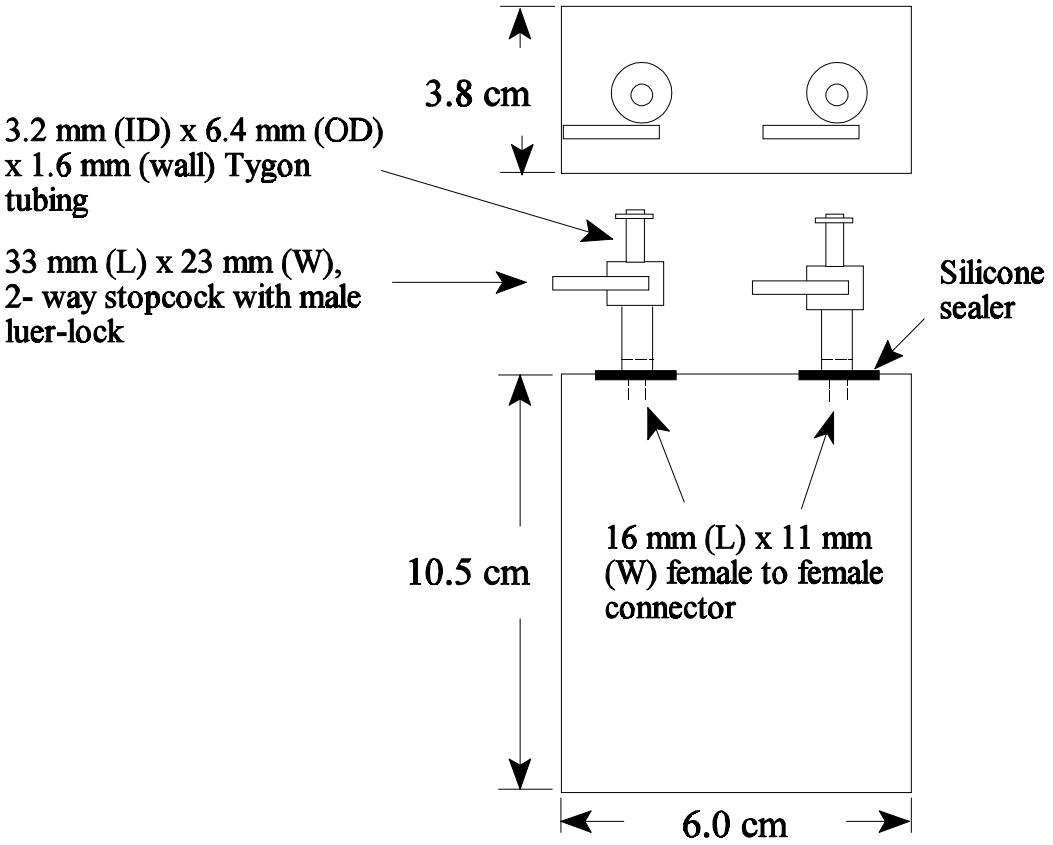

FI

GURE 1. *Illustration of fittings attached to an aseptic brick-pack used to measure imposed pressures generated within a package. All packages in this study were fitted with identical fixtures.*

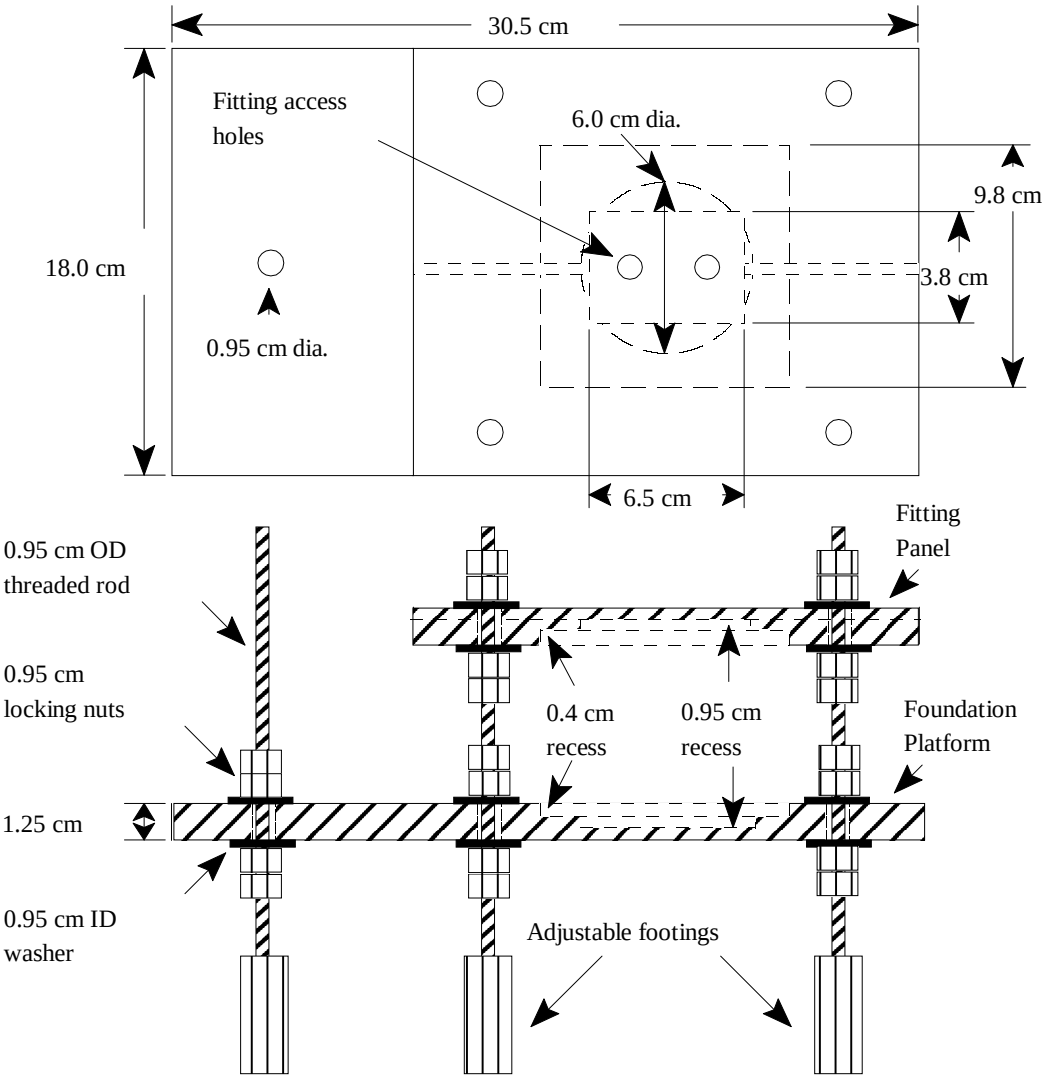

FIGURE 2. *Package holding device for distribution simulations. Adjustable for holding gable top cartons, brick packs, cans, half gallon and one gallon plastic milk jugs.*

SECTION III: APPLICATION OF FLUID AND STATISTICAL MODELING TO ESTABLISH THE LEAK SIZE CRITICAL TO PACKAGE STERILITY

(Paper formatted for submission to the Journal of Food Protection)

ABSTRACT

Onset of liquid flow through a defect as a result of imposed pressures or vacuum was linked to the sterility loss of a package. Five-hundred sixty-seven test cells with microtubes of 0, 2, 5, 7, 10, 20 or 50 μm, were manufactured to simulate packages with defects. They were biochallenged via an aerosol concentration of 10^6 cells/cm^3 of *Pseudomonas fragi* Lacy-1052, under conditions of imposed pressure or vacuum of 20.7, 13.8, 6.9, 0, -6.9, -13.8, -20.7 kPa, respectively and temperatures of 4°, 25° and 37°C. A statistically significant relationship between loss of sterility due to microbial ingress in test cells and the initiation of liquid flow were found ($p < 0.05$). Microbial ingress was not found in test cells with microtube internal diameters (IDs) of 2 μm under any conditions. Leak sizes critical to sterility maintenance were based on the relationship between liquid surface tension and imposed pressure. Threshold leak sizes where the onset of liquid flow was initiated, and critical leak sizes at which loss of sterility occured, were not significantly different ($p > 0.05$).

Key words: threshold leak size, critical leak size, package defect, sterility maintenance

INTRODUCTION

Sterility maintenance assurance continues to be a prominent concern for producers of aseptically packaged products. Such producers have aggressively embraced new technologies to manufacture flexible and semi-rigid packaging. Although many technologies have been developed to maintain package sterility, a problem that remains unresolved is the identification of the critical leak size. The critical leak size is that at which container sterility is jeopardized (*8*).

Presently, differences can be found in the scientific literature regarding the the critical leak size. Howard and Duberstein (*14*) found that under specific conditions certain types of water borne bacteria penetrated 0.2-μm membrane filters and therefore speculated that the minimum hole size critical to sterility maintenance and integrity of the package, or the critical leak size, is between 0.2-μm and 0.4-μm. This range was selected based on the size of membrane filters used routinely for aseptic packaging and clean room applications with little significant microbial contamination. Lampi (*21*) demonstrated bacterial penetration via holes of less than 10-μm was unlikely. Lake et al. (*20*), during an extensive 4-year study, found leaks must be considerably larger than 1-μm for bacterial penetration to occur. Gilchrist et al. (*11*) showed bacterial contamination of cans from cooling water requires pinholes larger than 5-μm. McEldowney and Fletcher (*24*, *25*) found that holes of 1-μm permitted microbial entry under certain conditions. Chen et al. (*6*) observed that 5-μm pin holes allowed microbial aerosol penetration. Board (*4*) found

the pores of eggs (7-μm and 10-μm IDs) would permit microbial ingress when washed in liquids warmer than the egg or when stored in conditions of high relative humidity. Jarrosson (*16*) found that a 20-μm diameter hole with a 5-mm channel length permitted microbiological contamination in Meal Ready to Eat (MRE) pouches.

Much of the discrepancy over the threshold leak size in the aforementioned studies rest in the inability to manufacture and maintain the integrity of the leak size during the process of experimentation. The problem is further magnified for small hole diameters such as 10-20 μm internal diameters (ID) (*12, 16*).

Differences can also be found with regards to the leak sizes which are readily detectable using current on-line technology versus the speculated value for the critical leak size. It has been suggested that package inspection systems are available which can provide sufficient safety assurance and detection for microleaks with IDs of 10-μm for pinholes and 50-μm for channel leaks (*33*). However, the critical leak size is believed to be $\leq$ 10-μm for channel leaks (*3*). The emphasis of research found in the scientific literature is sharply focused on package leak detection (*2, 11, 23, 28, 30, 32*).

A paradigm shift in package integrity research is currently underway. The emphasis of the most recent research suggest that physical factors, such as the development of a leaker, are responsible for the loss of package sterility *(2, 17, 24, 25, 26*). An equation was established to quantify the forces required to initiate flow of a liquid of a given surface tension, through a defect with a known diameter, to produce a leaker (*18*). The defect size at which the onset of liquid flow is initiated is called the threshold leak size

(*18*).

After liquid flow initiation, a liquid pathway through the defect linking the interior of a package to the exterior may be present (*18*). Liquid food product on the outside of a package as a result of passage through a defect from the package interior has been long suspected of facilitating post-process contamination (*2, 20, 26, 30*). The incidence of post-process contamination is well documented, however, the mechanism by which post-process contamination occurs remains unquantified (*20, 28,31,32*).

In this study, equations for the initiation of liquid flow, and the threhsold leak size will be used in an effort to establish a relationship between the threshold leak size, the critical leak size, and loss of package sterility (*18*). Variables of temperature, imposed pressure and vacuum were examined to determine their relationship to the leak size critical to the sterility of a package.

MATERIALS AND METHODS

Microtubes

Nickel microtubes were supplied by the Phillips Laboratory, Fundamental Technology Division, Carbon Research Laboratory, Edwards Air Force Base, CA through a Cooperative Research and Development Agreement (*13*). Sixty-three (nine of each size) microtubes with IDs of 0, 2, 5, 7, 10, 20 and 50 μm and 7 mm in length were used as the manufactured defects. Solid microtubes were used as a control (Fig. 1).

Exposure chamber

The exposure chamber was constructed of Lexan® in dimensions of 35-cm (L) x 25-cm (W) x 25-cm (H). The internal area of the exposure chamber is 21,875-cm^3, and is divided into two sections: 1) top; utility section, 2) bottom, the exposure section. The utility section (dimensions: 35-cm [L] x 25-cm [W] x 18-cm [H]; total area = 15,750-cm^3) housed the vacuum, water input and recovery manifolds, all related tubing, vacuum and compressor tubing, as well as the test cells (Figures 2 and 3). The neck of each test cell passed through one of seven 2.85-cm holes in the partition. The top and end panels of the exposure chamber had stainless steel handles and were removable. The entry ports were created using two brass male and female threaded fittings with rubber O-rings

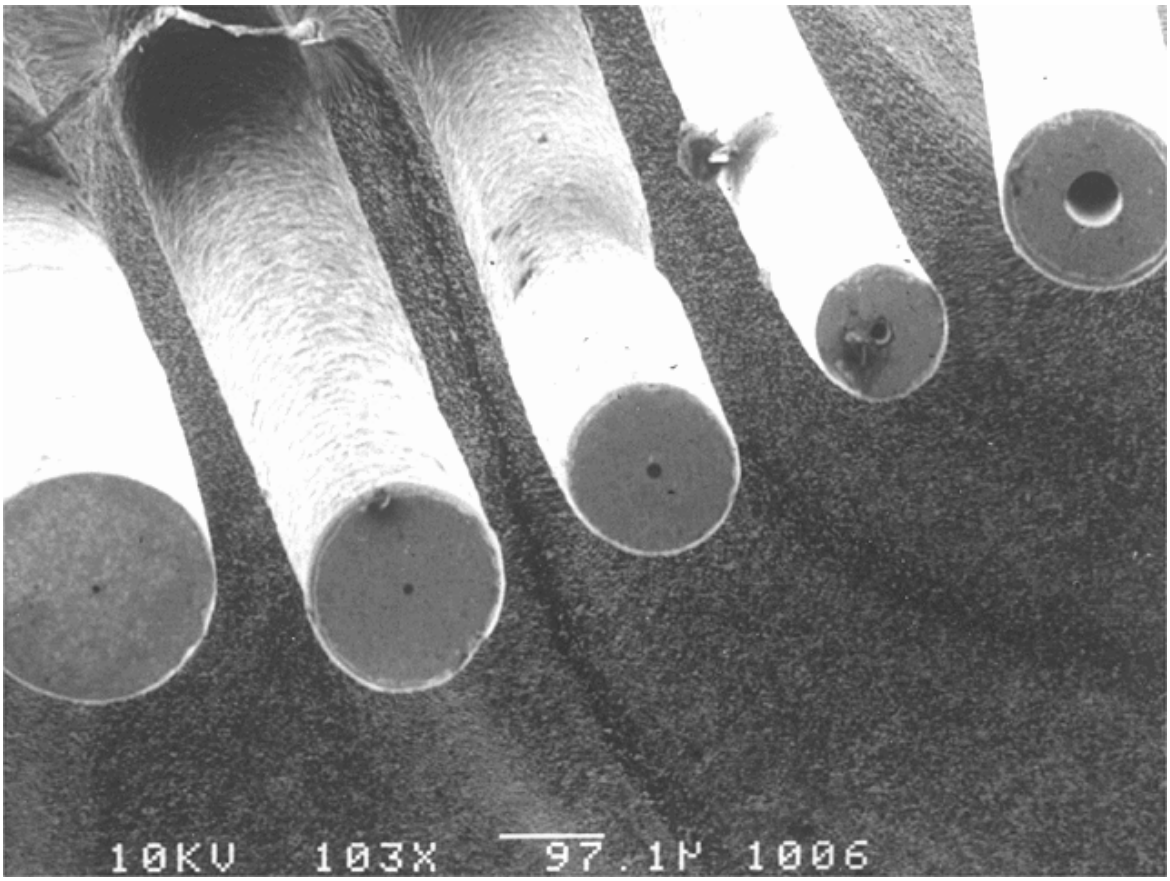

FIGURE 1. *Electron micrograph showing end views of nickel microtubes with IDs of 2μm, 5μm, 7μm, 10μm, and 50μm. Each of the microtubes are 7 mm in length.*

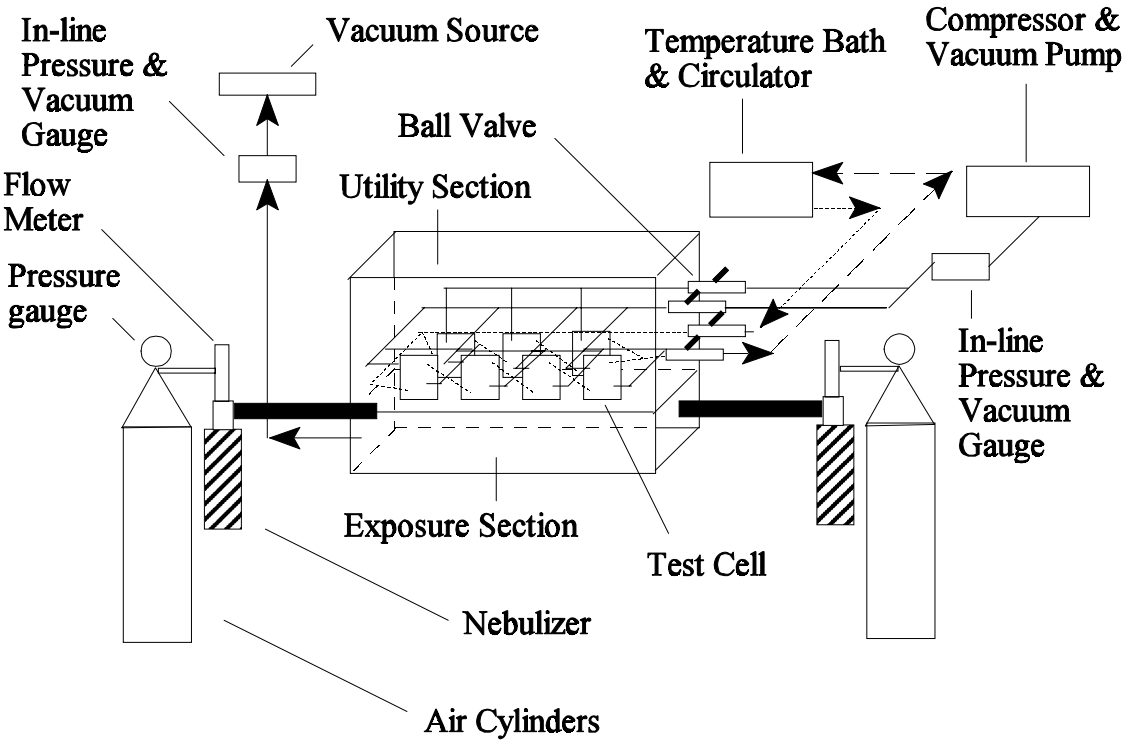

FIGURE 2. *Diagram of equipment set-up for bioaerosol challenge of test cells in the exposure chamber.*

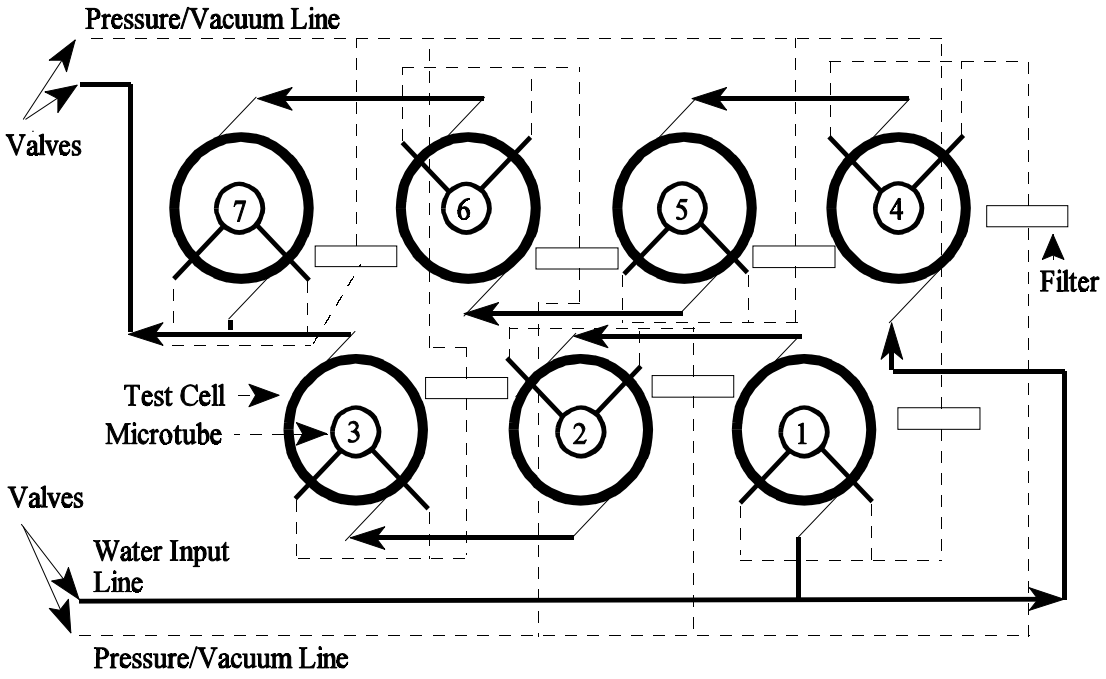

FIGURE 3. *Schematic of exposure chamber utility section showing test cell positions 1-7, water, imposed positive pressure/vacuum input, exit manifolds, valves, and in-line filters.*

The exposure section (dimensions: 35 cm [L] x 25 cm [W] x 7 cm [H]; total area = 6125 cm^3) has entry ports positioned in the center of opposing panels of the exposure chamber for bioaerosol delivery. Nebulizer kits (Baxter model 2D0807, Toronto, Ontario, Canada) with a mass median aerodynamic diameter of 2.68-μm, a geometric standard of 1.85 μm, and a mass of aerosol per minute of 1.1-μm and 4.7-μm were used. The maximum air flow (ml/h) at 10 Lpm was 21.9-ml/h. Four 6.9-m^3 size E cylinders, each equipped with CGA 346 air (0 - 15 Lpm) flow meters were used for the air supply. Twenty-one 37-mm, 0.33-μm inline bacterial air vents (product no. 4210, Gelman Sciences, Ann arbor, MI) were used to filter air flowing into the sterile test cells. The bacterial vents were also used on the pressure equalization ports for the utility and exposure sections of the exposure chamber. Pressure inside the exposure chamber was equilibrated and maintained at room pressure using 0.41 kPa of vacuum.

Test cells

Glass test cells were developed for the purpose of simulating imposed pressure within a package while maintaining sterility. The glass test cell dimensions are 8-cm [H] x 5-cm [D]. Each test cell consists of a 45-mm [H] x 15-mm [D] glass vial (3-ml capacity) encased in a 85-ml glass water jacket. The vial and the jacket have one entry and one exit port each. The vial has a glass lug for a septa closure (*18*).

Test organism

Pseudomonas fragi Lacy-1052, selected from the library of the Department of Plant Pathology, Physiology and Weed Science, Virginia Polytechnic Institute and State University, Blacksburg, VA was used as an indicator of sterility. *Pseudomonades* are aerobic, gram-negative, motile, nonsporeforming, catalase-positive rods with polar flagella, ranging from 0.5-1.0 μm in diameter and 1.5-5.0 μm in length. Optimal temperature and pH ranges are 25°-30°C and 6.6-8.5, respectively. *Pseudomonas fragi* L-1052 was differentiated by antibiotic resistance to kanomycin (30-μg/ml) and tetracycline (10-μg/ml).

Preparation of test cells

Microtubes were positioned inside a 27-gauge syringe needle. The needle was used to puncture and penetrate through the center of a silicone septum. The syringe needle was removed, leaving the microtube in place. The internal diameter of each microtube was measured to obtain the cross-sectional area using a light microscope (Olympus Model BH-2, Lake Success, NY) equipped with video callipers.

Septums containing microtubes were positioned on top of the test cell finish. Glass lugs of the test cell were wrapped with teflon tape, overlapping the top outside circular edge of the septum. Septa caps were placed over the septums and tightened. DAP™ silicone sealer (Dow Corning, Dayton, OH) was used to seal the septa surface around the microtube and the septum-septa cap contact area. Seal integrity of test cells were confirmed using the safranin red dye test, bubble leak test, and vacuum test (*18*).

Preparation of exposure chambers

Seven test cells, each with a microtube of a different internal diameter, were randomly assigned one of seven positions within the exposure chamber. Each test cell was filled with 3-ml of tryptic soy broth (Difco Laboratories, Detroit, MI) inverted to a septa cap down position, and secured on top of a rubber gasket. All rubber gaskets received a thin coat of high vacuum grease (Dow Corning Corp., Midland, MI) on both the top and bottom surfaces. Test cells were secured to the partition by bolt-down aluminum brackets. General purpose 6.4-mm ID rubber tubing (Fisher Scientific, Atlanta, GA) with a wall thickness of 2.4-cm, were connected to the entry and exports of the vial section of each test cell. Tubes were equipped with an in-line bacterial air vent (# 4210, Gelman Sciences, Ann Arbor, MI) positioned inside the holding section to prevent contamination during post autoclave cooling. Each tube was also connected to a brass ball valve, on the exterior of the chamber. The exposure chamber was positioned so that septa caps faced up to eliminate contact of the microtubes with the liquid tryptic soy broth within each of the test cells during autoclaving.

Exposure chambers were autoclaved separately, at 121°C for 55 min. Valves on each exposure chamber were opened prior to autoclaving to facilitate sterilization and to dampen the generation of pressure differentials between the test cells, the exposure chamber and the autoclave.

Prior to the introduction of the bioaerosol into the exposure section, each exposure chamber was inverted so that the septa caps faced downward. The inverted position of the

test cells facilitated continuous contact of the liquid growth medium with the microtubes.

Preparation of bioaerosol

Inocula of 10^9 CFU/ml *Pseudomonas fragi* Lacy-1052 motile organisms were prepared according to Keller et al. (*17*). The optical density of the tryptic soy broth with the test organism growth was measured and compared to a standard. Two cartridges, each filled with a source concentration of 10^9 cells/mL of *Pseudomonas fragi* L-1052 in 200-ml of tryptic soy broth were centrifuged at 16,270 x g for 10 min (RC-5B, Sorvall Instruments, Newtown, CT). The tryptic soy broth was aseptically decanted and replaced with 200 ml of sterile Butterfield's phosphate buffer adjusted to a pH of 6.8 to 7.0. The optical density of the decanted tryptic soy broth was measured and compared to a standard. Cartridges were oscillated for one minute to resuspend the microorganisms into the solution. The final challenge suspensions were aseptically transferred to the reservoirs of the nebulizer kits.

Aerosol biochallenge

Nebulizers were secured to the external ports centered on each of the two small end panels of the exposure chamber via a sterile 2.54 cm ID x 3.2 cm OD clear PVC tubing (Nalgene, Fisher Scientific, Atlanta, GA) with a wall thickness of 3.2-cm x 45-cm in length. The exposure period was divided into a 30-min come-up period, and a 5-min static period.

The 30-min come-up period is the time required to achieve the final desired

bioaerosol concentration of 10^6 CFU/cm^3 within the exposure section. A total of 6-ml of the source concentration of approximately 10^9 CFU/ml were introduced via aerosol into the 6,125-cm^3 exposure section, for a final airborne concentration of approximately 10^6 CFU/cm^3. A vacuum of 0.42 kPa was used to maintain a pressure equilibrium between the exposure chamber and ambient conditions.

Imposed pressure and vacuum

To measure the influence of imposed pressures or vacuums on the critical leak size, positive pressures or vacuums were imposed on the internal vial of the test cell at the onset of the come-up period. Internal positive pressures of 6.9, 13.8, or 20.7 kPa, or a vacuum of -6.9, -13.8, or -20.7 kPa were imposed on the test cells at 25°C. Positive pressures and vacuums were imposed via a compressor/vacuum pump (model ROA-P131-AA, Gast, Benton Harbor, MI). General purpose rubber tubing (Fisher Scientific, Atlanta, GA) with 37 mm, 0.33 μm inline bacterial air vents (product no. 4210, Gelman Sciences, Ann arbor, MI) were used to communicate the imposed pressure from the compressor to the test cell. A 500-ml vessel with brass entry and exit barbed ports were used to stabilize the air flow from the compressor to produce pressure fluxuations of $\leq$ 0.06 kPa. An in line pressure gauge (Model HHP701-2, Omega Engineering, Inc., Stamford, CT) with a detection range of 137.9 kPa of vacuum or positive pressure, and a resolution and accuracy of 0.05% and ± 0.15% FS, respectively, was used to measure the applied imposed pressure.

After completion of the come-up period, the bioaerosol and vacuum were

discontinued, thus initiating the static period. Each chamber remained in the static period for 5 minutes at a temperature of 25°C. The static period provided time for the aerosol to initiate fall out as a result of natural sedimentation (*9, 22, 29, 31*). Aerosol residual was removed via an exposure section vent port with an in-line bacterial vent under 20.7 kPa of vacuum.

Exposure chambers were incubated for 72 h at 25°C. Following the incubation period, test cells were removed from the utility section. Turbidity of TSB within a test cell indicated a positive for loss of sterility. To confirm that loss of sterility was due to ingress of the test organism, liquid samples were aseptically transferred and plated from test cells showing turbidity and plated on tryptic soy agar with kanomycin and tetracycline, 30-μg/mL and 10-μg/mL, respectively.

Imposed temperature

To determine the effect of temperature on the critical leak size independently of pressure, vacuums or positive pressures were not imposed on test cells challenged under temperature conditions. Test cells were challenged under temperature conditions of 4°C, 25°C, or 37°C at 0.0 kPa. Temperature control was maintained using a 1:1 v/v, solution of water and ethylene-glycol using a variable temperature bath and circulator (Masterline™ Model # 2095, Forma Scientific, Marietta, OH). Target temperatures were maintained for one hour prior to biochallenge initiation.

Relative humidity

The relative humidity created by nebulizers within the exposure section of the chamber during a simulated bioaerosol challenge (without test organism) was measured. Relative humidity was measured by eight thermocouples: four-wet-bulb, each with moist, 100% cotton covers, and four-dry-bulb. Paired wet-bulb and dry-bulb thermocouples were secured in the centers and on a side wall of both the exposure and holding sections. Distilled water was introduced into the exposure section of the chamber at a combined flow rate of 20 Lpm (i.e., 2 nebulizers @ 10 Lpm each) for 30 min.

Confirmation of airborne microorganism concentration

To verify that the concentration delivered to the microtubes attached to the test cells was a 10^6 cells/cm^3 concentration, filter papers (product no. 63077, Gelman Sciences, Ann arbor, MI), were positioned within the exposure chamber to catch settling airborne microorganism from the bioaerosol. Plate counts from the filter papers were measured against plate counts obtained as a result of aerosol trapping during chamber evacuation.

Filter papers were attached via sterile water contact to test cell positions, the bottom center, and to the geometric center of a long side panel in the exposure section of the chamber. A filter was attached on the partition within the utility section of the chamber as a control. The chamber was autoclaved at 121°C for 55 min and allowed to cool to 25°C.

The exposure section of the chamber was subjected to a bioaerosol with a 10^9 CFU/mL source concentration of of *Pseudomonas fragi* Lacy-1052 for 30 min. Bioaerosol residual was evacuated under 20.7 kPa of vacuum into a 1 L flask filled with sterile water containing peptone. The contents of the flask were serially diluted and plated.

Filters were aseptically transferred to bottles containing 100 ml sterile water with peptone. Each blank was placed on a shaker, model G-2 (Gyrotory™, New Brunswick Scientific Company, Inc., Edison, NJ), for 1 min. The contents of seven blanks were serially diluted, plated and incubated at 28°C for 24 hours.

Temperature verification of test cells

Temperature verifications were performed to determine the time required to achieve temperatures of 4° C and 37°C from a starting temperature of 25°C. Thermocouples were inserted into the center of each septum of the seven test cells with ends poised 1.5-cm from the septum surface facing inward. Each test cell was filled with 3 ml of tryptic soy broth and positioned inside the exposure chamber.

Experimental design

A randomized complete block design was employed. The purpose of the block design was to independently measure the influence of positive pressure, vacuum, and temperature on the threshold defect size critical to the sterility maintenance of a package.

Seven test cells with one microtube of each available size were represented within each exposure chamber. To reduce the potential for a position effect, the order of test cells

were randomized. Each exposure chamber was replicated. Nine randomized replicates were challenged via bioaerosol per imposed pressure, vacuum or temperature condition (i.e., 9 conditions; +20.7, +13.8, +6.9, 0, -6.9, -13.8, -20.7 kPa at 25°C, and 0 kPa at 4°C and 37°C).

Two models were employed in this study; the equation for the initiation of liquid flow (M1), and a statistical model (M2). M1 was used for the calculation of threshold imposed pressures required to initiate liquid flow per microtube ID size:

$$P_O > P_{ATM} + [(4\sigma/D_H - \rho gL) \; x \; 0.272] \qquad (2)$$

where the imposed pressure (P_o) must be greater than the surface tension (σ) for a given hydraulic diameter (D_H) with a given static head (ρgL) (*18*). When threshold imposed pressures are met or exceeded, a liquid pathway through the microtube is established, indicating the threshold leak size (*18*).

M2 was designed for a fixed temperature/pressure combination in a logistic regression analysis:

$$p = \begin{cases} (1 + \exp(\beta_0 + \beta_1(Size - e^T)))^{-1} & if \; Size - e^T \geq 0 \\ 0 & otherwise \end{cases} \qquad (3)$$

where is the portion of test cells that realized ingress, $\beta 0$ is the intercept, $\beta 1$ is the slope, and e^T is the threshold value (*5*).

It is also of interest to approximate the relationship between the threshold defect

size and pressures. The following model in a binary regression analysis was used (*5*):

$$p = \begin{cases} 1 - \exp\left(-\exp\left(\beta_0 + \beta_1 \left(Size - \exp\left(c_0 + c_1\ Pressure + c_2\ Pressure^2\right)\right)\right)\right) & if\ Size - \exp\left(c_0 + c_1\ Pressure + c_2\ Pressure^2\right) \geq 0 \\ 0 & otherwise \end{cases} \quad (4)$$

With this parameterization, the threshold defect size is estimated as the following function of pressure for a given temperature (*5*):

$$\exp\left(\delta_0 + \delta_1\ Pressure + \delta_2\ Pressure^2\right) \quad (5)$$

The method of maximum likelihood was used to estimate the parameters in each of the model equations listed above. This model was designed to relate the proportion of test cells identified as positives for microbial ingress to the microtube ID. This allowed a critical leak size per a set of conditions to be established.

Statistical analysis

A non-linear regression was used for data analysis to determine significance between threshold imposed pressures per microtube ID size by M1, predicted values for the critical leak size predicted by M2 versus observed critical leak sizes. Analyses were carried out using JMP® (SAS Institute, Cary, North Carolina).

RESULTS AND DISCUSSION

Test cells

Test cells with solid microtubes showed no indications of microbial presence. This confirmed that test cells positive for microbial contamination resulted due to ingress through holes in microtubes.

Relative humidity

A relative humidity of 98% ± 1% was achieved within three minutes of iniation of nebulizers. The target relative humidity was ≥ 55%. Maintenance of high relative humidities are important for challenge tests that employ bioaerosols. Relative humidities < 32% result in erratic aerosol particle size, poor aerosol distribution, reduction of airborne microbial population and difficulties in experimental reproduction (7, *9, 10, 15, 29*).

Confirmation of airborne microorganisms concentration

Plate counts of *Pseudomonas fragi* Lacy-1052 for filter papers extracted from the side panels and bottom center of the exposure section of the chamber were 5.3×10^5 CFU/ml to 1.5×10^6 CFU/ml, respectively, with an average of 8.7×10^5 CFU/ml. Plate counts of the bioaerosol evacuated form the exposure section of the chamber were 2.8×10^5 CFU/ml to 3.5×10^7 CFU/ml with an average of 2.5×10^6 CFU/ml. This confirmed that the target airborne micoorganism concentration of 10^6 cells/cm^3 was achieved using a

bioaerosol.

Temperature verification of test cells

Temperature verification for test cells biochallenged at 4.4°C and 37.7°C were perfomed. For test cells with a target temperature of 4.4°C, an average temperature within test cells of 5.1°C ±0.3°C was acheived in 126 min from a starting temperature of 23.8°C. For test cells with a target temperature of 37.7°C, an average temperature within the test cells of 36.8°C ± 1.6°C was achieved in 28 min from a starting temperature of 23.8°C.

Biochallenge via aerosol under imposed pressure and vacuum

Threshold imposed pressures necessary for flow initiation of tryptic soy broth with a surface tension of 44.09 mN/m through microtubes of 2, 5, 7, 10, 20 and 50 μm were experimentally correlated to the onset of ingress under similar imposed pressures (Tables 1 & 2). For example, the imposed pressure required to initiate the flow of TSB through a 20 μm ID microtube was 3.45 kPa. Ingress was found in test cells with a microtube ID of 20 μm under imposed pressures > 3.45 kPa.

An imposed pressure of -13.8 kPa resulted in 19 of 54 tests cells positive for microbial ingress contamination. Ambient pressure conditions (0.0 kPa) resulted in 2 positives for contamination of 54 test cells (Table 1). Microbial ingress occurred in test cells where the pressure or vacuum required for the initiation of flow of tryptic soy broth or distilled water, were met or exceeded. Water was important in that it was employed to

transport the test organism to the test cells in the exposure chamber. Therefore, the surface tension of water was an important consideration for the process of ingress into test cells under imposed vacuums. To illustrate, the surface tension of water is 64.67 mN/m and requires an imposed vacuum of -11 kPa to initiate flow through a micrtoube with an ID of 10-μm. Microbial ingress was found in test cells where the imposed vacuum exceeded -11 kPa (Table 1).

Imposed pressures of -13.9 kPa and -20.7 kPa resulted in 4 positive test cells for microbial ingress of 9, and 1 positive of 9, respectively. The number of positives did not increase with increased imposed vacuum. These findings agreed with that of McEldowney and Fletcher (*25*) in that the number of positives for microbial ingress found in their study were not proportional to the magnitude of imposed vacuum.

TABLE 1. *Microbial ingress into test cells as a result of bioaerosol exposure and imposed pressures at 25 °C.*

Microtube ID Size (μm)	Imposed Pressure (kPa)							Total Positives
	-20.7	-13.8	-6.9	0	6.9	13.8	20.7	
50	4/9	8/9	1/9	2/9	3/9	1/9	3/9	22/63
20	6/9	4/9	0/9	0/9	1/9	6/9	6/9	23/63
10	1/9	4/9	0/9	0/9	0/9	3/9	3/9	11/63
7	0/9	1/9	0/9	0/9	0/9	3/9	1/9	5/63
5	1/9	2/9	0/9	0/9	0/9	3/9	1/9	7/63
2	0/9	0/9	0/9	0/9	0/9	0/9	0/9	0/63
Total Positives	12/54	19/54	1/54	2/54	4/54	16/54	14/54	68/378

TABLE 2. *M1 predicted vales for liquid flow and the imposed pressures at which microbial ingress was found for tryptic soy broth with a surface tension of 44.09 mN/m, through microtubes of 50, 20, 10, 7, 5 or 2 μm at 25 °C.*

Imposed Pressures (P_O)		
Microtube ID Size (μm)	M1 (kPa)	Ingress *for* Imposed P_O (kPa)
50	1.47	6.9/-6.9
20	3.99	6.8/-13.7
10	8.22	13.7/-13.7
7	11.66	13.7/-13.7
5	15.43	13.7/-13.7
2	31.80	No Ingress

The incidence of ingress was highest in test cells with microtubes of 20 μm ID, where 23 of 63 test cells resulted positive for microbial ingress contamination. The lowest incidence of microbial ingress was 0 positives of 63, found for test cells with a microtube of 2 μm ID (Table 1). The hydrophilic nature of the nickel microtubes may have contributed to a low critical leak size. Larger critical leak sizes may have resulted if the microtubes were constructed of hydrophobic materials, such as polyethylene or polypropylene. Surface oxidation of nickel microtubes may facilitate fluid movement by creating a hydrophilic surface, potentially reducing the imposed pressure required for the initiation of flow.

For microtubes with IDs of $\leq$ 20 μm, imposed pressures of 6.9, 13.8, and 20.7 kPa produced a total of 27 positive test cells for microbial ingress versus 19 test cells for imposed pressures of -6.9, -13.8, and -20.7 kPa. Ingress was found for test cells with a microtube ID of 20 μm under an imposed pressure of 6.9 kPa. However, ingress was not found in test cells with a microtube ID of 20 μm under an imposed pressure of -6.9 kPa. The difference between values for positives between pressure conditions of 6.9 kPa and -6.9 kPa were a function of differences between liquid surface tensions of TSB and water. Surface tension values for TSB inside the test cells were lower than those of distilled water forming the aerosol used to transport the test organism; 44.09 mN/m compared to 64.67 mN/m (*18*). Therefore, TSB required less imposed pressure than water to initiate flow through microtube IDs used in this study.

Imposed pressure conditions of -13.8 and -20.7 kPa produced 12 positives for microbial ingress for test cells with microtubes IDs of 50 μm versus four positives for identical test cells under imposed pressures of 13.8 and 20.7 kPa. Under most pressure conditions, fewer positives were found for test cells with 50-μm ID microtubes than for test cells with 20-μm IDs (Table 1). An explanation rests in the dynamics of droplet formation (*33*). For microtubes with 50 μm IDs, positive pressures greater than 6.9 kPa incite a rapid increase in droplet size (*18*). When the droplet reached a sufficient size (a diameter of approximately 900 μm), detachment from the microtube occurred. As a result, microorganisms transported via bioaerosol and contacting the droplet were carried away from the microtube by the detached droplet, thwarting ingress into the test cell.

The absence of microbial ingress in test cells with microtube IDs of 2 μm can be explained via the relationship between the fluid surface tension and imposed pressure in relation to the hole size. The imposed pressure required to initiate the flow of TSB through a microtube ID of 2 μm is 39.29 kPa (Table 2). A maximum imposed pressure and vacuum of 20.7 kPa were used in this study. Therefore, microbial ingress was not found in test cells with a microtube ID of 2-μm because the maximum imposed pressure used, 20.7 kPa, did not exceed 39.29 kPa which is required to initiate the flow of TSB.

The threshold imposed pressure or vacuum required to initiate flow of tryptic soy broth and distilled water produced by M1, coincided with those associated with critical leak values (Table 2). Packages with a partial vacuum or that maintain constant pressure differences between the inside and the outside have been found to be at greater risks for

contamination than those at atmospheric pressure (*24*, *30*). Banks and Stringer (*2*) found that bacterial transfer through a 5 μm diameter channel leak was higher when a vacuum was applied. The findings of this study agree with that of McEldowney and Fletcher (*24*) in that packages with large vacuums may be at no greater risks than those with low internal vacuums. Data in this study suggest that packages under positive pressures may face greater risk than packages under vacuum. Such positive pressures may occur during distribution (*18*).

Effect of temperature

The number of test cells with microtube IDs of 20 μm positive for contamination under imposed temperatures of 4.4° C and 37.7° C were 1 of 9 and 2 of 9, respectively (Table 3). The critical leak size for test cells challenged with a bioaerosol at a temperature of 25°C was 50 μm (2 of 9). Lower critical leak sizes resulted for temperatures of 4.4° C and 37.7° C due to differences between the temperatures of the exposure chamber and the test cell. Temperatures within the exposure section of the chamber decreased as relative humidity increased as a result of the bioaerosol presence. From a starting temperature of 25°C, the temperature within the exposure section was 20°C ± 1.5°C after 5 min of bioaerosol initiation. Since the temperature of the test cell (4.4°C) was lower than that of the atmosphere in the exposure section of the chamber (20°C), airborne particles exhibited thermophoresis by moving from a high temperature zone within the chamber to a lower temperature zone within the test cell (*32*). For test

TABLE 3. *Comparison of temperature (4 °, 25 °, and 37 °C) effects, at 0 kPa, on the critical leak size.*

Microtube ID Size (μm)	Temperature (°C)		
	4.0	25.0	37.0
50	3/9	2/9	2/9
20	1/9	0/9	2/9
10	0/9	0/9	0/9
7	0/9	0/9	0/9
5	0/9	0/9	0/9
2	0/9	0/9	0/9

cells biochallenged at a temperature of 37.7° C, the surface tension of the TSB within the test cells accounted for the increased number of positives for ingress compared to test cells biochallenged at a temperature condition of 25°C. An increase in the temperature of TSB above the start temperature of 25°C produced a decrease in surface tension, and allowed the initiation of liquid flow under ambient pressure conditions (*27*).

Critical leak size comparison of M1, M2, and observed values

The critical leak size is the smallest microtube ID where microbial ingress was found per conditions of imposed pressures. Values for the M1, M2 and the observed values were significantly different from each other ($p < 0.05$). The logistic regression model (M2) predicted values for the critical leak size based on the observed data and did not consider physical properties of the liquid food product, such as surface tension. The liquid flow model (M1) predicted the threshold leak size based on the imposed pressure and surface tension of the liquid product. Analyses employing the ANOVA indicate that the threshold leak sizes produced by M1, and the observed critical leak sizes were not significantly different ($p > 0.05$) (*19*). Differences between the observed critical leak size and values produced by M1 are due to surface tension and the microtube sizes. Such was the case for the observed and predicted critical leak sizes under an imposed pressure of 20.7 kPa. The observed critical leak size under an imposed pressure of 20.7 kPa was 5-μm, compared to the M1 predicted of 3.9-μm. However, no microtube sizes between 2-μm and 5-μm were tested. An imposed pressure of 20.7 kPa was sufficient to initiate flow

of TSB through a microtube with an ID size of 5-μm, but not sufficient to initiate flow through a microtube with a 2-μm ID. Therefore, the defect size critical to the sterility of a package can be caculated if the liquid surface tension and the internal pressures the package will encounter during distribution are known.

Gnanasekharan and Floros (*12*) suggested that factors such as length to diameter ratio of the leak, the internal geometry of the leak (straight/tortuous or smooth/rough) and the pressure differential across the leak interface, should be considered to determine the critical leak size for a package. However, Amini and Morrow (*1*) suggested that the diameter to length ratio of microleaks, for example, those of pin holes in the micron range found in thin foil, is of a sufficiently small magnitude so as not to require a correction factor. In this study, the microtubes used as leaker channels were 7 mm in length and straight. Previous research produced no evidence that supported significant effects on microbial ingress into a package via a defect as a function of channel length, although leak diameter itself was significant (*16, 17*).

In this study, the critical leak size was found to be a function of liquid avialability within, and through the microtube. Liquid TSB was present in and through the microtube when the imposed pressure required to initiate liquid flow was met or exceeded for each microtube ID size.

CONCLUSIONS

Many fluid foods have surface tension values similar to that of tryptic soy broth (*18*). This study, in conjunction with Keller et al. (*18*), produced data that establishes a relationship between the liquid surface tension of a food product, the imposed pressures the package will be expected to tolerate during distribution, and the threshold leak size. This, in part, explains the previously elusive nature of the critical leak size.

The critical leak size is a changing range largely based on the surface tension, hole size and imposed positive pressure or vacuum the package will be expected to tolerate during distribution. By averting such conditions sufficient to initiate flow of a fluid food product through a defect, such as alteration of its surface tension, reduction of defect size or avoidance of comparatively adequate imposed pressures, package sterility can be maintained.

Critical leak values produced in this study, are potentially conservative in that they are smaller values than those that may be found using microtubes constructed of hydrophobic materials. Such values resulted as a function of the nickel used to construct the microtubes. Due to the possible presence of hydrophilic conditions as a result of surface oxidation of the nickel microtubes, less imposed pressure may have been required to initiate flow than for microtubes made of a material with hydrophobic characteristics. As a result, the value for the critical leak microtube ID may be smaller than those that would result using other materials found in the seal areas of aseptic packages, such as

polypropylene.

Conservative critical leak values produced by this study resulted as a function of the microtube placement. Readied test cells are inverted prior to bioaerosol exposure, making the end of the microtubes the low points of the test cells. Therefore, the liquid within the test cells exerted the maximum static head pressure through the microtube, and facilitated the initiation of fluid flow. Defects found in the seal area on top of the package, for example, are not exposed to imposed pressures that result from static head.

In this study, a relationship between the imposed pressure required to initiate flow of a liquid through a defect and the loss of sterility have been established. For the first time, manufacturers of liquid food products can determine the leak size critical to the sterility of their product based on the liquid surface tension and imposed pressures required to initiate the flow of their product through the defect sizes commonly found in their packaging. As a result, the manufacturer may engage in a proactive approach to package sterility maintenance.

REFERENCES

1. Amini, M.A. and D. R. Morrow. 1979. Leakage and permeation: Theory and practical applications. Pack. Develop. and Sys. May/June: 20-27.

2. Banks, P. and M. F. Stringer. 1988. The design and application of a model system to investigate physical factors affecting container leakage. Inter. J. Food Microbiol. 6:281-286.

3. Blakistone, B.A., S.W. Keller, J.E. Marcy, G.H. Lacy, C.R. Hackney, and W.H. Carter, Jr. 1996. Contamination of flexible pouches challenged by immersion biotesting. J. Food. Prot. 59(7): 764-767.

4. Board, R.G. 1980. The avian eggshell-A resistance network. J. Appl. Bacteriol. 48:303-313.

5. Carter, W.H. 1995. Personal correspondence.

6. Chen, C., B. Harte, C. Lai, J. Pestka, and D. Henyon. 1991. Assessment of package integrity using a spray cabinet technique. J. Food. Prot., 54(8):643-647.

7. Cooper, D. W. 1989. Monitoring containment particles in gases and liquids: A review. p. 1-33 *In* K.L. Mittal (ed). Particles in Gases and Liquids 1: Detection, Characterization and Control. Plenum Press, New York.

8. Floros, J.D. and V. Gnanasekharan. 1995. Determination of critical leak size by analysis of gas and aerosol flow. Symposium Proceedings: "Advances in Aseptic Processing and Packaging Technologies," Copenhagen, Denmark. September 11-12.

9. Friedlander, S. K. 1970. The characterization of aerosols distributed with respect to size and chemical composition. Aerosol Sci. 1:295-307.

10. Fuchs, N. A. 1972. Some new methods and devices for aerosol studies. p.200-211. *In* T.T. Mercerm P.E. Morrow and W. Stöber (ed.). Assessment of Airborne Particles, Fundamentals, Applications, and Implications to inhalation Toxicity. Charles C. Thomas Publisher, Springfield, IL.

11. Gilchrist, J. E., U. S. Rhea, R. W. Dickerson, and J. E. Campbell. 1985. Helium leak test for micron-sized holes in canned foods. J. Food Prot. 48(10):856-860.

12. Gnanasekharan, V. and J. D. Floros. 1994. Package integrity evaluation: Criteria for selecting a method. Part I. Pack. Technol. and Eng. 3(6):67-72.

13. Hoffman, W. 1996. Cooperative research and development agreement. Phillips Laboratory, OLAC PL/RKFE, Edwards, CA

14. Howard, G. and R. Duberstein. 1980. A case of penetration of 0.2 μm rated membrane filters by bacteria. J. Parental Drug Assoc. 34(2): 95-102.

15. Jaenicke, R. 1976. Methods for Determination of Aerosol Properties. p. 469-475. *In* Fine Particles, Aerosol Generation, Measurement, Sampling, and Analysis. Academic Press, Inc. New York.

16. Jarrosson, B. P. 1992. Closure Integrity of Heat Sealed Aseptic Packaging Using Scanning Acoustic Microscopy. Virginia Polytechnic Institute and State University, Department of Food Science and Technology, M.S. Thesis.

17. Keller, S.W., J.E. Marcy, B.A. Blakistone, G.H. Lacy, C.R. Hackney, and W.H. Carter, Jr. 1996. Bioaerosol exposure method for package integrity testing. J. Food Prot. 59(7): 768-771.

18. Keller, S.W., J.E. Marcy, B.A. Blakistone, G.H. Lacy, C.R. Hackney, R. M. Davis, and W.H. Carter, Jr. 1998. Application of fluid modeling to determine the threshold leak size for liquid foods. J. Food Prot.

19. Koopman, L.H. 1987. Appendix Tables. p. 604. *In* Introduction to Contemporary Statistical Methods, 2nd ed. Duxbury Press, Boston.

20. Lake, D.E., R. R. Graves, R. S. Lesniewski, and J. E. Anderson. 1985. Post-processing spoilage of low-acid canned foods by mesophilic anaerobic sporeformers. J. Food Prot. 48(3):221-226.

21. Lampi, R. A. 1980. Retort pouch: The development of a basic packaging concept in today's high technology era. J. Food Process Eng. 4:1-18.

22. Lushnikov, A. A. 1976. Evolution of coagulating systems; Part III., Coagulating mixtures. J. of Colliod and Interface Sci. 54(1): 94-101.

23. McEldowney, S. and M. Fletcher. 1988. Bacterial desorption from food container and food processing surfaces. Mirob. Ecol. 15:229-237.

24. McEldowney, S. and M. Fletcher. 1990. A model system for the study of food container leakage. J. Appl. Bacteriol. 69:206-210.

25. McEldowney, S. and M. Fletcher. 1990. The effect of physical and microbiological factors on food container leakage. J. Appl. Bacteriol. 69:190-205.

26. Morton, D.K., G. L. Nicholas, L. H. Troutman, and T. J. Ambrosio. 1989. Quantitative and mechanistic measurements of container/closure integrity. Bubble, liquid, and microbial leakage test. J. of Parenteral Sci. and Technol. 43(3): 104-108.

27. Paddy, J. F., A. R. Pitt and R. M. Pashley. 1975. Menisci at a free liquid surface tension from the maximum pull on a rod. J. Chem. Soc. 1(71):1919-1931.

28. Pflug, I. J., P. M. Davidson, and R. G. Holcome. 1981. Incidence of canned food spoilage at the retail level. J. Food. Prot. 44(9),682-685.

29. Pich, J. 1972. Theory of gravitational deposition of particles from laminar flows in channels. Aerosol Sci. 3:351-361.

30. Put, H.M.C., Witvoet, H.T. and Warner, W.R. 1980. Mechanism of microbiological leaker spoilage of canned foods: Biophysical aspects. J. Food. Prot. 43(6):488-497.

31. Stersky, A., E. Todd, and H. Pivnick. 1980. Food poisoning associated with post-process leakage (PPL) in canned foods. J. Food Prot. 43(6):465-476.

32. Simpson. D.R., M. M. R. Williams, and S. Simons. 1989. Modeling of an aerosol in coupled chambers. Nuclear Sci. and Eng. 101:259-268.

33. Yam, K. 1995. On-line, non-destruction system inspects integrity of pouches. Pack. Technol. and Eng. 4(5):46-49.

34. Zhang, X. and O. A. Basaran. 1996. Dynamics of droplet formation from a capillary in the presence of an electric field. J. Fluid Mech. (326):239-263.

APPENDIX A. EXPOSURE CHAMBER.

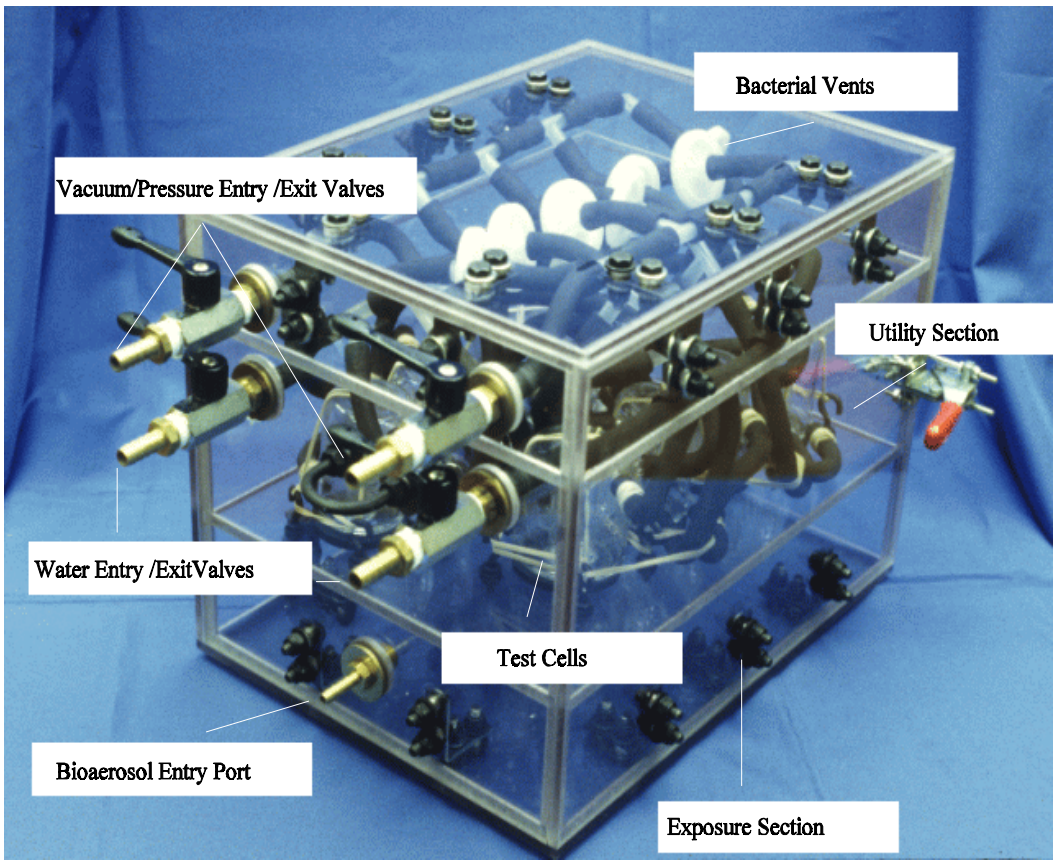

FIGURE 1. *Entry/exit ports, water entry/exit ports, bioaerosol entry ports, test cell holding area, exposure and utility sections, and inline bacterial vents.*

SECTION IV: EFFECT OF ORGANISM CHARACTERISTICS ON THE LEAK SIZE CRITICAL TO PACKAGE STERILITY

(Paper formatted for submission to the Journal of Food Protection)

ABSTRACT

The effects of microorganism size and motility, along with the imposed pressure required to initiate liquid flow on the leak size critical to the sterility of a package were measured. *Pseudomonas fragi* Lacy-1052, *Bacillus atrophaeus* ATCC 49337, and *Enterobacter aerogenes* ATCC 29007 were employed to indicate loss of package sterility. One hundred twenty-six microtubes with interior diameters (I.D.s) of 5, 10, and 20 μm and 7 mm in length were used as the manufactured defects. Forty-two solid microtubes were used as a control. No significant differences were found between test organisms with respect to size and motility for loss of sterility as a result of microbial ingress into test cells with microtube IDs of 5, 10, and 20 μm ($p > 0.05$). Interactions between the initiation of liquid flow as a result of applied threshold imposed pressures, and the sterility loss of test cells were significant ($p < 0.05$).

Key words: threshold imposed pressure, critical leak size, microbial ingress, package sterility

INTRODUCTION

The mechanism by which loss of package sterility occurs has eluded researchers for many years. Much emphasis has historically been placed on contaminated cooling water for loss of sterility in metal cans, as well as leakers in the double seam, rough handling after processing during distribution, and high relative humidity during storage *(1, 9, 10, 12, 13, 14*). As a by-product of such emphasis, package integrity tests such as immersion biochallenging were developed to simulate the conditions that metal cans were expected to tolerate during their life, through manufacturing to consumer use. Although the mechanism of microbial ingress into the package leading to post-process spoilage was not previously understood, precautions were implemented to reduce product loss as a result of loss of package sterility. For example, handling of hot metal cans and/or wet metal cans is discouraged until dry due to correlations made between poor package handling practices and spoilage (*12, 15, 16*). Documentation of such relationships can be found in decades of research throughout the scientific literature (*2, 3, 14, 15*).

Recently, quantitative links were established between the presence of liquid product on the outside of a package as a result of traversing through a defect, and loss of package sterility (*9*). Keller et al. (*8*) confirmed that liquid spoilage results when a liquid pathway is established through a defect (*11, 14*).

Investigation of contaminated packages consistently showed that microorganisms

were able to penetrate packages by traversing through a defect within the package (*14*). Microorganisms are thought to penetrate packages via defects by exercising motility, and/or by transport via a liquid passing through the defect as a result of pressure differentials *(2, 6, 8, 11, 12*). The purpose of this study was to determine the significance of microorganism characteristics, such as size and motility, on loss of package sterility..

MATERIALS AND METHODS

Microtubes

Nickel microtubes were supplied by the Phillips Laboratory, Fundamental Technology Division, Carbon Research Laboratory, Edwards Air Force Base, CA through a Cooperative Research and Development Agreement (*8*). One hundred twenty-six microtubes with interior diameters (IDs) of 5, 10, and 20 μm and 7 mm in length were used as the manufactured defects. Forty-two solid microtubes were used as a control.

Exposure chamber

The exposure chamber was constructed of Lexan® with dimensions of 35 cm (L) x 25 cm (W) x 25 cm (H). The internal area of the exposure chamber is 21,875 cm^3, and is divided into two sections: 1) utility section, 2) exposure section (*8*).

The utility section (dimensions: 35 cm [L] x 25 cm [W] x 18 cm [H]; total area = 15,750 cm^3) conatined the vacuum, water input and recovery manifolds, all related tubing,

vacuum and compressor tubing, as well as the test cells. The neck of each test cell passed through one of seven 2.85 cm holes in the partition. The top and end panels of the exposure chamber had stainless steel handles that were removable. The entry ports were created using two brass male and female threaded fittings with rubber O-rings

The exposure section (dimensions: 35 cm [L] x 25 cm [W] x 7 cm [H]; total area = 6125 cm^3) had entry ports positioned in the center of opposing panels of the exposure chamber for bioaerosol delivery. Nebulizer kits (Baxter model 2D0807, Toronto, Ontario, Canada) with mass median aerodynamic diameters of 2.68 μm, geometric standards of 1.85 μm, and masses of aerosols per minute of 1.1 μm and 4.7 μm were used. The maximum air flow (ml/hour) at 10 liters per minute (Lpm) was 21.9 ml/hour. Four 6.9 m^3 size E cylinders, each equipped with CGA 346 air (0 - 15 Lpm) flow meters were used for the air supply. Twenty-one 37 mm, 0.33-μm inline bacterial air vents (Gelman Sciences, Ann arbor, MI) were used to filter air flowing into the sterile test cells. The bacterial vents were also used on pressure equalization ports for the utility and exposure sections of the exposure chamber. Pressure inside the exposure chamber was monitored and maintained at 0.41 kPa via vacuum.

Test cells

Glass test cells were developed for the purpose of simulating imposed pressure within a package while maintaining sterility. The glass test cell dimensions were 8 cm [H] x 5 cm [D]. Each test cell consisted of a 45 mm [H] x 15 mm [D] glass vial (3 ml capacity)

encased in a 85-ml glass water jacket. The vial and the jacket have one entry and one exit port each. The vial was a glass lug for a septa closure (*6*).

Test organism

Three test organisms were used in this study; *Pseudomonas fragi* Lacy-1052, *Bacillus atrophaeus* ATCC 49337, and *Enterobacter aerogenes* ATCC 29007. These organisms were selected for their size, motility, and their wide use within the scientific literature (*10, 11*).

Pseudomonades used as an indicator of sterility are aerobic, gram-negative, motile, nonsporeforming rods with polar flagella, ranging from 0.5-1.0 μm in diameter and 1.5-5.0 μm in length. *Pseudomonas fragi* Lacy-1052, was selected from the library of the Department of Plant Pathology, Physiology and Weed Science, Virginia Polytechnic Institute and State University, Blacksburg, VA. Optimal temperature and pH ranges are 25°-30°C and 6.6-8.5, respectively.

Motile bacteria were used because of their suspected superior ability to penetrate a package via a defect when compared to nonmotile microorganisms (*10, 13*). Also, motile microorganisms are often associated with leaker spoilage (*10, 13*).

Bacillus atrophaeus ATCC 49337 are gram-positive, nonpathogenic, nonmotile, sporeforming rods, 1-1.5 μm in width and 4-10 μm in length. Optimal temperature and pH ranges are 27°-37°C and 5.5-8.5, respectively. *Bacillus atrophaeus* ATCC 49337, formerly *Bacillus subtilis* var. *niger* was selected because of its size and sporeforming

ability.

Enterobacter aerogenes ATCC 29007 are facultatively anaerobic, gram-negative, motile (peritrichous flagella), straight rods, 0.6-1.0 μm wide and 1.2-3.0 μm long. Optimal temperature and pH ranges are 37°-44.5°C and 6.0-8.0, respectively.

Preparation of test cells

Microtubes were positioned inside a 27-gauge syringe needle. The needle was used to puncture and penetrate through the center of a silicone septum. The syringe needle was removed, leaving the microtube in place. The internal diameter of each microtube was measured to obtain the cross-sectional area using a light microscope (Model BH-2, Olympus, Lake Success, NY) equipped with video callipers.

Septums containing microtubes were positioned on top of the test cell finish. Glass lugs of the test cell were wrapped with Teflon™ tape, overlapping the top outside circular edge of the septum. Septa caps were placed over the septums and tightened. Silicone (Dow Corning, Dayton, OH) was used to seal the septa surface around the microtube and the septum-septa cap contact area. Seal integrity for test cells was confirmed as described by Keller et al. (*6*).

Preparation of exposure chambers

Seven test cells with microtubes of the same ID size were randomly assigned one of seven positions within the exposure chamber. Each test cell was filled with 3 mL of tryptic

soy broth (Difco Laboratories, Detroit, MI) inverted to a septa cap down position, and secured on top of a rubber gasket. All rubber gaskets received a thin coat of high vacuum grease (Dow Corning Corp., Midland, MI) on both the top and bottom surfaces. Test cells were secured to the partition by bolt-down aluminum brackets. General purpose rubber tubing (Fisher Scientific, Atlanta, GA) was connected to the entry and exports of the vial section of each test cell. Tubes were equipped with an in-line 0.33-μm bacterial air vent (Gelman Sciences, Ann Arbor, MI) positioned inside the holding section to prevent contamination during post autoclave cooling. Each tube was also connected to a brass ball valve, on the exterior of the chamber. The exposure chamber was positioned so that septa caps faced up to eliminate contact of the microtubes with the liquid tryptic soy broth within each of the test cells during autoclaving.

Exposure chambers were autoclaved at 121°C for 55 minutes. Valves on each exposure chamber were opened prior to autoclaving to facilitate sterilization and to dampen the generation of pressure differentials between the test cells, the exposure chamber and the autoclave.

Prior to the introduction of the bioaerosol into the exposure section, each exposure chamber was inverted so that the septa caps faced downward. The inverted position of the test cells facilitated continuous contact of the liquid growth medium with the microtubes.

Preparation of bioaerosol

Inocula of 10^9 CFU/ml of each microorganism were prepared according to Keller et

al. (*8*). *Pseudomonas fragi* L-1052 was differentiated by antibiotic resistance to kanomycin (30 μg/ml) and tetracycline (10 μg/ml). *Bacillus atrophaeus* ATCC 49337 were differentiated by pigmentation from telluride in tryptic soy agar, which aids identification by turning CFUs black. Spores of *Bacillus atrophaeus* ATCC 49337 was verified by the Wirtz's method of staining with the exception of use of a 7.5% aqueous safranin red dye (*5*). *Enterobacter aerogenes* ATCC 29007 was identified using Biologic® gram-negative MicroPlates™ (Biolog, Hayward, CA) . The final challenge suspensions were aseptically transferred to the reservoirs of the nebulizer kits.

Aerosol biochallenge

Nebulizers were secured to the external ports centered on each of the two small end panels of the exposure chamber via sterile clear PVC tubing 2.54 cm ID x 3.2 cm OD x 45 cm in length (Fisher Scientific, Atlanta, GA). The exposure period was divided into a 30 minute come-up period, and a 5 minute static period.

The 30 minute come-up period is the time required to achieve the final desired bioaerosol concentration of 10^6 CFU/cm^3 within the exposure section. A total of 6 ml of the source concentration approximately 10^9 CFU/ml, was introduced via aerosol into the 6,125 cm^3 exposure section, for a final airborne concentration of approximately 10^6 CFU/cm^3. A vacuum of 0.06 kPa was used to maintain a pressure equilibrium between the exposure chamber and ambient conditions.

Imposed pressure

To measure the influence of threshold pressures required to initiate liquid flow on the critical leak size at which loss of sterility occurs, positive pressures were imposed on the internal vial of the test cell at the onset of the come-up period. Internal threshold positive pressures were calculated for the smallest of each microtube size by the criteria for liquid flow model (*7*):

$$P_O - P_L > 0, \quad P_O > P_{ATM} + [(4\sigma/D_H - \rho gL) \; x \; 0.272] \qquad (2)$$

where the imposed pressure (P_o) must be greater than the surface tension (σ) for a given hydraulic diameter (D_H) with a given static head (ρgL). When threshold imposed pressures were met or exceeded for tryptic soy broth per microtube ID size, a liquid pathway through the microtube was established, simulating a liquid filled defect within a package.

Positive pressures were imposed via a compressor (model ROA-P131-AA, Gast, Benton Harbor, MI). A 500-ml vessel, with brass entry and exit barbed ports, was used to stabilize the air flow from the compressor to produce pressure fluxuations of ≤ 0.06 kPa. An in line pressure gauge (Model HHP701-2, Omega Engineering, Inc., Stamford, CT) with a detection range of 137.9 kPa of vacuum or positive pressure, and a resolution and accuracy of 0.05% and ± 0.15% FS, respectively, was used to measure the applied imposed pressure.

After completion of the come-up period, the bioaerosol and vacuum were

discontinued, thus initiating the static period. Each chamber remained in the static period for 5 minutes at a temperature of 25°C. Aerosol residual in the exposure section of the chamber was removed through a port with an in-line bacterial vent under 20.7 kPa of vacuum.

Exposure chambers were incubated for 72 hours at 25°C. Following the incubation period, test cells were removed from the utility section. Liquid samples were aseptically transferred and plated from test cells showing turbidity to confirm test organism growth on tryptic soy agar with a differentiating agent as previously described.

Experimental design

A randomized complete block design was employed. The purpose of the block design was to independently determine the significance of microorganism characteristics such as size and motility on the leak size critical to package sterility, and determine the significance of liquid present in the defect on the sterility of the package.

Each exposure chamber contained seven randomly positioned test cells fixed with seven microtubes of the same ID size. Therefore, each exposure chamber contained seven replicates challenged via bioaerosol per imposed pressures at 25°C.

Statistical analysis

A chi-square test was carried out using StatXact 3® (Cytel Software Corp., Cambridge, MA) to determine significant differences within and between the randomized

complete blocks..

RESULTS

Test cells

Test cells with microtubes without holes (i.e., solid) showed no indications of microbial presence after aerosol biochallenge. This confirmed that test cells with positive microbial contamination resulted due to ingress through microtubes with holes.

Aerosol biochallenge

No significant differences were found between critical leak sizes for *Enterobacter aerogenes* ATCC 29007, *Pseudomonas fragi* L-1052, and *Bacillus atrophaeus* ATCC 49337 ($p < 0.05$). No significant differences for loss of sterility were found between ID sizes of 5, 10, and 20 μin ($p > 0.05$). The Chi-square test showed no significant differences in frequency of microbial ingress between microtube ID sizes or between microorganisms (Table 1). These findings conflict with those of McEldowney and Fletcher (*10, 11*), Banks and Stringer (*2*), and Hurme et al. (*4*). McEldowney and Fletcher (*10, 11*), using *Pseudomonas* sp., *Bacillus* sp., and *Enterobacter aerogenes* found that microbial ingress into test packages varied with, bacterial morphology, defect channel length and diameter. Likewise, Put et al., (*13, 14*) reported that leakage was largely a function of bacterial cell size. McEldowney and Fletcher (*11*) also found significant

differences between the indicator organisms ability to ingress through straight leakage channels into a container leakage model system (CLMS) with defect equivalent IDs of 0.9, 4.4, 7.1, 8.9, 10.6, and 10.9 μm, respectively. According to McEldowney and Fletcher (*10, 11*), loss of sterility increased as vacuum was increased from 6.8 to 40.7 kPa, although not proportionately. Positive imposed pressures were not examined in their study. Banks and Stringer (*2*) observed differences in the rate of microbial ingress between *Pseudomonas* sp., and a *Bacillus* sp. They reported the occurance of microbial ingress through 5-μm pores under ambient pressure conditions. Contrary to the findings of McEldowney and Fletcher (*11*), Banks and Stringer (*2*) found that microbial ingress increased proportionately to an increase of imposed vacuum. Keller et al. (*8*) found microbial ingress to be similiar for test cells under imposed vacuums and positive pressures of the same absolute value. Imposed positive pressures were not examined in the study by Banks and Stringer (*2*). Hurme et al. (*4*) found that microorganism size was a significant characteristic regarding microbial ingress into a package. They found the critical leak size for *Enterobacter aerogenes* and *Bacillus subtilis* to be $\geq$ 10-μm, and that penetration of *E. aerogenes* was unlikely to occur in IDs smaller than 10-μm when the channel length was 100μm. In the current study, microbial ingress were found for *E. aerogenes, B. subtilis*, and *Pseudomonas fra*gi in test cells with microtube IDs of 5, 10, and 20 -μm and a channel length of 7-mm.

In this study, microbial ingress increased significantly when the imposed pressure exceeded that which was required to initiate flow for each microtube ID size (Table 1).

Threshold pressures for test cells with microtubes IDs of 5, 10, and 20 μm, were 25.87 ±1.48 kPa, 10.82 ±1.83 kPa, and 4.14 ± 0.17 kPa, respectively. Therefore, when a liquid pathway through the defect was established, microbial ingress occured. Where a liquid pathway was not established, as for those test cells challenged under ambient pressure, microbial ingress did not occur. McEldowney and Fletcher (*11*) associated an increase of liquid viscosity with a decrease in microbial ingress. They used a phosphate buffer solution of which the surface tension was estimated to be approximately equal to that of water, or 65 mN/m (Keller 1998a). They found that an increase in viscosity produced a decrease in microbial leakage into the CLMS per level of imposed vacuum (*9*). Similar results were found by Banks and Stringer (*2*). Both attributed these findings to a subsequent reduced rate of flow. Keller et al. (*6, 8*) suggest that such differences resulted due to a change in the liquid surface tension of the phosphate buffer solution. An increase in the liquid surface tension increases the imposed pressure required to initiate flow through a defect of a given size, and creates a liquid pathway (*8*). However, once flow is established, a liquid pathway is available to the microorganism for direct passage through the defect and into the package either by its own motility, or by the movement of

Table 1. *Test cells positive for microbial ingress for each test organism at threshold pressures and 0 kPa.*

	Enterobacter aerogenes ATCC 29007		*Bacillus atrophaeus* ATCC 49337		*Pseudomonas fragi* L-1052		Total Positives
Microtube ID (μm)	Press (kPa)	Positives	Press (kPa)	Positives	Press (kPa)	Positives	
20	0.00	0/7	0.00	0/7	0.00	0/7	0/21
	4.14	4/7	4.48	4/7	4.14	3/7	11/21
10	0.00	0/7	0.00	0/7	0.00	0/7	0/21
	9.65	2/7	13.23	2/7	9.58	3/7	7/21
5	0.00	0/7	0.00	0/7	0.00	0/7	0/21
	26.81	2/7	23.92	2/7	26.89	3/7	7/21
Total Positives		8/42		8/42		9/42	

the liquids due to pressure differentials between the interior and the exterior of the package. Such pressure differentials may be inherent to the package, such as with metal cans, or they may be generated during distribution (*8*).

In this study, interactions between the initiation of liquid flow as a result of applied threshold pressures, and the sterility loss of test cells were significant ($p < 0.05$). Re-arranging Equation 1 to solve for defect ID, we can detemine the threshold ID

$$D_H = 4\sigma\left(\frac{P_0}{0.272} + \rho gL\right)^{-1} \qquad (2)$$

per a given set of conditions such as liquid surface tension, imposed pressure and defect ID size. Since microbial ingress occurs when liquid flow is initiated, the threshold leak size is equal to the critical leak size. Therefore, package sterility can be quantified and predicted.

CONCLUSIONS

Loss of package sterility based on leakage rates have been established (2, *9, 10*). From a sterility maintenance perspective, one package with loss of sterility is significant. Therefore, the rate of ingress beyond that required to initiate sterility loss of the first package is not significant. Also, the significance of imposed pressures generated within a package of sufficient magnitude to initiate flow of liquids through a defect have been neglected.

This study differs from that of previous leaker studies, in that initiation of a leak irrespective of its flow rate, is a of concern with respect to loss of sterility. Imposed pressures capable of initiating flow through a defect provide the necessary conditions for microbial ingress and loss of package sterility.

REFERENCES

1. Anema, P. J. and B. L. Schram. 1980. Prevention of post process contamination of semi-rigid and flexible containers. J. Food. Prot. 43(6):461-464.

2. Banks, P. and M. F. Stringer. 1988. The design and application of a model system to investigate physical factors affecting container leakage. Inter. J. Food Microbiol. 6:281-286.

3. Bashford, T. E. 1947. Infected cooling water and its effect on spoilage in canned foods. J. Appl. Bact. 10:46-49.

4. Hurme, E. U., G. Wirtanen, L. Axelson-Larsson, N. A. M. Pachero, and R. Ahvenainen. 1997. Penetration of bacteria through microholes in semirigid aseptic and retort packages. J. Food Prot. 60(5):520-524.

5. Jacobs, M. B. and M. J. Gerssstein. 1960. Table 10., p. 253. Stains and staining techniques. *In* Handbook of Microbiology. D. Van Nostrand Company, Inc., Princton, NJ.

6. Keller, S.W., J.E. Marcy, B.A. Blakistone, G.H. Lacy, C.R. Hackney, and W.H. Carter, Jr. 1996. Bioaerosol exposure method for package integrity testing. J. Food Prot. 59(7): 768-771.

7. Keller, S.W., J.E. Marcy, B.A. Blakistone, G.H. Lacy, C.R. Hackney, R. M. Davis, and W.H. Carter, Jr. 1998. Application of fluid modeling to determine the threshold leak size for liquid foods. J. Food Prot.

8. Keller, S.W., J.E. Marcy, B.A. Blakistone, G.H. Lacy, C.R. Hackney, and W.H. Carter, Jr. 1998. The imposed pressures and vacuums generated inside a package during simulated distribution testing. J. Food Prot.

9. Keller, S.W., J.E. Marcy, B.A. Blakistone, G.H. Lacy, C.R. Hackney, and W.H. Carter, Jr. 1998. The application of fluid and statistical modeling to establish the leak size critical to package sterility. J. of Food Prot.

10. McEldowney, S. and M. Fletcher[a]. 1990. A model system for the study of food container leakage. J. Appl. Bacteriol. 69:206-210.

11. McEldowney, S. and M. Fletcher[b]. 1990. The effect of physical and microbiological factors on food container leakage. J. Appl. Bacteriol. 69:190-205.

12. Michels, M. J. M. and B. L. Schram. 1979. Effect of handling procedures on the post process contamination of retort packages. J. Appl. Bacteriol. 47:105-111.

13. Put, H. M. C. and W. R. Warner. 1972. The Mechanism of microbiological leaker spoilage of canned foods: a review. J. Appl. Bacteriol. 35:7-27.

14. Put, H. M. C., H. T. Witvoet, and W. R. Warner. 1980. Mechanism of microbiological leaker spoilage of canned foods: Biophysical aspects. J. Food. Prot. 43(6):488-497.

15. Stersky, A., E. Todd, and H. Pivnick. 1980. Food poisoning associated with post process leakage (PPL) in canned foods. J. Food Prot. 43(6):465-476.

16. Thompson, P. J. and M. A. Griffith. 1983. Identity of mesophilic anaerobic sporeformers cultured from recycled cannery cooling water. J. Food Prot. 46(5):400-402.

VITA

Scott Keller was born August 29th, 1960 in Joplin, Missouri. He lived in Joplin until the age of 10, when he moved to St. Joseph, Missouri where he attended both Lafayette High School *(Home of the Fighting Irish*), and Missouri Western State College where he graduated with a B. S. in Psychology. He attended Northwest Missouri State University in Maryville, Missouri where he earned an M.B.A. In the spring of 1988, he was transferred to Richmond, Virginia as a result of a promotion within Best Products, Inc.

In the Spring of 1993, he moved to Blacksburg, Virginia to began course work towards an M.S. in Food Science and Technology at Virginia Polytechnic Institute and State University. In 1998, he earned a Ph.D. in Food Science and Technology at the same institution. During his studies at Virginia Tech, he traveled to Copenhagen, Denmark, and Taipei, Taiwan to present his research.